

# Muon anomalous magnetic moment, lepton flavor violation, and flavor changing neutral current processes in SUSY GUT with right-handed neutrino

Seungwon Baek,<sup>1</sup> Toru Goto,<sup>2</sup> Yasuhiro Okada,<sup>2,3</sup> and Ken-ichi Okumura<sup>4</sup>

<sup>1</sup>*Department of Physics, National Taiwan University, Taipei 106, Taiwan*

<sup>2</sup>*Theory Group, KEK, Tsukuba, Ibaraki, 305-0801 Japan*

<sup>3</sup>*Department of Particle and Nuclear Physics,  
The Graduate University of Advanced Studies, Tsukuba, Ibaraki, 305-0801 Japan*

<sup>4</sup>*Institute for Cosmic Ray Research, University of Tokyo,  
Kashiwanoha 5-1-5, Kashiwa, 277-8582 Japan*

(April 16, 2001)

## Abstract

Motivated by the large mixing angle solutions for the atmospheric and solar neutrino anomalies, flavor changing neutral current processes and lepton flavor violating processes as well as the muon anomalous magnetic moment are analyzed in the framework of SU(5) SUSY GUT with right-handed neutrino. In order to explain realistic mass relations for quarks and leptons, we take into account effects of higher dimensional operators above the GUT scale. It is shown that the supersymmetric (SUSY) contributions to the CP violation parameter in  $K^0 - \bar{K}^0$  mixing,  $\varepsilon_K$ , the  $\mu \rightarrow e \gamma$  branching ratio, and the muon

anomalous magnetic moment become large in a wide range of parameter space. We also investigate correlations among these quantities. Within the current experimental bound of  $B(\mu \rightarrow e\gamma)$ , large SUSY contributions are possible either in the muon anomalous magnetic moment or in  $\varepsilon_K$ . In the former case, the favorable value of the recent muon anomalous magnetic moment measurement at the BNL E821 experiment can be accommodated. In the latter case, the allowed region of the Kobayashi-Maskawa phase can be different from the prediction within the Standard Model (SM) and therefore the measurements of the CP asymmetry of  $B \rightarrow J/\psi K_S$  mode and  $\Delta m_{B_s}$  could discriminate this case from the SM. We also show that the  $\tau \rightarrow \mu\gamma$  branching ratio can be close to the current experimental upper bound and the mixing induced CP asymmetry of the radiative  $B$  decay can be enhanced in the case where the neutrino parameters correspond to the Mikheyev-Smirnov-Wolfenstein small mixing angle solution.

## I. INTRODUCTION

In order to explore physics beyond the Standard Model (SM), indirect searches play an important role complimentary to direct searches of new particles at high energy frontiers. The indirect searches include flavor changing neutral current (FCNC) processes, lepton flavor violation (LFV) and the muon anomalous magnetic moment. In the minimal SM, lepton flavor is conserved and FCNC is forbidden at tree level, so that  $B$ ,  $K$  and  $\mu$  decay experiments have supplied severe constraints on models beyond the SM. At the recent BNL E821 experiment, it was reported that the muon anomalous magnetic moment had  $2.6\sigma$  deviation from the SM prediction [1]. If the deviation is confirmed by improvement in both statistics and understanding theoretical uncertainty of the SM prediction, the muon anomalous magnetic moment becomes a clear signal of physics beyond the SM.

Among candidates of the physics beyond the SM, supersymmetry (SUSY) is the most

attractive one. Because of the cancellation of quadratic divergence in the renormalization of the Higgs field, SUSY models do not have the hierarchy problem of the SM. Furthermore, the gauge coupling unification is realized in the SUSY grand unified theories (SUSY GUT) based on SU(5) gauge group or its extensions.

In view of the flavor physics, it is important that the scalar partners of quarks and leptons, namely squarks and sleptons, have a new source of flavor mixing. Due to the new flavor mixing, LFV and FCNC such as  $\mu \rightarrow e \gamma$ ,  $b \rightarrow s \gamma$  and  $K^0 - \bar{K}^0/B^0 - \bar{B}^0$  mixing could be induced through SUSY loop diagrams. Because these processes receive too large contributions for generic flavor mixing in squark and slepton sector, the structure of SUSY breaking sector of the Lagrangian is required to have a special form, unless the masses of the SUSY particles are beyond multi-TeV region [2]. The simplest possibility to avoid this problem is that the SUSY breaking mechanism is assumed to be flavor blind. However, even in such a case, the squark and slepton mass matrices receive radiative corrections from interactions below the scale where the SUSY breaking is originated, and flavor blindness is broken [3,4]. In particular, effects of the large top Yukawa coupling constant can not be neglected. A number of analyses have been done in the context of minimal supergravity (minimal SUGRA) anzats where SUSY breaking parameters are assumed to be flavor blind at the Planck scale [5–8]. It was shown that the flavor mixing is controlled by the Cabibbo-Kobayashi-Maskawa (CKM) matrix element. As a result the maximal deviation from the SM in the CP violating parameter of  $K^0 - \bar{K}^0$  mixing,  $\varepsilon_K$ , and  $B_d - \bar{B}_d/B_s - \bar{B}_s$  mixing is of the order of 10 %, while the SUSY contribution to  $b \rightarrow s \gamma$  process can be much important [7,8]. In the GUT scenario, there are additional contributions to FCNC/LFV processes from GUT interactions [4,9–12]. As for LFV processes the  $\mu \rightarrow e \gamma$  branching ratio is close to the current experimental bound, especially for SO(10) model [10].

Recent experimental evidences of neutrino oscillation indicate existence of small neutrino mass and large flavor mixings in the lepton sector [13]. A natural explanation for small neutrino mass is the seesaw mechanism [14]. In this mechanism, heavy right-handed neutrinos are introduced, and these neutrinos have Majorana mass term and new Yukawa interactions.

Because the neutrino Yukawa coupling constants can be as large as the top Yukawa coupling constant if the right-handed neutrinos are  $O(10^{14})$  GeV, radiative corrections from these interactions contribute to the renormalization of slepton mass matrix above the mass scale of the right-handed neutrinos. Within the minimal SUGRA scenario, it was shown that the branching ratios of LFV processes becomes large enough to be measured in near-future experiments [15–17]. Some GUT models which have predictable neutrino mass and mixing are already constrained [18]. In the context of SUSY GUT, these new interactions in the lepton sector also contribute to the quark sector, because radiative corrections on the squark from neutrino interactions can become a new source of quark FCNC processes as well as the LFV processes. Recently, these processes are analyzed in the minimal SU(5) SUSY GUT with right-handed neutrino and large deviations from the SM are predicted [19,20]. However, in these analyses, simple flavor structure was assumed so that the correct mass relations between the down-type quarks and charged leptons in the first and second generations can not be realized.

Very recently, the BNL E821 experiment reported a new result on the muon anomalous magnetic moment [1]. The measured value of  $a_\mu = (g_\mu - 2)/2$  is  $a_\mu(\text{exp}) = 11659202(14)(6) \times 10^{-10}$ , which is compared to the SM prediction  $a_\mu(\text{SM}) = 11659159.6(6.7) \times 10^{-10}$ . It was concluded that the theory and experiment had  $2.6 \sigma$  difference  $a_\mu(\text{exp}) - a_\mu(\text{SM}) = 43(16) \times 10^{-10}$ . The deviation can be explained in the context of the SUSY model [21]. In contrast to the LFV and FCNC processes which are very sensitive to the origin on the flavor mixing at high energy scale, the muon anomalous magnetic moment can provide us information on the slepton masses, rather independent of the flavor structure of the slepton mass matrices.

In this paper, we discuss FCNC/LFV processes in the SU(5) supersymmetric grand unified theory with right-handed neutrino (SU(5)RN SUSY GUT) taking account of realistic mass relations. The seesaw mechanism generates small neutrino masses and large mixing angles which incorporate atmospheric and solar neutrino anomalies. In order to reproduce realistic mass relations, we introduce a higher dimensional operator including **24** superfield

which gives contributions to the Yukawa coupling matrices for the down-type quarks and the charged leptons in a different manner. Moreover, new degrees of freedom arise in the choice of the bases when the MSSM multiplets are embedded in the SU(5) multiplets. We show that the main effect of these new mixings is described by two mixing angles which parameterize rotations of the bases between the down-type quarks and charged leptons in the first and second generations. We perform numerical analysis on FCNC/LFV processes taking account of various sources of flavor mixing. We also calculate the muon anomalous magnetic moment and investigate the correlations among these quantities. Solving renormalization group equations for the Yukawa coupling matrices and the SUSY breaking parameters, the flavor mixing in the squark and slepton sectors is evaluated at the electroweak (EW) scale. In addition to the muon anomalous magnetic moment, we calculate following FCNC/LFV observables: the branching ratios of  $\mu \rightarrow e \gamma$ ,  $\tau \rightarrow \mu \gamma$  and  $b \rightarrow s \gamma$ ,  $\varepsilon_K$ , the mass differences in  $B_d - \bar{B}_d$  mixing and  $B_s - \bar{B}_s$  mixing, and the time-dependent CP asymmetries of  $B \rightarrow J/\psi K_S$  and  $B \rightarrow M_s \gamma$  where  $M_s$  is a CP eigenstate including a strange quark. We find that the SUSY contributions to  $\varepsilon_K$ , the  $\mu \rightarrow e \gamma$  branching ratio, and the muon anomalous magnetic moment become large in a wide range of parameter space. Within the current experimental bound on  $B(\mu \rightarrow e \gamma)$ , large SUSY contributions are possible either in the muon anomalous magnetic moment or in  $\varepsilon_K$ . In the former case, the favorable value of the recent muon anomalous magnetic moment measurement at the BNL experiment can be accommodated. In the latter case, the new contribution  $\varepsilon_K$  modifies the constraint for the CKM matrix elements and affects  $B$  decay observables because allowed region of  $\Delta m_{B_s}/\Delta m_{B_d}$  and the time-dependent CP asymmetry of the  $B \rightarrow J/\psi K_S$  mode can be quite different from that of the SM or MSSM without the new flavor mixing source. We also show that  $B(\tau \rightarrow \mu \gamma)$  and the indirect CP asymmetry of the radiative  $B$  decay can be large in the case where the neutrino parameters correspond to the small mixing angle Mikheyev-Smirnov-Wolfenstein (MSW) solution. We also notice that the branching ratio of  $\mu \rightarrow e \gamma$  can be close to the present experimental upper limit both in the large and small mixing angle MSW solutions.

The rest of this paper is organized as follows. In Sec. II, the SU(5)RN SUSY GUT is introduced. The higher dimensional operators are included to incorporate the realistic fermion mass relation. Two new mixing angles are defined to parameterize the effect of these operators. In Sec. III, the minimal SUGRA model is introduced for the SUSY breaking sector. Radiative corrections for the SUSY breaking parameters and FCNC/LFV processes are discussed qualitatively using approximated formulas. In Sec. IV, the numerical results for the muon anomalous magnetic moment and FCNC/LFV processes are presented. Sec. V is devoted for conclusion and discussions. In Appendices, useful formulas are collected.

## II. SU(5) SUSY GUT WITH RIGHT-HANDED NEUTRINO

In this section we discuss quark and lepton Yukawa couplings in the SU(5)RN SUSY GUT. Before introducing higher dimensional operators, we first discuss the case without them. Later, we introduce those operators to accommodate realistic mass relation. Without higher dimensional operators, the Yukawa coupling and the Majorana mass term of the superpotential for this model are given by

$$\begin{aligned} \mathcal{W}_{\text{SU(5)RN}} = & \frac{1}{8} \epsilon_{abcde} (\lambda_u)_{ij} (T^i)^{ab} (T^j)^{cd} H^e + (\lambda_d)_{ij} (\bar{F}^i)_a (T^j)^{ab} \bar{H}_b \\ & + (\lambda_\nu)_{ij} \bar{N}^i (\bar{F}^j)_a H^a + \frac{1}{2} (M_\nu)_{ij} \bar{N}^i \bar{N}^j, \end{aligned} \quad (1)$$

where  $T^i$ ,  $\bar{F}^i$  and  $\bar{N}^i$  are **10**,  $\bar{\mathbf{5}}$  and **1** representation of SU(5) gauge group, respectively.  $i, j$  are generation indices and  $a, b, c, d$  and  $e$  are SU(5) indices.  $\epsilon_{abcde}$  is the totally antisymmetric tensor of SU(5) gauge group.  $H$  and  $\bar{H}$  are Higgs superfields with **5** and  $\bar{\mathbf{5}}$  representations. In terms of SU(3)×SU(2)<sub>L</sub>×U(1)<sub>Y</sub>,  $T^i$  contains  $Q^i(\mathbf{3}, \mathbf{2}, \frac{1}{6})$ ,  $\bar{U}^i(\bar{\mathbf{3}}, \mathbf{1}, -\frac{2}{3})$  and  $\bar{E}^i(\mathbf{1}, \mathbf{1}, 1)$  superfields. Here the representations for SU(3) and SU(2) groups and the  $U(1)_Y$  charge are indicated in the parentheses.  $\bar{F}^i$  includes  $\bar{D}^i(\mathbf{3}, \mathbf{1}, \frac{1}{3})$  and  $L^i(\mathbf{1}, \mathbf{2}, -\frac{1}{2})$ , and  $\bar{N}^i$  is a singlet of SU(3)×SU(2)<sub>L</sub>×U(1)<sub>Y</sub>.  $H$  consists of  $H_C(\mathbf{3}, \mathbf{1}, 0)$  and  $H_2(\mathbf{1}, \mathbf{2}, \frac{1}{2})$  and  $\bar{H}$  contains  $\bar{H}_C(\bar{\mathbf{3}}, \mathbf{1}, 0)$  and  $H_1(\mathbf{1}, \mathbf{2}, -\frac{1}{2})$ .  $(\lambda_u)_{ij}$ ,  $(\lambda_d)_{ij}$  and  $(\lambda_\nu)_{ij}$  are Yukawa coupling matrices and  $(M_\nu)_{ij}$  is a Majorana mass matrix. In addition to the above formula, we also need a superpotential for

Higgs superfields,  $\mathcal{W}_H(H, \overline{H}, \Sigma)$  where  $\Sigma_b^a$  is a **24** representation of SU(5) group. It is assumed to develop vacuum expectation values as  $\langle \Sigma_b^a \rangle = \text{diag}(\frac{1}{3}, \frac{1}{3}, \frac{1}{3}, -\frac{1}{2}, -\frac{1}{2})v_G$  at the GUT scale ( $M_G \approx 2 \times 10^{16}$  GeV) and breaks the SU(5) symmetry to  $\text{SU}(3) \times \text{SU}(2)_L \times \text{U}(1)_Y$ .

Below the GUT scale, the heavy superfields such as  $H_C$ ,  $\overline{H}_C$  and  $\Sigma$  are integrated out and the superpotential of the MSSM with right-handed neutrino (MSSMRN) is given by

$$\begin{aligned} \mathcal{W}_{\text{MSSMRN}} = & (y_u)_{ij} \overline{U}^i Q^j H_2 + (y_d)_{ij} \overline{D}^i Q^j H_1 + (y_e)_{ij} \overline{E}^i L^j H_1 + \mu H_1 H_2 \\ & + (y_\nu)_{ij} \overline{N}^i L^j H_2 + \frac{1}{2} (M_\nu)_{ij} \overline{N}^i \overline{N}^j, \end{aligned} \quad (2)$$

where Yukawa coupling matrices are related to those of the SU(5)RN as  $(y_u)_{ij} = (\lambda_u)_{ij}$ ,  $(y_d)_{ij} = (y_l^T)_{ij} = (\lambda_d)_{ij}$  and  $(y_\nu)_{ij} = (\lambda_\nu)_{ij}$ . Below the Majorana mass scale ( $\equiv M_R$ ), the singlet fields are also integrated out from the superpotential and a dimension five operator is generated as follows:

$$\Delta \mathcal{W}_\nu = -\frac{1}{2} (K_\nu)_{ij} (L_i H_2) (L_j H_2), \quad K_\nu = (y_\nu^T)_{ik} \left( \frac{1}{M_\nu} \right)^{kl} (y_\nu)_{lj}. \quad (3)$$

After the EW symmetry breaking, this operator induces by the seesaw mechanism the following neutrino mass matrix,

$$(m_\nu)_{ij} = (K_\nu)_{ij} \langle H_2 \rangle^2. \quad (4)$$

In this model, the naive GUT relation is predicted at the GUT scale,

$$(y_e)_{ij} = (y_d)_{ji}. \quad (5)$$

Although this relation gives a reasonable agreement for  $m_b$  and  $m_\tau$ , it is well known that the mass ratio of down-type quarks and charged leptons in the first and the second generations can not be explained in this way. One possibility to remedy this defect is to introduce higher dimensional operators above the GUT scale because they can give different contributions to the Yukawa coupling matrices of down-type quarks and charged leptons after the SU(5) symmetry breaking.

We consider higher dimensional operators including the **24** Higgs superfield up to dimension five terms. Relevant parts of the superpotential is parameterized as follows:

$$\begin{aligned}
\Delta\mathcal{W}_{\text{SU}(5)\text{RN}} = \frac{1}{M_X} & \left[ \frac{1}{4}\epsilon_{abcde}(\kappa_u^+)_{ij}\{\Sigma_f^a(T^i)^{fb}(T^j)^{cd} + (T^i)^{ab}\Sigma_f^c(T^j)^{fd}\}H^e \right. \\
& + \frac{1}{4}\epsilon_{abcde}(\kappa_u^-)_{ij}\{\Sigma_f^a(T^i)^{fb}(T^j)^{cd} - (T^i)^{ab}\Sigma_f^c(T^j)^{fd}\}H^e \\
& + (\kappa_d)_{ij}(\overline{F}^i)_a\Sigma_b^a(T^j)^{bc}\overline{H}_c \\
& + (\overline{\kappa}_d)_{ij}(\overline{F}^j)_a(T^j)^{ab}\Sigma_b^c\overline{H}_c \\
& \left. + (\kappa_\nu)_{ij}\overline{N}^i(\overline{F}^j)_a\Sigma_b^aH^b \right], \tag{6}
\end{aligned}$$

where  $M_X$  is the cut-off scale which we take as the Planck mass  $M_P$ . We also assume that the elements of coupling matrices  $\kappa_u^\pm$ ,  $\kappa_d$ ,  $\overline{\kappa}_d$  and  $\kappa_\nu$  are smaller than  $O(1)$ . After  $\text{SU}(5)$  symmetry is broken, they give contributions of the order of  $\xi = v_G/M_X \approx 0.01$  to the Yukawa coupling constants of the MSSMRN as follows:

$$(y_u)_{ij} = (\lambda_u)_{ij} + \xi \left\{ \frac{1}{2}(\kappa_u^+)_{ij} + \frac{5}{6}(\kappa_u^-)_{ij} \right\}, \tag{7a}$$

$$(y_d)_{ij} = (\lambda_d)_{ij} + \xi \left\{ \frac{1}{3}(\kappa_d)_{ij} - \frac{1}{2}(\overline{\kappa}_d)_{ij} \right\}, \tag{7b}$$

$$(y_e)_{ij} = (\lambda_d^T)_{ij} + \xi \left\{ -\frac{1}{2}(\kappa_d^T)_{ij} - \frac{1}{2}(\overline{\kappa}_d^T)_{ij} \right\}, \tag{7c}$$

$$(y_\nu)_{ij} = (\lambda_\nu)_{ij} - \frac{\xi}{2}(\kappa_\nu)_{ij}. \tag{7d}$$

The naive GUT relation between the lepton and the down-type quark Yukawa coupling matrices in Eq. (5) is modified to

$$(y_e)_{ij} = (y_d)_{ji} + \frac{5}{6}\xi(\kappa_d)_{ji}. \tag{8}$$

With this small contribution from the higher dimensional operator, realistic mass relations between the down-type quarks and charged leptons can be incorporated in the model. In the following analysis we take  $(\kappa_u^+)_{ij} = (\kappa_u^-)_{ij} = (\overline{\kappa}_d)_{ij} = (\kappa_\nu)_{ij} = 0$  because they are not necessarily required to reproduce the realistic mass relations.

In the following, we show that new mixing angles are introduced at the GUT scale because of  $\kappa_d$ . Using  $\text{SU}(5)$  symmetry, we can rotate the generation indices of superfields in Eq. (2) so that the Yukawa coupling constants and the Majorana mass matrix are parameterized as follows:

$$(y_u)_{ij} = (V_{\text{CKM}}^T V_U^*)_i{}^k y_{uk} (V_{\text{CKM}})_j{}^k, \quad (9a)$$

$$(y_d)_{ij} = (V_D^*)_i{}^j y_{dj}, \quad (9b)$$

$$(y_e)_{ij} = (V_E^*)_i{}^j y_{ej}, \quad (9c)$$

$$(y_\nu)_{ij} = y_{\nu i} (V_L)^i{}_j, \quad (9d)$$

$$(M_\nu)_{ij} = (V_N^T)_i{}^k M_{\nu k} (V_N)_j{}^k, \quad (9e)$$

where  $V_U$ ,  $V_E$ ,  $V_D$  and  $V_N$  are unitary matrices and  $V_{\text{CKM}}$  is the CKM matrix at the GUT scale.  $y_{ui}$ ,  $y_{di}$ ,  $y_{ei}$ ,  $y_{\nu i}$ , and  $M_{\nu i}$  represent the eigenvalues of the Yukawa coupling matrices and the Majorana mass matrix. The GUT relation between the two Yukawa coupling constants is then given by

$$(V_D^*)_i{}^j y_{dj} - y_{ei} (V_E^\dagger)^i{}_j = \frac{5}{6} \xi (\kappa_d)_{ij}. \quad (10)$$

From this formula we can derive the following approximate relations for the 1-3 and 2-3 (3-1 and 3-2) elements of the mixing matrices because the Yukawa coupling constants of the first and second generations are much smaller than that of the third generation,

$$(V_D)^i{}_3 \approx \frac{5}{6} \frac{\xi}{y_b} (\kappa_d^*)_{i3}, \quad (11a)$$

$$(V_E)^i{}_3 \approx -\frac{5}{6} \frac{\xi}{y_\tau} (\kappa_d^\dagger)_{i3}, \quad (11b)$$

$$(V_E)^3{}_i \approx \frac{5}{6} \frac{\xi}{y_b} (V_D^T \kappa_d V_E)_{3i}, \quad (11c)$$

$$(V_D)^3{}_i \approx -\frac{5}{6} \frac{\xi}{y_\tau} (V_E^T \kappa_d^T V_D)_{3i}, \quad (11d)$$

for  $i = 1, 2$ . We can estimate  $\xi/y_b$  and  $\xi/y_\tau$  as

$$\frac{\xi}{y_b} \approx \frac{\xi}{y_\tau} \approx -\frac{\xi v \cos \beta}{\sqrt{2} m_\tau}, \quad \frac{v}{\sqrt{2}} = \sqrt{\langle H_1 \rangle^2 + \langle H_2 \rangle^2}, \quad (12)$$

where  $\beta$  is a vacuum angle of two Higgs vacuum expectation values ( $\tan \beta = \langle H_2^0 \rangle / \langle H_1^0 \rangle$ ). Assuming the condition  $(\kappa_d)_{ij} \lesssim O(1)$ , we can conclude that the magnitude of these elements are constrained to be smaller than  $(\tan \beta)^{-1}$  because lower  $\tan \beta$  region is excluded from Higgs boson search. On the other hand, 1-2 (2-1) element is not constrained from such a consideration. Motivated by this observation we assume the following form:

$$(V_D)^i_j = e^{i\gamma_D} \begin{pmatrix} e^{i\alpha_D} \cos \theta_D & -e^{-i\beta_D} \sin \theta_D & 0 \\ e^{i\beta_D} \sin \theta_D & e^{-i\alpha_D} \cos \theta_D & 0 \\ 0 & 0 & e^{i(-\gamma_D+\delta)} \end{pmatrix}, \quad (13a)$$

$$(V_E)^i_j = e^{i\gamma_E} \begin{pmatrix} e^{i\alpha_E} \cos \theta_E & -e^{-i\beta_E} \sin \theta_E & 0 \\ e^{i\beta_E} \sin \theta_E & e^{-i\alpha_E} \cos \theta_E & 0 \\ 0 & 0 & e^{i(-\gamma_E+\delta)} \end{pmatrix}. \quad (13b)$$

The antisymmetric part of the Yukawa matrix for the up-type quarks is also written by the coefficients of the dimension five operator as follows:

$$(V_U^*)_i^j y_{uj} - y_{ui} (V_U^\dagger)^i_j = \frac{5}{6} \xi (V_{\text{CKM}}^* \kappa_u^- V_{\text{CKM}}^\dagger)_{ij}. \quad (14)$$

Because we set  $(\kappa_u^-)_{ij} = 0$  for simplicity,  $(V_U)^i_j$  becomes  $e^{i\phi_{U,i}} \delta^i_j$  in our analysis.

The neutrino Yukawa coupling matrix and the Majorana mass matrix are constrained from the oscillation solutions of the atmospheric and solar neutrino anomalies. In the basis where the charged lepton mass matrix is diagonal, the neutrino mass matrix is written as follows:

$$(m_\nu)_{ij} = (V_{\text{MNS}}^*)_i^k m_{\nu k} (V_{\text{MNS}}^\dagger)^k_j, \quad (15)$$

where  $V_{\text{MNS}}$  is the Maki-Nakagawa-Sakata (MNS) matrix [22]. At the Majorana mass scale Eqs. (3) and (4) are solved as follows:

$$(V_N^*)_i^k y_{\nu k} (V_L)^k_j = \frac{1}{\langle H_2 \rangle} \sqrt{M_{\nu i}} (O_\nu^T)_i^k \sqrt{m_{\nu k}} (V_{\text{MNS}}^\dagger)^k_j, \quad (16)$$

where  $O_\nu$  is a complex orthogonal matrix which can not be determined from the low energy experiments. Although we neglect a running effect of the neutrino mass matrix between the low energy scale and the GUT scale in Eqs. (15) and (16), later we fully take account of this effect in the numerical calculation in Sec. IV.

### III. MINIMAL SUGRA AND THE MUON ANOMALOUS MAGNETIC MOMENT AND THE FCNC/LFV PROCESSES

In Subsection III A we first discuss the flavor mixing of squark and slepton mass matrices induced by the radiative correction due to the Yukawa coupling constants. In order to explain qualitative features we show the one-loop logarithmic terms for SUSY breaking parameters. In the numerical calculation in Sec. IV, however, we use the full renormalization group equation (RGE) and solve them numerically. In Subsection III B, we give a brief description on the SUSY contribution to the muon anomalous magnetic moment and various FCNC and LFV processes.

#### A. Minimal SUGRA and radiative corrections to the SUSY breaking parameters

The soft SUSY breaking terms of the MSSM are given by

$$\begin{aligned}
\mathcal{L}_{\text{soft}} = & -(m_Q^2)^i_j \tilde{Q}_i^\dagger \tilde{Q}^j - (m_U^2)_i^j \tilde{U}^{i*} \tilde{U}_j - (m_D^2)_i^j \tilde{D}^{i*} \tilde{D}_j \\
& -(m_L^2)^i_j \tilde{L}_i^\dagger \tilde{L}^j - (m_E^2)_i^j \tilde{E}^{i*} \tilde{E}_j - m_{H_2}^2 H_2^\dagger H_2 - m_{H_1}^2 H_1^\dagger H_1 \\
& - \left\{ (\tilde{y}_u)_{ij} \tilde{U}^{i*} \tilde{Q}^j H_2 + (\tilde{y}_d)_{ij} \tilde{D}^{i*} \tilde{Q}^j H_1 \right. \\
& \left. + (\tilde{y}_e)_{ij} \tilde{E}^{i*} \tilde{L}^j H_1 + \mu B H_1 H_2 + \text{H.c.} \right\} \\
& + \frac{1}{2} M_1 \overline{\tilde{B}} \tilde{B} + \frac{1}{2} M_2 \overline{\tilde{W}} \tilde{W} + \frac{1}{2} M_3 \overline{\tilde{G}} \tilde{G},
\end{aligned} \tag{17}$$

where  $\tilde{Q}^i$ ,  $\tilde{U}^{i*}$ ,  $\tilde{D}^{i*}$ ,  $\tilde{L}^i$  and  $\tilde{E}^{i*}$  are scalar components of  $Q^i$ ,  $\overline{U}^i$ ,  $\overline{D}^i$ ,  $L^i$  and  $\overline{E}^i$ , respectively. We use the same symbols as superfields for scalar components of the Higgs supermultiplets.  $\tilde{B}$ ,  $\tilde{W}$  and  $\tilde{G}$  are U(1), SU(2) and SU(3) gauginos, respectively. At the GUT scale, these soft SUSY breaking parameters are determined by the following SUSY breaking terms of the SU(5)RN SUSY GUT,

$$\begin{aligned}
\mathcal{L} = & -(m_T^2)^i_j (\tilde{T}_i^*)_{ab} (\tilde{T}^j)^{ab} - (m_{\tilde{F}}^2)_i^j (\tilde{F}_i^*)^a (\tilde{F}^j)_a - (m_{\tilde{N}}^2)^i_j \tilde{N}_i^* \tilde{N}^j \\
& -(m_H^2) H^*_a H^a - (m_{\tilde{H}}^2) \overline{\tilde{H}}^{*a} \tilde{H}_a \\
& - \left\{ \frac{1}{8} \epsilon_{abcde} (\tilde{\lambda}_u)_{ij} (\tilde{T}^i)^{ab} (\tilde{T}^j)^{cd} H^e + (\tilde{\lambda}_d)_{ij} (\tilde{F}^i)_a (\tilde{T}^j)^{ab} \tilde{H}_b \right.
\end{aligned}$$

$$\begin{aligned}
& +(\tilde{\lambda}_\nu)_{ij}\widetilde{\overline{N}}^i(\widetilde{\overline{F}}^j)_a H^a + \frac{1}{2}(\widetilde{M}_\nu)_{ij}\widetilde{\overline{N}}^i\widetilde{\overline{N}}^j + \text{H.c.} \Big\} \\
& -\frac{1}{M_X} \left[ \frac{1}{4}\epsilon_{abcde}(\tilde{\kappa}_u^+)_{ij} \left\{ \Sigma_f^a(\tilde{T}^i)^{fb}(\tilde{T}^j)^{cd} + (\tilde{T}^i)^{ab}\Sigma_f^c(\tilde{T}^j)^{fd} \right\} H^e \right. \\
& \quad + \frac{1}{4}\epsilon_{abcde}(\tilde{\kappa}_u^-)_{ij} \left\{ \Sigma_f^a(\tilde{T}^i)^{fb}(\tilde{T}^j)^{cd} - (\tilde{T}^i)^{ab}\Sigma_f^c(\tilde{T}^j)^{fd} \right\} H^e \\
& \quad + (\tilde{\kappa}_d)_{ij}(\widetilde{\overline{F}}^i)_a \Sigma_b^a(\tilde{T}^j)^{bc}\overline{H}_c \\
& \quad + (\tilde{\kappa}_d)_{ij}(\widetilde{\overline{F}}^j)_a (\tilde{T}^j)^b \Sigma_b^c \overline{H}_c \\
& \quad \left. + (\tilde{\kappa}_\nu)_{ij}\widetilde{\overline{N}}^i(\widetilde{\overline{F}}^j)_a \Sigma_b^a H^b + \text{H.c.} \right] \\
& + \frac{1}{2}M_5\widetilde{\overline{G}}_5\widetilde{G}_5, \tag{18}
\end{aligned}$$

where  $\tilde{T}^i$ ,  $\widetilde{\overline{F}}^i$  and  $\widetilde{\overline{N}}^i$  are scalar components of  $T^i$ ,  $\overline{F}^i$  and  $\overline{N}^i$  and  $\widetilde{G}_5$  represents SU(5) gaugino. We assume the minimal supergravity scenario for the origin of SUSY breaking and set the following boundary conditions for the SUSY breaking parameters at the Planck scale,

$$(m_T^2)^i{}_j = (m_F^2)^i{}_j = (m_N^2)^i{}_j = m_0^2\delta_j^i, \tag{19a}$$

$$(\tilde{\lambda})_{ij} = m_0 A_0(\lambda)_{ij}, \quad (\lambda = \lambda_u, \lambda_d, \lambda_\nu), \tag{19b}$$

$$(\tilde{\kappa})_{ij} = m_0(A_0 + \Delta A_0)(\kappa)_{ij}, \quad (\kappa = \kappa_u^\pm, \kappa_d, \overline{\kappa}_d, \kappa_\nu), \tag{19c}$$

$$M_5 = M_0. \tag{19d}$$

If we ignore radiative corrections from the gauge and Yukawa coupling constants and assume  $\Delta A_0 = 0$ , the soft SUSY breaking terms are given by

$$(m_Q^2)^i{}_j = (m_L^2)^i{}_j = (m_U^2)_i{}^j = (m_E^2)_i{}^j = (m_D^2)_i{}^j = m_0^2\delta_i^j, \tag{20a}$$

$$(\tilde{y})_{ij} = m_0 A_0(y)_{ij}, \quad (y = y_u, y_d, y_e). \tag{20b}$$

Then LFV processes are forbidden and SUSY contributions to FCNC processes are suppressed. We consider  $\Delta A_0 \neq 0$  case later.

Radiative corrections between the Planck scale and the EW scale modify the above structure of the soft SUSY breaking terms. In particular, the corrections from the Yukawa

coupling constants associated with the colored Higgs supermultiplets and right-handed neutrino supermultiplets are important because they have different flavor structure from the Yukawa coupling constants of the MSSM.

Let us estimate these corrections using approximate formulas only considering logarithmic terms to see qualitative features of FCNC/LFV processes in the model. The Yukawa couplings including colored Higgs supermultiplets are parameterized as follows:

$$\begin{aligned}\mathcal{W}_C = & -(y_{CR})_{ij}H_C\overline{U}^i\overline{E}^j - \frac{1}{2}(y_{CL})_{ij}H_CQ^iQ^j \\ & -(y_{\overline{C}R})_{ij}\overline{H}_C\overline{D}^i\overline{U}^j - (y_{\overline{C}L})_{ij}\overline{H}_CL^iQ^j + (y_{CN})_{ij}H_C\overline{N}^i\overline{D}^j.\end{aligned}\quad (21)$$

It is convenient to work in the basis where the down-type quark and charged lepton mass matrices are diagonal,

$$(y_u)_{ij} = y_{ui}(V_{\text{CKM}})^i{}_j, \quad (22a)$$

$$(y_d)_{ij} = y_{di}\delta_j^i, \quad (22b)$$

$$(y_e)_{ij} = y_{ei}\delta_j^i, \quad (22c)$$

$$(y_\nu)_{ij} = y_{\nu i}(V_L)^i{}_j. \quad (22d)$$

In this basis, Yukawa coupling matrices in Eq. (21) are given by

$$(y_{CR})_{ij} = y_{ui}(V_{\text{CKM}}V_E)^i{}_j, \quad (23a)$$

$$(y_{CL})_{ij} = \frac{1}{2}\{(V_{\text{CKM}}^T)_i{}^je^{i\phi_{Uj}}y_{uj} + e^{i\phi_{Ui}}y_{ui}(V_{\text{CKM}})^i{}_j\}, \quad (23b)$$

$$(y_{\overline{C}R})_{ij} = y_{di}e^{i\phi_{Ui}}\delta_j^i, \quad (23c)$$

$$(y_{\overline{C}L})_{ij} = y_{ei}(V_E^\dagger)^i{}_j, \quad (23d)$$

$$(y_{CN})_{ij} = y_{\nu i}(V_LV_D)^i{}_j. \quad (23e)$$

The radiative corrections to squark and slepton mass matrices from these Yukawa coupling constants are approximated as follows:

$$\begin{aligned}\Delta m_Q^2 \approx & -2\left(y_u^\dagger y_u + 2y_{CL}^\dagger y_{CL} + y_d^\dagger y_d + y_{\overline{C}L}^\dagger y_{\overline{C}L}\right)(3 + |A_0|^2)m_0^2 t_G \\ & -2\left(y_u^\dagger y_u + y_d^\dagger y_d\right)(3 + |A_0|^2)m_0^2 t_W,\end{aligned}\quad (24a)$$

$$\begin{aligned}\Delta m_U^2 \approx & -2 \left( 2y_u y_u^\dagger + y_{CR} y_{CR}^\dagger + 2y_{CR}^T y_{CR}^* \right) (3 + |A_0|^2) m_0^2 t_G \\ & - 4y_u y_u^\dagger (3 + |A_0|^2) m_0^2 t_W,\end{aligned}\quad (24b)$$

$$\begin{aligned}\Delta m_E^2 \approx & -2 \left( 2y_e y_e^\dagger + 3y_{CR}^T y_{CR}^* \right) (3 + |A_0|^2) m_0^2 t_G \\ & - 4y_e y_e^\dagger (3 + |A_0|^2) m_0^2 t_W,\end{aligned}\quad (24c)$$

$$\begin{aligned}\Delta m_D^2 \approx & -2 \left( 2y_d y_d^\dagger + 2y_{CR}^T y_{CR}^\dagger + y_{CN}^T y_{CN}^* \right) (3 + |A_0|^2) m_0^2 t_G \\ & - 4y_d y_d^\dagger (3 + |A_0|^2) m_0^2 t_W,\end{aligned}\quad (24d)$$

$$\begin{aligned}\Delta m_L^2 \approx & -2 \left( y_e^\dagger y_e + 3y_{CL}^* y_{CL}^T + y_\nu^\dagger y_\nu \right) (3 + |A_0|^2) m_0^2 t_G \\ & - 2y_e^\dagger y_e (3 + |A_0|^2) m_0^2 t_W - 2y_\nu^\dagger y_\nu (3 + |A_0|^2) m_0^2 t_R,\end{aligned}\quad (24e)$$

where we only take account of logarithmic terms so that  $t_G = \frac{1}{(4\pi)^2} \ln(\frac{M_P}{M_G})$ ,  $t_R = \frac{1}{(4\pi)^2} \ln(\frac{M_G}{M_R})$  and  $t_W = \frac{1}{(4\pi)^2} \ln(\frac{M_G}{M_{\text{SUSY}}})$ .  $M_{\text{SUSY}}$  is a characteristic mass scale of the SUSY particles and identified to the EW scale. The off-diagonal elements of the above formulas are sources of the LFV and FCNC processes. Keeping only possible large Yukawa coupling constants, the off-diagonal elements of the mass matrices are approximated as follows:

$$\begin{aligned}(m_Q^2)_j^i \approx & -2(V_{\text{CKM}}^\dagger)^i{}_3 y_t^2 (V_{\text{CKM}})^3{}_j (3 + |A_0|^2) m_0^2 (t_G + t_W) \\ & - \left\{ (V_{\text{CKM}}^\dagger)^i{}_3 y_t^2 \delta_j^3 + \delta^i{}_3 y_t^2 (V_{\text{CKM}})^3{}_j \right. \\ & \left. + (V_{\text{CKM}}^\dagger)^i{}_3 y_t^2 (V_{\text{CKM}})^3{}_j \right\} (3 + |A_0|^2) m_0^2 t_G, \quad (i \neq j),\end{aligned}\quad (25a)$$

$$(m_E^2)_i^j \approx -6(V_E^T V_{\text{CKM}}^T)_i{}^3 y_t^2 (V_{\text{CKM}}^* V_E^*)_3^j (3 + |A_0|^2) m_0^2 t_G, \quad (i \neq j), \quad (25b)$$

$$(m_D^2)_i^j \approx -2(V_D^T V_L^T)_i{}^k y_{\nu k}^2 (V_L^* V_D^*)_k^j (3 + |A_0|^2) m_0^2 t_G, \quad (i \neq j), \quad (25c)$$

$$(m_L^2)_j^i \approx -2(V_L^\dagger)^i{}_k y_{\nu k}^2 (V_L)^k{}_j (3 + |A_0|^2) m_0^2 (t_G + t_R), \quad (i \neq j). \quad (25d)$$

$(m_Q^2)_j^i$  corresponds to the flavor mixing due to the large top Yukawa coupling constant which already exists within the MSSM based on the minimal SUGRA.  $(m_E^2)_i^j$  receives radiative correction from the up-type Yukawa coupling constant between the Planck scale and the GUT scale. This is a well-known mechanism to induce LFV processes in the SUSY GUT [4]. We notice that the following important features.

- There are flavor mixings in the right-handed down-type squark and the left-handed

slepton sectors. These mixings are absent in the minimal SUGRA model without right-handed neutrino supermultiplet.

- Because  $V_L$  can be related to the MNS matrix, large mixing is possible.
- The main effect of the higher dimensional operator under assumption of Eq. (13) is only rotating the basis of light fermions between  $d_R$  and  $s_R$ ,  $e_R$  and  $\mu_R$ . For each of these mixings the rotation is described by one parameter  $\theta_D$  in  $V_D$  or  $\theta_E$  in  $V_E$ .

In the above discussion, we only considered the radiative correction to squarks and slepton mass matrices, however, the trilinear scalar coupling constants,  $\tilde{y}_u$ ,  $\tilde{y}_d$  and  $\tilde{y}_e$  also receive corrections as follows:

$$(\tilde{y}_u)_{ij} \approx m_0 A_u y_{ui} (V_{\text{CKM}})^i_j - \frac{m_0 A_0}{3 + |A_0|^2} \frac{(\Delta m_U^2)_i^k y_{uk} (V_{\text{CKM}})^k_j + y_{ui} (V_{\text{CKM}})^i_k (\Delta m_Q^2)^k_j}{m_0^2}, \quad (26a)$$

$$(\tilde{y}_d)_{ij} \approx m_0 A_d y_{di} \delta_j^i - \frac{m_0 A_0}{3 + |A_0|^2} \frac{(\Delta m_D^2)_i^j y_{dj} + y_{di} (\Delta m_Q^2)^i_j}{m_0^2} - \frac{2}{5} m_0 \Delta A \left\{ y_{di} \delta_j^i - (V_D^T)_i^k y_{ek} (V_E^\dagger)^k_j \right\}, \quad (26b)$$

$$(\tilde{y}_e)_{ij} \approx m_0 A_e y_{ei} \delta_j^i - \frac{m_0 A_0}{3 + |A_0|^2} \frac{(\Delta m_E^2)_i^j y_{ej} + y_{ei} (\Delta m_L^2)^i_j}{m_0^2} - \frac{3}{5} m_0 \Delta A \left\{ y_{ei} \delta_j^i - (V_E^T)_i^k y_{dk} (V_D^\dagger)^k_j \right\}, \quad (26c)$$

where  $A_u$ ,  $A_d$ ,  $A_e$  and  $\Delta A$  are given by

$$A_u \approx A_0 - \frac{192}{5} g_5^2 \frac{M_0}{m_0} t_G - \frac{276}{15} g_5^2 \frac{M_0}{m_0} t_W + 3y_t^2 (t_G + t_W) + \sum_{i=1}^3 y_{\nu_i}^2 (t_G + t_R), \quad (27a)$$

$$A_d \approx A_0 - \frac{168}{5} g_5^2 \frac{M_0}{m_0} t_G - \frac{88}{5} g_5^2 \frac{M_0}{m_0} t_W, \quad (27b)$$

$$A_e \approx A_0 - \frac{168}{5} g_5^2 \frac{M_0}{m_0} t_G - \frac{48}{5} g_5^2 \frac{M_0}{m_0} t_W, \quad (27c)$$

$$\Delta A \approx -20 g_5^2 \frac{M_0}{m_0} t_G. \quad (27d)$$

The second terms in the right-hand side of Eqs. (26) are induced by the radiative corrections from the Yukawa interactions. The third terms in Eqs. (26b) and (26c) come from the higher dimensional operators. They break proportionality between the trilinear scalar coupling matrix and the corresponding Yukawa coupling matrix and generate flavor mixings in the left-right mixing mass matrices of squarks and sleptons after the EW symmetry breaking. If  $\Delta A_0 \neq 0$  in Eq. (19c), we have an extra contribution,  $\Delta A_0$  to Eq. (27d) and there are corrections of order  $m_0^2 A_0 \Delta A_0 \xi t_G$  to Eqs. (25) and corrections of order  $m_0 \Delta A_0 \xi t_X$  ( $X = G, R, W$ ) to Eqs. (26). Notice that even if we assume  $\Delta A_0 = 0$  at the Planck scale  $\Delta A$  is induced by the gauge interaction as shown in Eq. (27d) because the renormalization of  $\tilde{\lambda}_d$  and  $\tilde{\kappa}_d$  are different due to the wave-function renormalization of  $\Sigma$ . We therefore expect analysis with  $\Delta A_0 = 0$  gives us a qualitative feature for general cases.

### B. The muon anomalous magnetic moment, FCNC and LFV processes

Let us discuss the muon anomalous magnetic moment, FCNC and LFV processes in the model according to the approximations of the previous section. In the following we make a simplification in the neutrino sector to estimate possible deviations from the SM in the FCNC/LFV processes. We assume the Majorana masses of the right-handed neutrinos are universal at the Majorana mass scale  $M_R$  as  $(M_\nu)_{ij} = \delta_{ij} M_R$ . We also neglect any CP violating phase in the model except for the Kobayashi-Maskawa phase and assume that  $V_N$ ,  $V_L$ ,  $O_\nu$  and  $V_{\text{MNS}}$  are real matrices and  $\alpha_{D,E} = \beta_{D,E} = \gamma_{D,E} = \delta = 0$  in Eq. (13) and  $\phi_{U_i} = 0$  in Eq. (23). If we include these phases, new contributions to the electron and neutron electric dipole moments (EDMs) are induced so that we have to take into account constraints to SUSY parameters from the upper bound of the EDMs. In the numerical calculation we evaluate these EDMs and check that these constraints are satisfied in the case that new CP phases are set to vanish. With the above simplification, the mixing matrix  $V_L$  and the neutrino Yukawa coupling can be related to the low energy observables according to Eq. (16),

$$V_L = V_{\text{MNS}}^\dagger, \quad y_{\nu i} = \sqrt{M_R m_{\nu i}} / \langle H_2 \rangle. \quad (28)$$

We parameterize the MNS matrix assuming maximal mixing for the atmospheric neutrino oscillation as follows:

$$V_{\text{MNS}} = \begin{pmatrix} \cos \theta_{\text{sun}} & \sin \theta_{\text{sun}} & 0 \\ -\frac{\sin \theta_{\text{sun}}}{\sqrt{2}} & \frac{\cos \theta_{\text{sun}}}{\sqrt{2}} & \frac{1}{\sqrt{2}} \\ \frac{\sin \theta_{\text{sun}}}{\sqrt{2}} & -\frac{\cos \theta_{\text{sun}}}{\sqrt{2}} & \frac{1}{\sqrt{2}} \end{pmatrix}, \quad (29)$$

where  $\theta_{\text{sun}}$  is the mixing angle for the solar neutrino oscillation. We assume the 1-3 element of the MNS matrix is zero in our analysis because it is known to be small from the result of the CHOOZ experiment [23]. We will comment on the nonzero case later. We assume the hierarchical pattern of neutrino mass, namely  $m_{\nu 1} < m_{\nu 2} \ll m_{\nu 3}$ . From the following relation,

$$m_{\nu 2}^2 = \Delta m_{\text{sun}}^2 + m_{\nu 1}^2, \quad m_{\nu 3}^2 = \Delta m_{\text{atm}}^2 + m_{\nu 2}^2, \quad (30)$$

where  $\Delta m_{\text{sun}}^2$  and  $\Delta m_{\text{atm}}^2$  are the mass differences of solar and atmospheric neutrino oscillation,  $m_{\nu 3}$  and  $m_{\nu 2}$  are determined once we fix  $m_{\nu 1}$ . Then using Eq. (28) we can calculate  $y_{\nu i}$  for a fixed value of  $M_R$ .

### 1. The muon anomalous magnetic moment

We consider the SUSY contribution to the muon anomalous magnetic moment [8,21,24,25]. The muon anomalous magnetic moment  $a_\mu$  is defined by the following effective Lagrangian:

$$\mathcal{L}^{g-2} = \frac{1}{2} \left( \frac{e}{2m_\mu} \right) a_\mu \bar{\mu} \sigma^{\alpha\beta} \mu F_{\alpha\beta}, \quad (31)$$

where  $e$  is the positron charge,  $m_\mu$  is the muon mass,  $F_{\alpha\beta}$  is the electromagnetic field tensor and  $\sigma_{\alpha\beta} = i[\gamma_\alpha, \gamma_\beta]/2$ . The SUSY contribution to  $a_\mu$  ( $\equiv a_\mu^{\text{SUSY}}$ ) is obtained from the flavor diagonal parts of photon-penguin diagrams including smuon-neutralino and sneutrino-chargino.  $a_\mu^{\text{SUSY}}$  depends on the slepton mass and the neutralino/chargino mass and mixing, but it is rather insensitive to the flavor mixing of the slepton sector. Therefore we expect

$a_\mu^{\text{SUSY}}$  is almost the same as a result in the minimal SUGRA model. In the MSSM based on the minimal SUGRA, it is known that the main contribution comes from the sneutrino-chargino diagram which contains a component proportional to  $\mu \tan \beta$  [25]. Then  $a_\mu^{\text{SUSY}}$  preferred by the recent results from BNL E821 experiment is achieved in the large  $\tan \beta$  region of the parameter space. In this region the sign of  $a_\mu^{\text{SUSY}}$  is correlated to the branching ratio of  $b \rightarrow s \gamma$  through the sign of the Higgsino mass parameter  $\mu$  so that  $a_\mu^{\text{SUSY}}$  is positive when  $b \rightarrow s \gamma$  is suppressed and negative when  $b \rightarrow s \gamma$  is enhanced.

## 2. $\mu \rightarrow e \gamma, \tau \rightarrow \mu \gamma$

We consider LFV decays of charged leptons. Radiative decays of charged leptons occur through photon-penguin diagrams including sleptons, neutralinos and charginos. The effective Lagrangian for these processes is described as follows:

$$\mathcal{L}^{\text{LFV}} = -\frac{4G_F}{\sqrt{2}} \left\{ m_{ei} A_R^{ij} (\overline{l_{Ri}} \sigma^{\mu\nu} l_{Lj}) F_{\mu\nu} + m_{ei} A_L^{ij} (\overline{l_{Li}} \sigma^{\mu\nu} l_{Rj}) F_{\mu\nu} \right\} + \text{H.c.} \quad (i > j), \quad (32)$$

where  $G_F$  is the Fermi constant and  $i, j$  denote generation indices.  $A_R^{ij}$  corresponds to the amplitude for  $l_i^+ \rightarrow l_j^+ \gamma_R$  and  $A_L^{ij}$  for  $l_i^+ \rightarrow l_j^+ \gamma_L$ . The branching ratios are calculated from these amplitudes as  $\text{B}(l_i^+ \rightarrow l_j^+ \gamma) = 384\pi^2 (|A_R^{ij}|^2 + |A_L^{ij}|^2)$ .

For  $\mu \rightarrow e \gamma$ , it is known that if both left-handed and right-handed sectors have flavor mixing, there are the diagrams which have an enhancement factor  $m_\tau$  as shown in Fig. 1 [10,16,17]. In our model we find that diagrams corresponding to Figs. 2 and 3 also give large contributions. The flavor mixing in the left-right mixing term in Fig. 3 is induced by renormalization between the Planck and GUT scale as shown in Eq. (26c). Approximate formulas for  $A_R^{21}$  and  $A_L^{21}$  from these contributions are given by

$$A_R^{21} \approx \frac{1}{\sqrt{2}} \sin 2\theta_{\text{sun}} (y_{\nu 2}^2 - y_{\nu 1}^2) y_t^2 \left[ \left\{ (V_{\text{CKM}})^3_1 \sin \theta_E + (V_{\text{CKM}})^3_2 \cos \theta_E \right\} \frac{m_\tau}{m_\mu} a_2^n - a^c \right] - \cos \theta_E \sin \theta_D a_1^n, \quad (33a)$$

$$A_L^{21} \approx -(y_{\nu 3}^2 - y_{\nu 2}^2) y_t^2 \left\{ (V_{\text{CKM}})^3_1 \cos \theta_E - (V_{\text{CKM}})^3_2 \sin \theta_E \right\} \frac{m_\tau}{m_\mu} a_2^n + \sin \theta_E \cos \theta_D a_1^n, \quad (33b)$$

where we explicitly show  $\theta_{\text{sun}}$ ,  $y_{\nu_i}$ ,  $y_t$ ,  $\theta_E$  and  $\theta_D$  dependence.  $a_2^n$ ,  $a^c$  and  $a_1^n$  are functions of the slepton masses and the chargino and neutralino masses and mixings. These contributions correspond to Fig. 1, Fig. 2 and Fig. 3, respectively. The explicit forms of the functions are given in Appendix B. Because  $(V_{\text{CKM}})_2^3 \gg (V_{\text{CKM}})_1^3$ , the mixing angle  $\theta_E$  can enhance the amplitude  $A_L^{21}$  compared to the case  $\theta_E = 0$ .

The ratio of the magnitudes of  $A_L^{21}$  and  $A_R^{21}$  can be measured by the P-odd asymmetry of  $\mu \rightarrow e \gamma$  process,  $A(\mu \rightarrow e \gamma)$  [26]. With the help of initial muon polarization, we define  $A(\mu \rightarrow e \gamma)$  as follows:

$$\frac{dB(\mu^+ \rightarrow e^+ \gamma)}{d \cos \theta} = \frac{1}{2} B(\mu^+ \rightarrow e^+ \gamma) \{1 + A(\mu^+ \rightarrow e^+ \gamma) P \cos \theta\}, \quad (34a)$$

$$A(\mu^+ \rightarrow e^+ \gamma) = \frac{|A_L^{21}|^2 - |A_R^{21}|^2}{|A_L^{21}|^2 + |A_R^{21}|^2}, \quad (34b)$$

where  $P$  is the polarization of initial  $\mu^+$  and  $\theta$  is the angle between the polarization and the momentum of the decay positron. For  $\tau \rightarrow \mu \gamma$ , a similar P-odd asymmetry can be measured in the  $e^+ e^- \rightarrow \tau^+ \tau^-$  process using spin correlation of the  $\tau$  pair [27].

### 3. $b \rightarrow s \gamma$

The  $\Delta B = 1$  FCNC effective Lagrangian for the radiative  $B$  decay is written as follows:

$$\mathcal{L}^{\Delta S=1} = -\frac{4G_F}{\sqrt{2}} \{C'_7(\overline{s}_R \sigma^{\mu\nu} b_L) F_{\mu\nu} + C_7(\overline{s}_L \sigma^{\mu\nu} b_R) F_{\mu\nu}\} + \text{H.c.} \quad (35)$$

In the SM case, the process occurs through photon penguin diagrams which exchange a  $W$  boson as Fig. 4 and  $C'_7$  is suppressed by a factor of  $m_s/m_b$  compared to  $C_7$ . In the minimal SUGRA model without the right-handed neutrino supermultiplets, the flavor mixing in the squark mass matrices only appears in that of left-handed squark and the same argument can be applied. In the present model, however, a gluino exchanging diagram (Fig. 5) can give a large contribution to  $C'_7$  because of the new flavor mixing in the right-handed down-type squarks  $(m_D^2)_2^3$ .

If  $C'_7$  has a similar magnitude as  $C_7$ , the time-dependent CP asymmetry of  $B \rightarrow M_s \gamma$  may be observed where  $M_s$  is a CP eigenstate which includes a strange quark such as  $K_1$  ( $\rightarrow K_S \rho^0$ ) or  $K^*$  ( $\rightarrow K_S \pi^0$ ) [19,28]. The asymmetry is defined as follows:

$$\frac{\Gamma(t) - \bar{\Gamma}(t)}{\Gamma(t) + \bar{\Gamma}(t)} = \eta A_{CP}(B \rightarrow M_s \gamma) \sin \Delta m_{B_d} t, \quad A_{CP}(B \rightarrow M_s \gamma) = \frac{2\text{Im}(e^{-i\theta_B} C_7 C'_7)}{|C_7|^2 + |C'_7|^2}, \quad (36)$$

where  $\Gamma(t)$  ( $\bar{\Gamma}(t)$ ) is the decay width of  $B^0(t) \rightarrow M_s \gamma$  ( $\bar{B}^0(t) \rightarrow M_s \gamma$ ).  $\eta$  is +1 if  $M_s$  is a CP even state and -1 if  $M_s$  is a CP odd state.  $\theta_B$  is the phase of  $B_d - \bar{B}_d$  mixing amplitude  $M_{12}(B_d)$  which defined below in Eq. (40). In the SM case, this asymmetry is only a few percent, however, it may be considerably enhanced by the new SUSY contribution to  $C'_7$ .

#### 4. $\varepsilon_K$

$K^0 - \bar{K}^0$  mixing is described by the  $\Delta S = 2$  FCNC effective Lagrangian. The general form is given by

$$\begin{aligned} \mathcal{L}^{\Delta S=2} = & -\frac{8G_F}{\sqrt{2}} \left\{ \frac{1}{2} g_R^V (\bar{d}_R^\alpha \gamma^\mu s_{R\alpha}) (\bar{d}_R^\beta \gamma_\mu s_{R\beta}) + \frac{1}{2} g_L^V (\bar{d}_L^\alpha \gamma^\mu s_{L\alpha}) (\bar{d}_L^\beta \gamma_\mu s_{L\beta}) \right. \\ & + \frac{1}{2} g_{RR}^S (\bar{d}_L^\alpha s_{R\alpha}) (\bar{d}_L^\beta s_{R\beta}) + \frac{1}{2} g_{LL}^S (\bar{d}_R^\alpha s_{L\alpha}) (\bar{d}_R^\beta s_{L\beta}) \\ & + \frac{1}{2} g_{RR}^{S'} (\bar{d}_L^\alpha s_{R\beta}) (\bar{d}_L^\beta s_{R\alpha}) + \frac{1}{2} g_{LL}^{S'} (\bar{d}_R^\alpha s_{L\beta}) (\bar{d}_R^\beta s_{L\alpha}) \\ & \left. + g_{RL}^S (\bar{d}_L^\alpha s_{R\alpha}) (\bar{d}_R^\beta s_{L\beta}) + g_{RL}^{S'} (\bar{d}_L^\alpha s_{R\beta}) (\bar{d}_R^\beta s_{L\alpha}) \right\} + \text{H.c.}, \quad (37) \end{aligned}$$

where  $\alpha$  and  $\beta$  denote color indices. The explicit forms of effective coupling constants in the above formula are given in Appendix C. The CP violation parameter in  $K^0 - \bar{K}^0$  mixing,  $\varepsilon_K$  is calculated from the above formula as follows:

$$\varepsilon_K = \frac{e^{\frac{\pi}{4}i} \text{Im}\{M_{12}(K)\}}{\sqrt{2} \Delta m_K}, \quad M_{12}(K) = -\frac{\langle K^0 | \mathcal{L}^{\Delta S=2} | \bar{K}^0 \rangle}{2m_K}. \quad (38)$$

In the case of the SM, the process occurs through a box diagram in which two  $W$  bosons are exchanged between the down-type quarks (Fig. 6) so that it is dominated by the  $g_L^V$ -term. However, we have a new flavor mixing,  $(m_D^2)_1^2$  in the right-handed down-type squark sector. We can draw gluino exchanging diagrams as Fig. 7 which include the CP violating phase

of CKM matrix in  $(m_Q^2)_2^1$  on one of the squark lines and large flavor mixing in  $(m_D^2)_1^2$  on the other. These diagrams contribute to the coupling constants  $g_{RL}^S$  and  $g_{RL}^{S'}$ . In the actual numerical calculation we first derive the effective Lagrangian at the energy scale  $M_{\text{SUSY}}$ . According to the reference [29], we include QCD corrections and derive the effective Lagrangian at the hadronic scale. The matrix elements for the dominant operators are parameterized as follows:

$$\langle K^0 | (\bar{d}_L^\alpha \gamma^\mu s_{L\alpha}) (\bar{d}_L^\beta \gamma_\mu s_{L\beta}) | \bar{K}^0 \rangle = \frac{2}{3} m_K^2 f_K^2 B_K, \quad (39a)$$

$$\langle K^0 | (\bar{d}_R^\alpha s_{L\alpha}) (\bar{d}_L^\beta s_{R\beta}) | \bar{K}^0 \rangle = \frac{1}{2} \left( \frac{m_K}{m_s + m_d} \right)^2 m_K^2 f_K^2 (B_K)_{RL}^S, \quad (39b)$$

$$\langle K^0 | (\bar{d}_R^\alpha s_{L\beta}) (\bar{d}_L^\beta s_{R\alpha}) | \bar{K}^0 \rangle = \frac{1}{6} \left( \frac{m_K}{m_s + m_d} \right)^2 m_K^2 f_K^2 (B_K)_{RL}^{S'}, \quad (39c)$$

where  $B_K$ ,  $(B_K)_{RL}^S$  and  $(B_K)_{RL}^{S'}$  are bag parameters calculated by the lattice QCD method. Because there is a large enhancement factor of order  $(m_K/m_s)^2$  in the matrix elements and large mixings originate from the MNS matrix, SUSY contribution to  $\varepsilon_K$  is expected to be large in this model.

### 5. $B_d - \bar{B}_d/B_s - \bar{B}_s$ mixing

The  $\Delta B = 2$  effective Lagrangians for  $B_d - \bar{B}_d$  and  $B_s - \bar{B}_s$  mixings are parameterized in the same manner as  $K^0 - \bar{K}^0$  mixing. For  $B_d - \bar{B}_d$  mixing, it is obtained by replacing the strange quark with the bottom quark in Eq. (37). For  $B_s - \bar{B}_s$  mixing, we further replace the down quark by the strange quark. The mass difference of  $B_d - \bar{B}_d$  mixing,  $\Delta m_{B_d}$  is calculated from the effective Lagrangian as follows:

$$\Delta m_{B_d} = 2 |M_{12}(B_d)|, \quad M_{12}(B_d) = - \frac{\langle B_d^0 | \mathcal{L}^{\Delta B=2} | \bar{B}_d^0 \rangle}{2m_{B_d}}. \quad (40)$$

In the SM case, this process occurs through the  $W$  boson exchanging diagram and the  $g_L^V$ -term gives a dominant contribution. In the present case, there are new diagrams as shown in Fig. 8 which contain the new flavor mixing in  $(m_D^2)_1^3$  on one of the down-type squark lines or on the both of them. The former contributes to  $g_{RL}^S$  and  $g_{RL}^{S'}$  and the latter to  $g_R^V$ . Unlike

$K^0 - \bar{K}^0$  mixing, the scalar-scalar matrix elements do not have an enhancement factor for  $B_d - \bar{B}_d$  mixing case because  $m_{B_d}/m_b$  is  $O(1)$ . Similar argument holds for  $B_s - \bar{B}_s$  mixing. In the numerical calculation we use next leading order QCD correction for  $g_R^V$  and  $g_L^V$  and leading order QCD formulas for other contributions [29] and bag parameters are calculated by the lattice QCD. Numerical values are shown later.

#### IV. RESULTS OF NUMERICAL CALCULATIONS

In this section we present our numerical results on the FCNC/LFV processes in the SU(5)RN SUSY GUT.

In the present analysis we assume that the SUSY breaking terms have the minimal SUGRA type boundary condition at the Planck scale and that the Kähler potential is flat. Adopting the simplifications discussed in the previous section, we have the following input parameters.

- Parameters at the Planck scale: the universal scalar mass  $m_0$ , the universal gaugino mass  $M_0$ , and the universal coefficient for the scalar couplings  $A_0$ .
- Parameters at the GUT scale: mixing angles  $\theta_D$  and  $\theta_E$ .
- Parameter at the right-handed neutrino mass scale: Majorana mass of the right-handed neutrino  $M_R$ , which is also used as the matching scale.
- Parameters at the EW scale: quark, lepton and neutrino masses, mixing matrices  $V_{\text{CKM}}$  and  $V_{\text{MNS}}$ ,  $\tan\beta$  and the sign of the Higgsino mass parameter  $\mu$  in Eq. (2).

Throughout the following calculation, we fix some of the parameters as shown in Table I. We consider two cases for the neutrino parameters, corresponding to the large mixing angle (LMA) and the small mixing angle (SMA) MSW solutions of the solar neutrino anomaly. The parameters we used in the neutrino sector for each case are given in Table II. For  $M_R$  and  $\tan\beta$ , we take several cases to see the dependences (see Table III). SUSY breaking parameters  $m_0$ ,  $M_0$  and  $A_0$  are varied and  $\Delta A_0$  is fixed to zero.

With these parameters, we solve the RGEs of the mass parameters and the coupling constants between the Planck and the EW scale taking all the flavor mixings into account. Detail of our method is explained in Appendix A. The magnitude of  $\mu$  is determined by the radiative EW symmetry breaking condition, in which the minimum of the one-loop effective potential for the Higgs fields is evaluated. Then we obtain all the masses and mixings of the SUSY particles at the EW scale and calculate the FCNC/LFV observables as functions of above parameters. We calculate the following quantities:

- The SUSY contribution to the muon anomalous magnetic moment  $a_\mu^{\text{SUSY}}$ ;
- Branching ratios of  $b \rightarrow s \gamma$ ,  $\mu \rightarrow e \gamma$  and  $\tau \rightarrow \mu \gamma$ ;
- P-odd asymmetry of  $\mu \rightarrow e \gamma$ ;
- $B^0 - \bar{B}^0$  mass splittings  $\Delta m_{B_d}$  and  $\Delta m_{B_s}$ ;
- CP violation parameter  $\varepsilon_K$ ;
- Time-dependent CP asymmetries of  $B \rightarrow M_s \gamma$  and  $B \rightarrow J/\psi K_S$ .

In order to find the allowed region in the parameter space, we impose the constraints from the experimental results of the direct searches of SUSY particles [30] and Higgs bosons [31] and the measurements of  $B(b \rightarrow s \gamma)$  [32]. Also it turns out that, in some parameter region, the branching ratio of  $\mu \rightarrow e \gamma$  exceeds the present upper limit and hence this process already gives an important constraint on the parameter space. We discuss the constraints from the measured values of  $\varepsilon_K$  and  $\Delta m_{B_d}$  and the lower bound of  $\Delta m_{B_s}$  later, since it depends on the CKM parameters, namely  $|V_{ub}|$  and  $\delta_{13}$  [33].

#### A. $\theta_E$ and $\theta_D$ dependence of $\mu \rightarrow e \gamma$ and $\varepsilon_K$

Let us first discuss the  $\theta_E$  and  $\theta_D$  dependence of the  $\mu \rightarrow e \gamma$  decay and  $\varepsilon_K$ .

As given in Eq. (33), the decay amplitudes  $A_R^{21}$  and  $A_L^{21}$  depend on  $\theta_E$  and  $\theta_D$  differently, so that both of the branching ratio and P-odd asymmetry are affected. In Fig. 9 we show

$B(\mu \rightarrow e \gamma)$  and  $A(\mu \rightarrow e \gamma)$  as functions of  $\theta_E$  and  $\theta_D$ . The shaded regions are excluded by the upper bound of  $B(\mu \rightarrow e \gamma)$  [34]. Here we take the LMA case for the neutrino parameters,  $M_R = 4 \times 10^{13}$  GeV,  $\tan \beta = 20$ ,  $\mu > 0$ . SUSY breaking parameters are also fixed as  $M_0 = 300$  GeV,  $A_0 = 0$  and  $m_0 = 0, 300, 600, 900$  GeV. For the fixed  $\theta_D = 0$  case ((a) and (b)), we can see that the amplitude  $A_L^{21}$  is enhanced for a nonvanishing  $\theta_E$  and relatively small  $m_0$ . In the parameter region  $\theta_E \sim 90^\circ$ ,  $B(\mu \rightarrow e \gamma)$  becomes larger than that for  $\theta_E \sim 0$  and  $A(\mu \rightarrow e \gamma)$  approaches to +1, reflecting that  $A_L^{21}$  is enhanced and dominates over  $A_R^{21}$ . For  $\theta_E = 0$  case ((c) and (d)),  $A_R^{21}$  dominates in the most of the range of  $\theta_D$  and hence  $A(\mu \rightarrow e \gamma)$  is close to -1. In some special case,  $\theta_D = -30^\circ$  and  $m_0 = 300$  GeV for example, a cancellation among contributions to  $A_R^{21}$  occurs and the branching ratio is suppressed. In such a case the P-odd asymmetry approaches to +1.

Fig. 10 shows the  $\theta_D$  dependence of  $\varepsilon_K$  for the same parameter set as Fig. 9(c) and (d). This dependence comes from  $g_{RL}^S$  and  $g_{RL}'^S$  in Eq. (37) since  $\theta_D$  directly affects the mixing between the right-handed down-type squarks of the first and the second generations. We have checked that  $\theta_E$  dependence is negligible for  $\varepsilon_K$ .

Hereafter we fix  $\theta_E$  as  $\theta_E = 0$  and in most cases we also fix  $\theta_D = 0$ .

## B. $a_\mu^{\text{SUSY}}$ , FCNC and LFV observables for different sets of the neutrino and the SUSY parameters

In Fig. 11 we show contour plots of the SUSY contribution to the muon anomalous magnetic moment  $a_\mu^{\text{SUSY}}$ , branching ratios of  $\mu \rightarrow e \gamma$  and  $\tau \rightarrow \mu \gamma$ , and the deviations from the SM values of  $\varepsilon_K$ ,  $\Delta m_{B_d}$  and  $\Delta m_{B_s}$ . The input parameters used in each figure are given in Table III. We also fix the sign of  $\mu$  as  $\mu > 0$  in these figures.  $\mu < 0$  region is disfavored because the SUSY contributions to  $b \rightarrow s \gamma$  decay amplitude interferes with the SM contribution constructively, so that the branching ratio becomes too large in a large portion of the parameter space. Note that the constraints from  $\varepsilon_K$ ,  $\Delta m_{B_d}$  and  $\Delta m_{B_s}$  are not imposed in Fig. 11 since these constraints depend on  $\delta_{13}$  and  $|V_{ub}|$ . We show our result

for each of these observables by taking a ratio to the corresponding SM value, expecting that the most of the dependences on the CKM parameters cancel. In fact we have checked that the plots do not change when a different value of  $\delta_{13}$  is used. The dependences of  $a_\mu^{\text{SUSY}}$ ,  $B(\mu \rightarrow e \gamma)$  and  $B(\tau \rightarrow \mu \gamma)$  on the CKM parameters are also small.

In Fig. 11(a) we take the LMA case for the neutrino masses and mixing,  $M_R = 4 \times 10^{13}$  GeV,  $\theta_E = \theta_D = 0$ ,  $\tan \beta = 20$  and  $A_0 = 0$  as a reference point. Shaded regions are experimentally excluded region. The constraints mainly come from the LEP II Higgs boson search and the upper bound on  $B(\mu \rightarrow e \gamma)$ . We see that there is a parameter region with  $20 \times 10^{-10} \lesssim a_\mu^{\text{SUSY}} \lesssim 60 \times 10^{-10}$ , which is favored by the E821 result and in that region  $B(\mu \rightarrow e \gamma)$  becomes larger than  $10^{-12}$ . In the allowed parameter region within the plotted range  $M_0 < 1$  TeV and  $m_0 < 4$  TeV,  $B(\mu \rightarrow e \gamma)$  varies  $O(10^{-14})$  to  $O(10^{-11})$  and  $B(\tau \rightarrow \mu \gamma)$  varies  $O(10^{-11})$  to  $O(10^{-9})$ . Both branching ratios depend similarly on  $M_0$  and  $m_0$ . Also we see that the deviation of  $\varepsilon_K$  from the SM value is about ten percent at most and the deviations of  $\Delta m_{B_d}$  and  $\Delta m_{B_s}$  are small.

In Fig. 11(b) plots for  $A_0 = 2$  are given. In this case the stop mass squared becomes negative in some parameter region, which is shown in the figure. The excluded region by the  $B(\mu \rightarrow e \gamma)$  constraint is enlarged, due to the enhancement of the branching ratio by the change in the left-right mixing in the slepton mass matrices. The deviation of  $\varepsilon_K$  is also enhanced and there is an allowed parameter region where  $\varepsilon_K$  is enhanced by more than 25 percent. It is noticeable that the allowed parameter region with a large enhancement of  $\varepsilon_K$  is different from the E821-favored region. The region which corresponds to both a favorable  $a_\mu^{\text{SUSY}}$  and a large enhancement of  $\varepsilon_K$  is excluded by other constraint, such as  $B(\mu \rightarrow e \gamma)$ .

Comparing Fig. 11(a) and (c), we can see the dependence on  $\theta_D$ . Since  $\theta_D$  affects the mixing between the first and the second generations, the difference appears mainly for  $B(\mu \rightarrow e \gamma)$  and  $\varepsilon_K$ . For a nonvanishing  $\theta_D = 45^\circ$  (Fig. 11(c)),  $B(\mu \rightarrow e \gamma)$  is enhanced for  $m_0 \lesssim 700$  GeV and the excluded region is enlarged. Also the SUSY contribution to  $\varepsilon_K$  can be larger than the SM contribution in a part of the allowed parameter region as shown in

Fig. 10.  $a_\mu^{\text{SUSY}}$  does not depend on  $\theta_D$  so that the parameter region with  $a_\mu^{\text{SUSY}} \gtrsim 10 \times 10^{-10}$  is excluded in the case (c). The behavior of  $B(\tau \rightarrow \mu \gamma)$  and  $\Delta m_{B_s}$  are unchanged also. Although  $\Delta m_{B_d}$  depends on  $\theta_D$ , the deviation is quite small in either case.

The plots for  $\tan \beta = 5$  are given in Fig. 11(d). Since both  $B(\mu \rightarrow e \gamma)$  and  $B(\tau \rightarrow \mu \gamma)$  are proportional to  $\tan^2 \beta$ , possible values are suppressed as  $B(\mu \rightarrow e \gamma) \lesssim 10^{-13}$  and  $B(\tau \rightarrow \mu \gamma) \lesssim 10^{-10}$ .  $a_\mu^{\text{SUSY}}$  is proportional to  $\tan \beta$  and is also suppressed. The excluded region is larger than the  $\tan \beta = 20$  case because the constraint from the Higgs mass bound is stronger for a smaller  $\tan \beta$ . The plots for  $\varepsilon_K$ ,  $\Delta m_{B_d}$  and  $\Delta m_{B_s}$  are the same as those in the case (a) except that the excluded region is enlarged.

Fig. 11(e) shows the case with a larger  $M_R = 4 \times 10^{14}$  GeV. Since the magnitude of the neutrino Yukawa coupling constants are proportional to  $\sqrt{M_R}$ , the flavor mixings in  $m_D^2$  and  $m_L^2$  are enhanced for a larger  $M_R$ . As a result we see that  $B(\mu \rightarrow e \gamma)$ ,  $B(\tau \rightarrow \mu \gamma)$  and  $\varepsilon_K$  are significantly enhanced in this case, compared to the  $M_R = 4 \times 10^{13}$  GeV case (a). Although the excluded region due to the constraint from  $B(\mu \rightarrow e \gamma)$  is enlarged, there is still an allowed parameter region where  $\varepsilon_K$  is enhanced more than fifty percent of the SM value. Also  $B(\tau \rightarrow \mu \gamma)$  can be close to  $O(10^{-8})$ . In the allowed parameter region, the deviations of  $\Delta m_{B_d}$  and  $\Delta m_{B_s}$  are small.  $a_\mu^{\text{SUSY}}$  is unaffected by the change of  $M_R$  and the E821-favored region is excluded by the  $B(\mu \rightarrow e \gamma)$  constraint.

Fig. 11(f) shows the SMA case. Other parameters are taken to be the same as those in the case (a). In this case, the mixing between the first and the second generations is suppressed compared to the LMA case. Consequently  $B(\mu \rightarrow e \gamma)$  is at most  $O(10^{-13})$  in the allowed region and the deviation of  $\varepsilon_K$  is smaller.  $a_\mu^{\text{SUSY}}$ ,  $B(\tau \rightarrow \mu \gamma)$ ,  $\Delta m_{B_d}$  and  $\Delta m_{B_s}$  look the same as those in the case (a).

In all the above cases the deviation of the  $B^0 - \bar{B}^0$  mixing from the SM value is small. Let us now show an example with a large enhancement of the  $B_s - \bar{B}_s$  mixing in Fig. 11(g). We see that  $\Delta m_{B_s}$  differs from the SM value by more than 50 percent in a parameter region  $m_0 \gtrsim 700$  GeV and  $M_0 \lesssim 200$  GeV. In the same region  $\varepsilon_K$  is also enhanced by a similar amount. Note that this enhancement comes from the mixing in the right-handed down-type

squarks induced by the neutrino Yukawa coupling. In such a case the time-dependent CP asymmetry of  $B \rightarrow M_s \gamma$  decay is also enhanced. Fig. 12 shows  $A_{CP}(B \rightarrow M_s \gamma)$  with the same parameter set. We see that this asymmetry can be larger than 25 percent in the parameter region where  $\Delta m_{B_s}$  is enhanced. In this case  $B(\tau \rightarrow \mu \gamma)$  can be close to  $10^{-7}$ .

In Table V we summarize the possible SUSY contributions to the observables given in Fig. 11. We can see that, except for the case (g), a large deviation from the SM is possible only in  $a_\mu^{\text{SUSY}}$ ,  $B(\mu \rightarrow e \gamma)$  and  $\varepsilon_K$ .

Let us see the correlation among  $a_\mu^{\text{SUSY}}$ ,  $B(\mu \rightarrow e \gamma)$  and  $\varepsilon_K$  more closely. Fig. 13 shows the correlation between  $a_\mu^{\text{SUSY}}$  and  $B(\mu \rightarrow e \gamma)$ ,  $a_\mu^{\text{SUSY}}$  and  $\varepsilon_K/(\varepsilon_K)_{\text{SM}}$ , and  $\varepsilon_K/(\varepsilon_K)_{\text{SM}}$  and  $B(\mu \rightarrow e \gamma)$ . Here SUSY breaking parameters  $m_0$ ,  $M_0$  and  $A_0$  are scanned within the range  $m_0, M_0 < 3 \text{ TeV}$  and  $-5 < A_0 < 5$ . Other parameters are taken to be the same as those in Fig. 11(a) and (b). In the plot of the correlation between  $a_\mu^{\text{SUSY}}$  and  $B(\mu \rightarrow e \gamma)$ , The  $a_\mu^{\text{SUSY}} < 0$  branch corresponds to  $\mu < 0$  and  $a_\mu^{\text{SUSY}} \lesssim -20 \times 10^{-10}$  region is excluded by the  $B(b \rightarrow s \gamma)$  constraint. Notice that the parameter region where  $a_\mu^{\text{SUSY}}$  saturates the E821 result is different from that with a large  $\varepsilon_K/(\varepsilon_K)_{\text{SM}}$ . As can be seen in the plot of  $a_\mu^{\text{SUSY}}$  and  $\varepsilon_K/(\varepsilon_K)_{\text{SM}}$ , when  $\varepsilon_K$  is enhanced by  $\sim 50$  percent, the magnitude of  $a_\mu^{\text{SUSY}}$  is small.

### C. Allowed region of $\Delta m_{B_s}/\Delta m_{B_d}$ and the CP asymmetry of $B \rightarrow J/\psi K_S$

Finally, let us discuss the effect of varying the CKM parameters  $|V_{ub}/V_{cb}|$  and  $\delta_{13}$ . Within the SM, these parameters are determined by combining the measurements of several observables:  $b \rightarrow u \ell \bar{\nu}$  semileptonic decays,  $\varepsilon_K$ ,  $\Delta m_{B_d}$ ,  $\Delta m_{B_s}/\Delta m_{B_d}$  and the time-dependent CP asymmetry of  $B \rightarrow J/\psi K_S$  decay. However, in the present case we have shown that there can be a significant SUSY contributions to these observables, especially for  $\varepsilon_K$ . In such a case the allowed range of  $\delta_{13}$  given by the measured value of  $\varepsilon_K$  is different from the SM case, and then this change affects the other observables. As for  $|V_{ub}/V_{cb}|$ , we have no change since the  $b \rightarrow u \ell \bar{\nu}$  decay is dominated by the tree-level SM amplitude.

We show how this effect will be observed in Fig. 14, where the possible region in the

space of  $\Delta m_{B_s}/\Delta m_{B_d}$  and the time-dependent CP asymmetry of  $B \rightarrow J/\psi K_S$  is presented. In this figure, we vary  $|V_{ub}/V_{cb}|$  and  $\delta_{13}$  within the ranges  $0.08 < |V_{ub}/V_{cb}| < 0.1$  and  $0 < \delta_{13} < 360^\circ$ . The dotted lines in each plot show the SM values of  $\Delta m_{B_s}/\Delta m_{B_d}$  and  $A_{CP}(B \rightarrow J/\psi K_S)$  for the whole range of  $\delta_{13}$  and  $|V_{ub}/V_{cb}| = 0.1$  (outer line) and 0.08 (inner line). The shaded region is allowed in the SM case. We impose the constraints from the measured values of  $\varepsilon_K = 2.28 \times 10^{-3}$  and  $\Delta m_{B_d} = 0.482 \text{ ps}^{-1}$  and from the lower limit of  $\Delta m_{B_s} > 14.3 \text{ ps}^{-1}$ . In the calculation of  $\varepsilon_K$ ,  $\Delta m_{B_d}$  and  $\Delta m_{B_s}$  we fix the bag parameters and the decay constant of the  $B$  meson  $f_{B_d, B_s}$  as given in Table IV [36]. When we impose the experimental constraints, we allow  $\pm 15\%$  and  $\pm 40\%$  deviations for  $\varepsilon_K$  and  $\Delta m_{B_d}$ , respectively, in order to take theoretical uncertainties in the bag parameters into account. Since this uncertainty is expected to be reduced in the ratio  $\Delta m_{B_s}/\Delta m_{B_d}$ , we use the lower limit of the ratio  $\Delta m_{B_s}/\Delta m_{B_d}$  instead of  $\Delta m_{B_s}$  itself.

Fig. 14(a) shows the result with the same parameter set as Fig. 11(a) except that  $A_0$  is scanned within  $-5 < A_0 < +5$  (see Table III). As shown in Fig. 11(a) and (b), the SUSY contributions to  $B_d - \bar{B}_d$  mixing and  $B_s - \bar{B}_s$  mixing are quite small in this case so that the allowed region lies between the dotted lines. The difference of the allowed regions from the SM one comes from the fact that the SUSY contribution to  $\varepsilon_K$  can be as large as 50 percent of the SM value, which can be seen in Fig. 13.

In Fig. 14(b) we take  $\theta_D = 45^\circ$  as in Fig. 11(c) and  $A_0$  is scanned within  $-5 < A_0 < +5$ . In this case the enhancement of  $\varepsilon_K$  is more significant compared to the  $\theta_D = 0$  case. Consequently a region with smaller  $\delta_{13}$  is now allowed and hence a smaller  $A_{CP}(B \rightarrow J/\psi K_S) \sim 0.4$  is possible, compared to the SM value  $A_{CP}(B \rightarrow J/\psi K_S) \sim 0.7$ . At the same time  $\Delta m_{B_s}/\Delta m_{B_d}$  can be as large as 60.

Fig. 14(c) is the case corresponding to Fig. 11(g) with  $-5 < A_0 < +5$ . In this case the allowed region can be outside of the dotted circles, since a large deviation of  $\Delta m_{B_s}$  is possible. On the other hand, we see that the deviation of  $A_{CP}(B \rightarrow J/\psi K_S)$  from the SM value is small.

At present we only have lower bound for  $\Delta m_{B_s}$  and the CP asymmetry of  $B \rightarrow J/\psi K_S$

and related modes is not precise enough [35,37]. In a few years we expect that the  $\Delta m_{B_s}$  will be measured at Tevatron and the precision of the CP violating asymmetry will be improved to 10 percent level at Belle, BaBar and Tevatron experiments. It is conceivable that the deviation shown in Fig. 14 will be clearly seen in these experiments.

## V. CONCLUSION AND DISCUSSIONS

In this paper we have studied the FCNC and LFV processes as well as the muon anomalous magnetic moment in the framework of SU(5) SUSY GUT with right-handed neutrino motivated by the large mixing angle solutions for the atmospheric and solar neutrino anomalies. In order to explain realistic mass relations for quarks and leptons, we have taken into account effects of higher dimensional operators above the GUT scale. It has been shown that there appear new mixing angles in the right-handed charged leptons and the right-handed down-type quarks due to the higher dimensional operators. We have calculated various low-energy observables by changing parameters of the model, namely SUSY parameters, neutrino parameters (LMA or SMA, and  $M_R$ ) and the above new mixing angles. We have shown that, within the current experimental bound of  $B(\mu \rightarrow e \gamma)$ , large SUSY contributions are possible either in the muon anomalous magnetic moment or in  $\varepsilon_K$ . The parameter regions which have a large correction in one case is different from that in the other case. In the former case, the favorable value of the recent result of the BNL E821 experiment can be accommodated. In the latter case, the allowed region of the Kobayashi-Maskawa phase can be different from the predictions within the SM, and therefore the measurements of the CP asymmetry of  $B \rightarrow J/\psi K_S$  mode and  $\Delta m_{B_s}$  can discriminate this case from the SM. We also show that the  $\tau \rightarrow \mu \gamma$  branching ratio can be close to the current experimental upper bound and the mixing-induced CP asymmetry of the radiative  $B$  decay can be enhanced in the case where the neutrino parameters correspond to the small mixing angle MSW solution.

Finally there are several remarks.

- In this paper we have neglected the constraint from the nucleon decay. If we take the

minimal model for the Higgs sector at the GUT scale, it is likely that the nucleon decay experiments excludes most of the parameter space even if the squark mass is multi-TeV [38]. It is known, however, that there are several ways to suppress the nucleon decay without changing the flavor signals discussed here [39].

- For LFV search,  $\mu \rightarrow e e e$  decay and  $\mu - e$  conversion in a muonic atom are also promising experimentally [40]. The rates of these processes have simple relations with  $B(\mu \rightarrow e \gamma)$  if the photonic operator Eq. (32) gives dominant contribution [17,41]:

$$\frac{B(\mu^+ \rightarrow e^+ e^+ e^-)}{B(\mu^+ \rightarrow e^+ \gamma)} \approx \frac{\alpha}{3\pi} \left[ \log \frac{m_\mu^2}{m_e^2} - \frac{11}{4} \right] \approx 0.006, \quad (41a)$$

$$\frac{B(\mu^- N \rightarrow e^- N)}{B(\mu^+ \rightarrow e^+ \gamma)} \approx \frac{B(A, Z)}{428}, \quad (41b)$$

where  $B(A, Z)$  represents the rate dependence on the mass number  $A$  and the atomic number  $Z$  of the target nucleus:  $B(A, Z) \approx 1.1$  for  $^{27}\text{Al}$ ,  $B(A, Z) \approx 1.8$  for  $^{48}\text{Ti}$  and  $B(A, Z) \approx 1.25$  for  $^{208}\text{Pb}$ . These relations hold also in our case.

- We also calculated  $\tau \rightarrow e \gamma$  branching ratio. In all cases  $B(\tau \rightarrow e \gamma)$  is smaller by two or three orders of magnitude than  $B(\tau \rightarrow \mu \gamma)$ .
- As shown in Fig. 11(a) and (e), the flavor mixing effect due to the neutrino Yukawa coupling is enhanced (suppressed) for a large (small)  $M_R$  since the neutrino Yukawa coupling constants are proportional to  $\sqrt{M_R}$  for given neutrino masses. When we take a small value of  $M_R$ , such as  $M_R \lesssim 10^{10}$  GeV, the contributions of  $y_\nu$  in  $m_L^2$  and  $m_D^2$  given in Eqs. (25c) and (25d) are suppressed and hence the SUSY contribution to  $\varepsilon_K$  becomes smaller than  $\sim 10$  percent. Even in this case, however, there are contributions to the  $\mu \rightarrow e \gamma$  decay amplitudes independent of the magnitude of  $y_\nu$ , as shown in Eq. (33). The terms proportional to  $a_1^n$  dominate the amplitude for  $\theta_{D,E} = O(1)$  and the branching ratio can be as large as the experimental upper bound in some parameter region.

- We have assumed 1-3 element of the MNS matrix to be vanishing. However, present experimental upper bound is given as  $\sin^2 2\theta_{13} < 0.1$  [23]. When a nonvanishing  $\theta_{13}$  is introduced,  $\mu \rightarrow e \gamma$  and  $\varepsilon_K$  are generally enhanced since the loop diagrams including the third-generation squarks/sleptons in the internal lines give large contributions [17]. Consequently, the constraint from the upper bound of  $B(\mu \rightarrow e \gamma)$  is significant even in the SMA case. In the allowed region,  $a_\mu^{\text{SUSY}}$  and the SUSY contributions to  $\Delta m_{B_d}$  and  $\Delta m_{B_s}$  are smaller than those in the  $\theta_{13} = 0$  case shown in Fig. 11. We see that the large deviation of  $\Delta m_{B_s}/\Delta m_{B_d}$  outside of the dotted lines given in Fig. 14(c) disappears when we take  $\sin^2 2\theta_{13} \gtrsim 0.001$ , and the corresponding plot looks similar to Fig. 14(b).
- Let us now discuss about the validity of the simplification imposed in the mixing matrices  $V_D$  and  $V_E$ . We have numerically checked that, when we require  $|(\kappa_d)_{ij}| < 4$  for example, the mixing angles for the second-third and first-third generation mixings are restricted to be smaller than  $\sim 15^\circ$  for the  $\tan \beta = 20$  case. In this case  $B(\mu \rightarrow e \gamma)$  varies within the range which is several times larger than those shown in Fig. 9. In addition to the mixing angles, CP-violating complex phases of  $O(1)$  can be introduced in  $V_D$  and  $V_E$ . It turns out that the SUSY contributions to  $\varepsilon_K$  can be twice as large as those given in Fig. 10. These complex phases also contribute to the EDMs of the neutron ( $d_n$ ) and the electron ( $d_e$ ). We calculated EDMs and obtained that  $|d_n| \lesssim 10^{-26} e \text{ cm}$  and  $|d_e| \lesssim 10^{-27} e \text{ cm}$  for  $m_0 = 600 \text{ GeV}$ ,  $M_0 = 300 \text{ GeV}$  and  $A_0 = 0$ . Thus the EDMs can be close to the present upper bounds  $|d_n| < 6.3 \times 10^{-26} e \text{ cm}$  [42] and  $|d_e| < 4.0 \times 10^{-27} e \text{ cm}$  [43].

As discussed above, if we relax the simple assumptions for the mixing matrices  $V_D$ ,  $V_E$  and  $V_{\text{MNS}}$ , typical patterns of the deviation from the SM can be summarized in the following way. (1)  $B(\mu \rightarrow e \gamma)$  can be close to  $10^{-11}$  and the deviation in  $\Delta m_{B_s}/\Delta m_{B_d}$ - $A_{CP}(B \rightarrow J/\psi K_S)$  plane appears like Fig. 14(b). In this case,  $a_\mu^{\text{SUSY}}$  is quite small and the SUSY contribution does not saturate the observed discrepancy of  $a_\mu$ . (2)  $a_\mu^{\text{SUSY}}$  is compatible with the E821

result and  $B(\mu \rightarrow e \gamma)$  can be as large as  $10^{-11}$ . However, no deviation may be seen in  $\varepsilon_K$ ,  $B_d - \bar{B}_d$  and  $B_s - \bar{B}_s$  mixings in this case. From these observations we can conclude that it is important to search for new physics effects in the ongoing and near-future experiments, namely the BNL muon  $g - 2$  experiment,  $\mu \rightarrow e \gamma$  and  $\mu - e$  conversion experiments [44,45],  $B$  physics experiments at  $B$ -factories and Tevatron. Combining results obtained in these experiments we may be able to get some insights on interactions at the GUT or right-handed neutrino scales.

## ACKNOWLEDGMENTS

The work of Y. O. was supported in part by the Grant-in-Aid of the Ministry of Education, Culture, Sports, Science and Technology, Government of Japan (No. 09640381), Priority area “Supersymmetry and Unified Theory of Elementary Particles” (No. 707), and “Physics of CP violation” (No. 09246105).

## APPENDIX A: RGE AND MATCHING CONDITION AT THE GUT SCALE

In this appendix we show the detail of our numerical calculation taking account of the effects of higher dimensional operators. An outline of the calculation is as follows:

- We solve the RGEs for the gauge and Yukawa coupling constants between the EW scale and the GUT scale. The neutrino Yukawa coupling constants are calculated with Eq. (28) at the Majorana mass scale.
- At the GUT scale, the coupling constants in the superpotential of the SU(5)RN SUSY GUT are determined from the Yukawa coupling constants for quarks and leptons using the matching condition explained in Subsection A 2. Then we solve the RGEs for these constants between the GUT scale and the Planck scale.
- At the Planck scale, we set the boundary conditions for the SUSY breaking parameters

as Eq. (19) and solve the RGEs for these parameters between the Planck scale to the EW scale.

The RGEs for the MSSM and MSSMRN are given for example in the reference [6,17] and we show the RGEs for the SU(5)RN SUSY GUT in Subsection A 1. In Subsection A 2 we explain the matching condition at the GUT scale taking account of the higher dimensional terms in the Kähler potential.

### 1. RGE for the SU(5) SUSY GUT with right-handed neutrino

In this subsection we show one-loop RGEs for the SU(5)RN SUSY GUT. In the derivation of RGEs, we only take account of diagrams to which the higher dimensional operators are inserted at most one time. In this approximation, the quadratic divergence does not appear in the calculation.

The RGEs for the SU(5) gauge coupling constant  $g_5$  and the gaugino mass parameter  $M_5$  are given by

$$(4\pi)^2 M \frac{d}{dM} g_5 = b_5 g_5^3, \quad (\text{A1a})$$

$$(4\pi)^2 M \frac{d}{dM} M_5 = 2b_5 g_5^2 M_5, \quad (\text{A1b})$$

where  $M$  is the renormalization scale. The coefficient of the beta function is given as  $b_5 = -3$  for the minimal field contents.

The RGEs for the coupling constants in the superpotentials, Eqs. (1) and (6) are represented as follows:

$$(4\pi)^2 M \frac{d}{dM} (\lambda_u)_{ij} = (\lambda_u)_{kj} (\Theta_T)^k_i + (\lambda_u)_{ik} (\Theta_T)^k_j + (\lambda_u)_{ij} \Theta_H, \quad (\text{A2a})$$

$$(4\pi)^2 M \frac{d}{dM} (\lambda_d)_{ij} = (\lambda_d)_{kj} (\Theta_{\bar{F}})^k_i + (\lambda_d)_{ik} (\Theta_T)^k_j + (\lambda_d)_{ij} \Theta_{\bar{H}}, \quad (\text{A2b})$$

$$(4\pi)^2 M \frac{d}{dM} (\lambda_\nu)_{ij} = (\lambda_\nu)_{kj} (\Theta_{\bar{N}})^k_i + (\lambda_\nu)_{ik} (\Theta_{\bar{F}})^k_j + (\lambda_\nu)_{ij} \Theta_H, \quad (\text{A2c})$$

$$(4\pi)^2 M \frac{d}{dM} (\kappa_u^\pm)_{ij} = (\kappa_u^\pm)_{kj} (\Theta_T)^k_i + (\kappa_u^\pm)_{ik} (\Theta_T)^k_j + (\kappa_u^\pm)_{ij} (\Theta_H + \Theta_\Sigma), \quad (\text{A2d})$$

$$(4\pi)^2 M \frac{d}{dM} (\kappa_d)_{ij} = (\kappa_d)_{kj} (\Theta_{\overline{F}})^k_i + (\kappa_d)_{ik} (\Theta_T)^k_j + (\kappa_d)_{ij} (\Theta_{\overline{H}} + \Theta_\Sigma), \quad (\text{A2e})$$

$$(4\pi)^2 M \frac{d}{dM} (\overline{\kappa}_d)_{ij} = (\overline{\kappa}_d)_{kj} (\Theta_{\overline{F}})^k_i + (\overline{\kappa}_d)_{ik} (\Theta_T)^k_j + (\overline{\kappa}_d)_{ij} (\Theta_{\overline{H}} + \Theta_\Sigma), \quad (\text{A2f})$$

$$(4\pi)^2 M \frac{d}{dM} (\kappa_\nu)_{ij} = (\kappa_\nu)_{kj} (\Theta_{\overline{N}})^k_i + (\kappa_\nu)_{ik} (\Theta_T)^k_j + (\kappa_\nu)_{ij} (\Theta_H + \Theta_\Sigma), \quad (\text{A2g})$$

where  $\Theta$ 's are given by

$$(\Theta_T)^i_j = 2(\lambda_d^\dagger)^{ik} (\lambda_d)_{kj} + 3(\lambda_u^\dagger)^{ik} (\lambda_u)_{kj} - \frac{36}{5} g_5^2 \delta_j^i, \quad (\text{A3a})$$

$$(\Theta_{\overline{F}})^i_j = 4(\lambda_d^*)^{ik} (\lambda_d^T)_{kj} + (\lambda_\nu^\dagger)^{ik} (\lambda_\nu)_{kj} - \frac{24}{5} g_5^2 \delta_j^i, \quad (\text{A3b})$$

$$(\Theta_{\overline{N}})^i_j = 5(\lambda_\nu^*)^{ik} (\lambda_\nu^T)_{kj}, \quad (\text{A3c})$$

$$\Theta_{\overline{H}} = 4\text{Tr} \left( \lambda_d^\dagger \lambda_d \right) - \frac{24}{5} g_5^2, \quad (\text{A3d})$$

$$\Theta_H = \frac{3}{2} \text{Tr} \left( \lambda_u^\dagger \lambda_u \right) + \text{Tr} \left( \lambda_\nu^\dagger \lambda_\nu \right) - \frac{24}{5} g_5^2, \quad (\text{A3e})$$

$$\Theta_\Sigma = -10g_5^2. \quad (\text{A3f})$$

The RGEs for the SUSY breaking parameters in Eq. (18) are written as follows:

$$(4\pi)^2 M \frac{d}{dM} (\tilde{\lambda}_u)_{ij} = (\tilde{\lambda}_u)_{kj} (\Theta_T)^k_i + (\tilde{\lambda}_u)_{ik} (\Theta_T)^k_j + (\tilde{\lambda}_u)_{ij} \Theta_H \\ + 2 \left\{ (\lambda_u)_{kj} (\tilde{\Theta}_T)^k_i + (\lambda_u)_{ik} (\tilde{\Theta}_T)^k_j + (\lambda_u)_{ij} \tilde{\Theta}_H \right\}, \quad (\text{A4a})$$

$$(4\pi)^2 M \frac{d}{dM} (\tilde{\lambda}_d)_{ij} = (\tilde{\lambda}_d)_{kj} (\Theta_{\overline{F}})^k_i + (\tilde{\lambda}_d)_{ik} (\Theta_T)^k_j + (\tilde{\lambda}_d)_{ij} \Theta_{\overline{H}} \\ + 2 \left\{ (\lambda_d)_{kj} (\tilde{\Theta}_{\overline{F}})^k_i + (\lambda_d)_{ik} (\tilde{\Theta}_T)^k_j + (\lambda_d)_{ij} \tilde{\Theta}_{\overline{H}} \right\}, \quad (\text{A4b})$$

$$(4\pi)^2 M \frac{d}{dM} (\tilde{\lambda}_\nu)_{ij} = (\tilde{\lambda}_\nu)_{kj} (\Theta_{\overline{N}})^k_i + (\tilde{\lambda}_\nu)_{ik} (\Theta_{\overline{F}})^k_j + (\tilde{\lambda}_\nu)_{ij} \Theta_H \\ + 2 \left\{ (\lambda_\nu)_{kj} (\tilde{\Theta}_{\overline{N}})^k_i + (\lambda_\nu)_{ik} (\tilde{\Theta}_{\overline{F}})^k_j + (\lambda_\nu)_{ij} \tilde{\Theta}_H \right\}, \quad (\text{A4c})$$

$$(4\pi)^2 M \frac{d}{dM} (\tilde{\kappa}_u^\pm)_{ij} = (\tilde{\kappa}_u^\pm)_{kj} (\Theta_T)^k_i + (\tilde{\kappa}_u^\pm)_{ik} (\Theta_T)^k_j + (\tilde{\kappa}_u^\pm)_{ij} (\Theta_\Sigma + \Theta_H) \\ + 2 \left\{ (\kappa_u^\pm)_{kj} (\tilde{\Theta}_T)^k_i + (\kappa_u^\pm)_{ik} (\tilde{\Theta}_T)^k_j + (\kappa_u^\pm)_{ij} (\tilde{\Theta}_\Sigma + \tilde{\Theta}_H) \right\} \quad (\text{A4d})$$

$$(4\pi)^2 M \frac{d}{dM} (\tilde{\kappa}_d)_{ij} = (\tilde{\kappa}_d)_{kj} (\Theta_{\overline{F}})^k_i + (\tilde{\kappa}_d)_{ik} (\Theta_T)^k_j + (\tilde{\kappa}_d)_{ij} (\Theta_\Sigma + \Theta_{\overline{H}}) \\ + 2 \left\{ (\kappa_d)_{kj} (\tilde{\Theta}_{\overline{F}})^k_i + (\kappa_d)_{ik} (\tilde{\Theta}_T)^k_j + (\kappa_d)_{ij} (\tilde{\Theta}_\Sigma + \tilde{\Theta}_{\overline{H}}) \right\}, \quad (\text{A4e})$$

$$(4\pi)^2 M \frac{d}{dM} (\tilde{\overline{\kappa}}_d)_{ij} = (\tilde{\overline{\kappa}}_d)_{kj} (\Theta_{\overline{F}})^k_i + (\tilde{\overline{\kappa}}_d)_{ik} (\Theta_T)^k_j + (\tilde{\overline{\kappa}}_d)_{ij} (\Theta_\Sigma + \Theta_{\overline{H}}) \\ + 2 \left\{ (\overline{\kappa}_d)_{kj} (\tilde{\Theta}_{\overline{F}})^k_i + (\overline{\kappa}_d)_{ik} (\tilde{\Theta}_T)^k_j + (\overline{\kappa}_d)_{ij} (\tilde{\Theta}_\Sigma + \tilde{\Theta}_{\overline{H}}) \right\}, \quad (\text{A4f})$$

$$(4\pi)^2 M \frac{d}{dM} (\tilde{\kappa}_\nu)_{ij} = (\tilde{\kappa}_\nu)_{kj} (\Theta_{\overline{N}})^k{}_i + (\tilde{\kappa}_\nu)_{ik} (\Theta_{\overline{F}})^k{}_j + (\tilde{\kappa}_\nu)_{ij} (\Theta_\Sigma + \Theta_H),$$

$$+ 2 \left\{ (\kappa_\nu)_{kj} (\tilde{\Theta}_{\overline{N}})^k{}_i + (\kappa_\nu)_{ik} (\tilde{\Theta}_{\overline{F}})^k{}_j + (\kappa_\nu)_{ij} (\tilde{\Theta}_\Sigma + \tilde{\Theta}_H) \right\}, \quad (\text{A4g})$$

$$(4\pi)^2 M \frac{d}{dM} (m_T^2)^i{}_j = (\Theta_T)^i{}_k (m_T^2)^k{}_j + (m_T^2)^i{}_k (\Theta_T)^k{}_j$$

$$+ 2 \left[ 3(\lambda_u^\dagger)^{ik} \left\{ (m_T^2)^T{}_k{}^l + (m_H^2) \delta_k^l \right\} (\lambda_u)_{lj} \right.$$

$$+ 2(\lambda_d^\dagger)^{ik} \left\{ (m_{\overline{F}}^2)^T{}_k{}^l + (m_H^2) \delta_k^l \right\} (\lambda_d)_{lj}$$

$$+ 3(\tilde{\lambda}_u^\dagger)^{ik} (\tilde{\lambda}_u)_{kj} + 2(\tilde{\lambda}_d^\dagger)^{ik} (\tilde{\lambda}_d)_{kj} \Big]$$

$$+ \frac{72}{5} g_5^2 \left\{ (m_T^2)^i{}_j - 2|M_5|^2 \delta_j^i \right\}, \quad (\text{A4h})$$

$$(4\pi)^2 M \frac{d}{dM} (m_{\overline{F}}^2)^i{}_j = (\Theta_{\overline{F}})^i{}_k (m_{\overline{F}}^2)^k{}_j + (m_{\overline{F}}^2)^i{}_k (\Theta_{\overline{F}})^k{}_j$$

$$+ 2 \left[ 4(\lambda_d^*)^{ik} \left\{ (m_T^2)^T{}_k{}^l + (m_H^2) \delta_k^l \right\} (\lambda_d^T)_{lj} \right.$$

$$+ (\lambda_\nu^\dagger)^{ik} \left\{ (m_N^2)^T{}_k{}^l + (m_H^2) \delta_k^l \right\} (\lambda_\nu)_{lj}$$

$$+ 4(\tilde{\lambda}_d^*)^{ik} (\tilde{\lambda}_d^T)_{kj} + (\tilde{\lambda}_\nu^\dagger)^{ik} (\tilde{\lambda}_\nu)_{kj} \Big]$$

$$+ \frac{48}{5} g_5^2 \left\{ (m_{\overline{F}}^2)^i{}_j - 2|M_5|^2 \delta_j^i \right\}, \quad (\text{A4i})$$

$$(4\pi)^2 M \frac{d}{dM} (m_{\overline{N}}^2)^i{}_j = (\Theta_{\overline{N}})^i{}_k (m_{\overline{N}}^2)^k{}_j + (m_{\overline{N}}^2)^i{}_k (\Theta_{\overline{N}})^k{}_j$$

$$+ 2 \left[ 5(\lambda_\nu^*)^{ik} \left\{ (m_{\overline{F}}^2)^T{}_k{}^l + (m_H^2) \delta_k^l \right\} (\lambda_\nu^T)_{lj} + 5(\tilde{\lambda}_\nu^*)^{ik} (\tilde{\lambda}_\nu^T)_{kj} \right], \quad (\text{A4j})$$

$$(4\pi)^2 M \frac{d}{dM} m_H^2 = 2\Theta_H m_H^2 + 2 \left\{ 6\text{Tr} \left( \lambda_u^\dagger m_T^2{}^T \lambda_u \right) + \text{Tr} \left( \lambda_\nu^\dagger m_{\overline{N}}^2{}^T \lambda_\nu \right) \right.$$

$$+ \text{Tr} \left( \lambda_\nu^* m_{\overline{F}}^2{}^T \lambda_\nu^T \right) + 3\text{Tr} \left( \tilde{\lambda}_u^\dagger \tilde{\lambda}_u \right) + \text{Tr} \left( \tilde{\lambda}_\nu^\dagger \tilde{\lambda}_\nu \right) \Big\}$$

$$+ \frac{48}{5} g_5^2 \left( m_H^2 - 2|M_5|^2 \right), \quad (\text{A4k})$$

$$(4\pi)^2 M \frac{d}{dM} (m_{\overline{H}}^2) = 2\Theta_{\overline{H}} m_{\overline{H}}^2 + 2 \left\{ 4\text{Tr} \left( \lambda_d^* m_T^2{}^T \lambda_d^T \right) + 4\text{Tr} \left( \lambda_d^\dagger m_{\overline{F}}^2{}^T \lambda_d \right) \right.$$

$$+ 4\text{Tr} \left( \tilde{\lambda}_d^* \tilde{\lambda}_d^T \right) \Big\} + \frac{48}{5} g_5^2 \left( m_{\overline{H}}^2 - 2|M_5|^2 \right), \quad (\text{A4l})$$

where  $\tilde{\Theta}$ 's are given by

$$(\tilde{\Theta}_T)^i{}_j = 2(\lambda_d^\dagger)^{ik} (\tilde{\lambda}_d)_{kj} + 3(\lambda_u^\dagger)^{ik} (\tilde{\lambda}_u)_{kj} - \frac{36}{5} g_5^2 M_5 \delta_j^i, \quad (\text{A5a})$$

$$(\tilde{\Theta}_{\overline{F}})^i{}_j = 4(\lambda_d^*)^{ik} (\tilde{\lambda}_d^T)_{kj} + (\lambda_\nu^\dagger)^{ik} (\tilde{\lambda}_\nu)_{kj} - \frac{24}{5} g_5^2 M_5 \delta_j^i, \quad (\text{A5b})$$

$$(\tilde{\Theta}_{\overline{N}})^i{}_j = 5(\lambda_\nu^*)^{ik} (\tilde{\lambda}_\nu^T)_{kj}, \quad (\text{A5c})$$

$$\tilde{\Theta}_{\overline{H}} = 4\text{Tr}\left(\lambda_d^\dagger \tilde{\lambda}_d\right) - \frac{24}{5}g_5^2 M_5, \quad (\text{A5d})$$

$$\tilde{\Theta}_H = \frac{3}{2}\text{Tr}\left(\lambda_u^\dagger \tilde{\lambda}_u\right) + \text{Tr}\left(\lambda_\nu^\dagger \tilde{\lambda}_\nu\right) - \frac{24}{5}g_5^2 M_5, \quad (\text{A5e})$$

$$\tilde{\Theta}_\Sigma = -10g_5^2 M_5. \quad (\text{A5f})$$

## 2. Matching conditions at the GUT scale

In this subsection we show the matching conditions between the SU(5)RN SUSY GUT and the MSSMRN at the GUT scale taking account of the dimension five terms in the Kähler potential. Although we include only the renormalizable terms in the Kähler potential at the Planck scale, higher dimensional terms are induced by the renormalization effects between the Planck scale and the GUT scale, because we introduce the higher dimensional operators in the superpotential. In order to simplify the treatment, we use logarithmic approximation for induced terms in the Kähler potential. For other coupling constants, we explicitly solve the RGEs in the previous subsection.

Up to dimension five terms, the corrections for the Kähler potential in the present model are parameterized as follows:

$$\begin{aligned} \Delta\mathcal{K}_{\text{SU}(5)\text{RN}} = \frac{1}{M_X} \Big\{ & (\overline{k}_T)^i{}_j (T_i^\dagger)_{ab} (\Sigma)^b{}_c (T^j)^{ca} + (\overline{k}_{\overline{F}})^i{}_j (\overline{F}_i^\dagger)^a (\Sigma)^b{}_a (\overline{F}_j)_b \\ & + \overline{k}_H (H^\dagger)_a (\Sigma)^a{}_b (H)^b + \overline{k}_{\overline{H}} (\overline{H}^\dagger)^a (\Sigma)^b{}_a (\overline{H})_b \Big\} + \text{H.c.}, \end{aligned} \quad (\text{A6})$$

where we include SUSY breaking parts in the coupling constants using the spurion method as follows:

$$\overline{k}_X = k_X + \hat{k}_X \theta^2 + \check{k}_X \overline{\theta}^2 + \tilde{k}_X \theta^2 \overline{\theta}^2 \quad (X = T, \overline{F}, H, \overline{H}). \quad (\text{A7})$$

At the Planck scale, we assume all the components of Eq. (A7) are zero. These coupling constants are induced from the renormalization between the Planck scale and the GUT scale.

In the logarithmic approximation,  $k$ 's at the GUT scale are given by,

$$(k_T)^i{}_j \approx -2 \left\{ (\lambda_u^\dagger)^{ik} (\kappa_u^+)_{kj} - 5(\lambda_u^\dagger)^{ik} (\kappa_u^-)_{kj} + (\lambda_d^\dagger)^{ik} (\kappa_d)_{kj} + (\lambda_d^\dagger)^{ik} (\overline{\kappa}_d)_{kj} \right\} t_G, \quad (\text{A8a})$$

$$(k_{\overline{F}})^i{}_j \approx -2 \left\{ (\lambda_d^*) (\kappa_d)_{jk} - 4(\lambda_d^*)_{ik} (\overline{\kappa}_d)_{jk} - (\lambda_\nu^\dagger)^{ik} (\kappa_\nu)_{kj} \right\} t_G, \quad (\text{A8b})$$

$$k_H \approx -2 \left\{ 3\text{Tr} \left( \lambda_u^\dagger \kappa_u \right) - \text{Tr} \left( \lambda_\nu^\dagger \kappa_\nu \right) \right\} t_G, \quad (\text{A8c})$$

$$k_{\overline{H}} \approx -2 \left\{ \text{Tr} \left( \lambda_d^\dagger \kappa_d \right) - 4\text{Tr} \left( \lambda_d^\dagger \overline{\kappa}_d \right) \right\} t_G. \quad (\text{A8d})$$

In the same approximation,  $\hat{k}_X$ ,  $\check{k}_X$  and  $\tilde{k}_X$  at the GUT scale are proportional to  $k_X$  as follows:

$$\hat{k}_X \approx m_0 (A_0 + \Delta A_0) k_X, \quad (\text{A9a})$$

$$\check{k}_X \approx m_0 A_0 k_X, \quad (\text{A9b})$$

$$\tilde{k}_X \approx m_0^2 \{ A_0^* (A_0 + \Delta A_0) + 2 \} k_X, \quad (X = T, \overline{F}, H, \overline{H}). \quad (\text{A9c})$$

The dimension five terms in Eq. (A6) modify the normalization of the Kähler potential after the SU(5) symmetry breaking. In order to obtain the correct normalization up to  $O(\xi)$ , we introduce the following new chiral superfields:

$$(T^{i'})^{ab} = (T^i)^{ab} + \frac{1}{M_X} \left\{ (k_T)^i{}_j + \theta^2 (\hat{k}_T)^i{}_j \right\} \left\{ (\Sigma)_c^a (T^j)^{cb} - (\Sigma)_c^b (T^j)^{ca} \right\}, \quad (\text{A10a})$$

$$(\overline{F}^{i'})_a = (\overline{F}^i)_a + \frac{1}{M_X} \left\{ (k_{\overline{F}})^i{}_j + \theta^2 (\hat{k}_{\overline{F}})^i{}_j \right\} (\Sigma)_a^b (\overline{F}^j)_b, \quad (\text{A10b})$$

$$(H')^a = (H)^a + \frac{1}{M_X} \left( k_H + \theta^2 \hat{k}_H \right) (\Sigma)_a^b H^b \quad (\text{A10c})$$

$$(\overline{H}')_a = (\overline{H})_a + \frac{1}{M_X} \left( k_{\overline{H}} + \theta^2 \hat{k}_{\overline{H}} \right) (\Sigma)_a^b (\overline{H})_b. \quad (\text{A10d})$$

Substituting these superfields for Eqs. (1) and (6), we can define the coupling constants in terms of the new chiral superfields as follows:

$$(\kappa_u^{+'})_{ij} = (\kappa_u^+)_{ij} - \frac{1}{2} (\lambda_u)_{ik} (k_T)^k{}_j - \frac{1}{2} (\lambda_u)_{kj} (k_T)^k{}_i + (\lambda_u)_{ij} k_H, \quad (\text{A11a})$$

$$(\kappa_u^{-'})_{ij} = (\kappa_u^-)_{ij} + \frac{1}{2} (\lambda_u)_{ik} (k_T)^k{}_j - \frac{1}{2} (\lambda_u)_{kj} (k_T)^k{}_i, \quad (\text{A11b})$$

$$(\kappa_d')_{ij} = (\kappa_d)_{ij} - (\lambda_d)_{ik} (k_T)^k{}_j - (\lambda_d)_{kj} (k_{\overline{F}})^k{}_i, \quad (\text{A11c})$$

$$(\overline{\kappa}_d')_{ij} = (\overline{\kappa}_d)_{ij} - (\lambda_d)_{ik} (k_T)^k{}_j - (\lambda_d)_{ij} k_{\overline{H}}, \quad (\text{A11d})$$

$$(\kappa_\nu')_{ij} = (\kappa_\nu)_{ij} - (\lambda_\nu)_{ik} (k_{\overline{F}})^k{}_j - (\lambda_\nu)_{ij} k_H. \quad (\text{A11e})$$

The matching conditions for the Yukawa coupling matrices for quarks and leptons are written with the above new coupling constants as follows <sup>1</sup>:

$$(y_u)_{ij} = (\lambda_u)_{ij} + \xi \left\{ \frac{1}{2}(\kappa_u^{+'})_{ij} + \frac{5}{6}(\kappa_u^{-'})_{ij} \right\}, \quad (\text{A12a})$$

$$(y_d)_{ij} = (\lambda_d)_{ij} + \xi \left\{ \frac{1}{3}(\kappa_d')_{ij} - \frac{1}{2}(\bar{\kappa}_d')_{ij} \right\}, \quad (\text{A12b})$$

$$(y_e)_{ij} = (\lambda_d^T)_{ij} + \xi \left\{ -\frac{1}{2}(\kappa_d'^T)_{ij} - \frac{1}{2}(\bar{\kappa}_d'^T)_{ij} \right\}, \quad (\text{A12c})$$

$$(y_\nu)_{ij} = (\lambda_\nu)_{ij} - \frac{\xi}{2}(\kappa_\nu')_{ij}. \quad (\text{A12d})$$

Using Eqs. (A8)–(A12) we can relate  $y$ 's and  $\lambda$ 's and  $\kappa$ 's at the GUT scale. The SUSY breaking parameters are also defined in terms of the new superfields as follows:

$$\begin{aligned} (\tilde{\kappa}_u^{+'})_{ij} &= (\tilde{\kappa}_u^+)_{ij} - \frac{1}{2}(\tilde{\lambda}_u)_{ik}(k_T)^k_j - \frac{1}{2}(\tilde{\lambda}_u)_{kj}(k_T)^k_i + (\tilde{\lambda}_u)_{ij}k_H \\ &\quad - \frac{1}{2}(\lambda_u)_{ik}(\hat{k}_T)^k_j - \frac{1}{2}(\lambda_u)_{kj}(\hat{k}_T)^k_i + (\lambda_u)_{ij}\hat{k}_H, \end{aligned} \quad (\text{A13a})$$

$$\begin{aligned} (\tilde{\kappa}_u^{-'})_{ij} &= (\tilde{\kappa}_u^-)_{ij} - \frac{1}{2}(\tilde{\lambda}_u)_{ik}(k_T)^k_j + \frac{1}{2}(\tilde{\lambda}_u)_{kj}(k_T)^k_i \\ &\quad - \frac{1}{2}(\lambda_u)_{ik}(\hat{k}_T)^k_j + \frac{1}{2}(\lambda_u)_{kj}(\hat{k}_T)^k_i, \end{aligned} \quad (\text{A13b})$$

$$(\tilde{\kappa}_d')_{ij} = (\tilde{\kappa}_d)_{ij} - (\tilde{\lambda}_d)_{ik}(k_T)^k_j - (\tilde{\lambda}_d)_{kj}(k_{\overline{F}})^k_i - (\lambda_d)_{ik}(\hat{k}_T)^k_j - (\lambda_d)_{kj}(\hat{k}_{\overline{F}})^k_i, \quad (\text{A13c})$$

$$\begin{aligned} (\tilde{\kappa}_d)_{ij} &= (\tilde{\kappa}_d)_{ij} - (\tilde{\lambda}_d)_{ik}(k_T)^k_j - (\tilde{\lambda}_d)_{ij}k_{\overline{H}} \\ &\quad - (\lambda_d)_{ik}(\hat{k}_T)^k_j - (\lambda_d)_{ij}\hat{k}_{\overline{H}}, \end{aligned} \quad (\text{A13d})$$

$$(\tilde{\kappa}_\nu')_{ij} = (\tilde{\kappa}_\nu)_{ij} - (\tilde{\lambda}_\nu)_{ik}(k_{\overline{F}})^k_j - (\tilde{\lambda}_\nu)_{ij}k_H - (\lambda_\nu)_{ik}(\hat{k}_{\overline{F}})^k_j - (\lambda_\nu)_{ij}\hat{k}_H, \quad (\text{A13e})$$

$$(\tilde{k}_T')^i_j = (\tilde{k}_T)^i_j + (m_T^2)^i_k(k_T)^k_j, \quad (\text{A13f})$$

$$(\tilde{k}_{\overline{F}}')^i_j = (\tilde{k}_{\overline{F}})^i_j + (m_{\overline{F}}^2)^i_k(k_{\overline{F}})^k_j, \quad (\text{A13g})$$

$$\tilde{k}_H' = \tilde{k}_H + m_H^2 k_H, \quad (\text{A13h})$$

$$\tilde{k}_{\overline{H}}' = \tilde{k}_{\overline{H}} + m_{\overline{H}}^2 k_{\overline{H}}. \quad (\text{A13i})$$

---

<sup>1</sup> $\kappa$ 's in Eqs. (7) of Sec. II should be read as those with prime if we take account of the higher dimensional terms radiatively induced in the Kähler potential.

The soft SUSY breaking parameters can be expressed using the above new coupling constants as follows:

$$(\tilde{y}_u)_{ij} = (\tilde{\lambda}_u)_{ij} + \xi \left\{ \frac{1}{2}(\tilde{\kappa}_u^{+'})_{ij} + \frac{5}{6}(\tilde{\kappa}_u^{-'})_{ij} + \frac{1}{6}(\lambda_u)_{ik}(\tilde{k}_T^\dagger)_j^k - \frac{2}{3}(\lambda_u)_{kj}(\tilde{k}_T^\dagger)_i^k + \frac{1}{2}(\lambda_u)_{ij}\tilde{k}_H^* \right\}, \quad (\text{A14a})$$

$$(\tilde{y}_d)_{ij} = (\tilde{\lambda}_d)_{ij} + \xi \left\{ \frac{1}{3}(\tilde{\kappa}_d')_{ij} - \frac{1}{2}(\tilde{\kappa}_d'')_{ij} - \frac{1}{6}(\lambda_d)_{ik}(\tilde{k}_T^\dagger)_j^k - \frac{1}{3}(\lambda_d)_{kj}(\tilde{k}_F^\dagger)_i^k + \frac{1}{2}(\lambda_d)_{ij}\tilde{k}_H^* \right\}, \quad (\text{A14b})$$

$$(\tilde{y}_e)_{ij} = (\tilde{\lambda}_d^T)_{ij} + \xi \left\{ -\frac{1}{2}(\tilde{\kappa}_d'^T)_{ij} - \frac{1}{2}(\tilde{\kappa}_d''^T)_{ij} + (\lambda_d^T)_{kj}(\tilde{k}_T^\dagger)_i^k + \frac{1}{2}(\lambda_d^T)_{ik}(\tilde{k}_F^\dagger)_j^k + \frac{1}{2}(\lambda_d^T)_{ij}\tilde{k}_H^* \right\}, \quad (\text{A14c})$$

$$(\tilde{y}_\nu)_{ij} = (\tilde{\lambda}_\nu)_{ij} + \xi \left\{ -\frac{1}{2}(\tilde{\kappa}_\nu')_{ij} + \frac{1}{2}(\lambda_\nu)_{ik}(\tilde{k}_F^\dagger)_j^k + \frac{1}{2}(\lambda_\nu)_{ij}\tilde{k}_H^* \right\}, \quad (\text{A14d})$$

$$(m_Q^2)_j^i = (m_T^2)_j^i + \frac{1}{6}\xi \left\{ (\tilde{k}_T')_j^i + (\tilde{k}_T'')_j^i \right\}, \quad (\text{A14e})$$

$$(m_U^2)_i^j = (m_T^2)_i^j - \frac{2}{3}\xi \left\{ (\tilde{k}_T')_i^j + (\tilde{k}_T'')_i^j \right\}, \quad (\text{A14f})$$

$$(m_E^2)_i^j = (m_T^2)_i^j + \xi \left\{ (\tilde{k}_T')_i^j + (\tilde{k}_T'')_i^j \right\}, \quad (\text{A14g})$$

$$(m_D^2)_i^j = (m_F^2)_i^j - \frac{1}{3}\xi \left\{ (\tilde{k}_F')_i^j + (\tilde{k}_F'')_i^j \right\}, \quad (\text{A14h})$$

$$(m_L^2)_j^i = (m_F^2)_j^i + \frac{1}{2}\xi \left\{ (\tilde{k}_F')_j^i + (\tilde{k}_F'')_j^i \right\}, \quad (\text{A14i})$$

$$m_{H_1}^2 = m_H^2 + \xi \tilde{k}_H', \quad (\text{A14j})$$

$$m_{H_2}^2 = m_H^2 + \xi \tilde{k}_H'. \quad (\text{A14k})$$

Using Eqs. (A13) and (A14), we can express the soft SUSY breaking terms of the MSSMRN by the input parameters at the Planck scale, Eq. (19).

## APPENDIX B: APPROXIMATE EXPRESSIONS OF THE PHOTON-PENGUIN AMPLITUDES FOR $\mu \rightarrow e \gamma$ PROCESS

In this appendix we show the explicit forms of the functions which appear in the approximated expressions of the photon-penguin amplitudes given in Eq. (33). We assume the following conditions to derive the expressions:

- The off-diagonal elements of the slepton mass matrices,  $(m_E^2)_i^j$  and  $(m_L^2)_j^i$  are given by Eqs. (25b) and (25d), and they are diagonalized with good approximation in the basis where  $(y_\nu)_{ij}$  and  $(y_{CR})_{ij}$  in Eqs. (22) and (23) are diagonal.
- In this basis, the left-right mixing mass of the slepton can be treated as perturbation to diagonalize the  $6 \times 6$  charged slepton mass matrix.
- The eigenvalues of the slepton mass matrices are almost degenerate and represented by  $\overline{m}^2$ .

With these conditions, the SUSY contributions to the photon-penguin amplitudes correspond to Figs. (1)-(3) are expressed as Eq. (33). In this formula,  $a_2^n$ ,  $a^c$  and  $a_1^n$  are given by

$$a_2^n = -\frac{e}{32\pi^2} \tan \theta_W \sum_{A=1}^4 (O_N^*)_{A1} \{ (O_N)_{A2} + \tan \theta_W (O_N)_{A1} \} f_2^n \left( \frac{\overline{m}^2}{m_{\tilde{\chi}_A^0}^2} \right) \left( \frac{m_W}{\overline{m}} \right)^2 \left( \frac{m_0}{\overline{m}} \right)^4 \\ \times \frac{m_0(A_e + \frac{3}{5}\Delta A) + \mu^* \tan \beta}{\overline{m}} (3 + |A_0|^2)^2 t_G (t_G + t_R), \quad (\text{B1a})$$

$$a^c = \frac{\sqrt{2}e}{32\pi^2 \cos \beta} \sum_{A=1}^2 (O_{CL}^*)_{A2} (O_{CR})_{A1} f^c \left( \frac{\overline{m}^2}{m_{\tilde{\chi}_A^-}^2} \right) \left( \frac{m_W}{\overline{m}} \right) (3 + |A_0|^2) (t_G + t_R), \quad (\text{B1b})$$

$$a_1^n = -\frac{e}{32\pi^2} \tan \theta_W \sum_{A=1}^4 (O_N^*)_{A1} \{ (O_N)_{A2} + \tan \theta_W (O_N)_{A1} \} f_1^n \left( \frac{\overline{m}^2}{m_{\tilde{\chi}_A^0}^2} \right) \\ \times \left( \frac{m_W}{\overline{m}} \right)^2 \left( \frac{m_0}{\overline{m}} \right) \frac{3}{5} \frac{m_s}{m_\mu} \Delta A, \quad (\text{B1c})$$

where  $\theta_W$  is the Weinberg angle.  $m_{\tilde{\chi}_A^0}$  and  $m_{\tilde{\chi}_A^-}$  represent the masses of neutralinos and charginos, respectively and  $O_N$ ,  $O_{CR}$  and  $O_{CL}$  are unitary matrices which are used to diagonalize the neutralino and chargino mass matrices,  $M_{\tilde{\chi}^0}$  and  $M_{\tilde{\chi}^-}$  as follows:

$$O_N M_{\tilde{\chi}^0} O_N^T = \text{diag}(m_{\tilde{\chi}_1^0}, m_{\tilde{\chi}_2^0}, m_{\tilde{\chi}_3^0}, m_{\tilde{\chi}_4^0}), \quad (\text{B2a})$$

$$M_{\tilde{\chi}^0} = \begin{pmatrix} M_1 & 0 & -m_Z s_W \cos \beta & m_Z s_W \sin \beta \\ 0 & M_2 & m_Z c_W \cos \beta & -m_Z c_W \sin \beta \\ -m_Z s_W \cos \beta & m_Z c_W \cos \beta & 0 & -\mu \\ m_Z s_W \sin \beta & -m_Z c_W \sin \beta & -\mu & 0 \end{pmatrix}, \quad (\text{B2b})$$

$$O_{CR}M_{\tilde{\chi}^-}O_{CL}^\dagger = \text{diag}(m_{\tilde{\chi}_1^-}, m_{\tilde{\chi}_2^-}), \quad (\text{B2c})$$

$$M_{\tilde{\chi}^-} = \begin{pmatrix} M_2 & \sqrt{2}m_W \cos \beta \\ \sqrt{2}m_W \sin \beta & \mu \end{pmatrix}. \quad (\text{B2d})$$

$$(\text{B2e})$$

where  $m_Z$  and  $m_W$  are the  $Z$  boson mass and the  $W$  boson mass, respectively and  $s_W = \sin \theta_W$  and  $c_W = \cos \theta_W$ . The mass functions  $f_2^n$ ,  $f^c$  and  $f_1^n$  in the above formulas are given by

$$f_2^n(x) = -\frac{x^{\frac{7}{2}}}{(1-x)^4} \{x^2 + 4x - 5 + 2(2x+1) \ln(x)\}, \quad (\text{B3a})$$

$$f^c(x) = -\frac{\sqrt{x}}{2x^3(1-x)^4} \{14x^3 - 25x^2 + 14x - 3 - 2x^2(4x-1) \ln(x)\}, \quad (\text{B3b})$$

$$f_1^n(x) = \frac{1}{x^4(1-x)^5} \{5x^4 - 37x^3 + 27x^2 + 13x - 8 + 6x(7x-3) \ln(x)\}. \quad (\text{B3c})$$

### APPENDIX C: FCNC EFFECTIVE COUPLINGS IN MSSM

In this appendix we present the explicit forms of FCNC effective coupling constants for  $K^0 - \bar{K}^0$ ,  $B_d - \bar{B}_d$  and  $B_s - \bar{B}_s$  mixings. For  $K^0 - \bar{K}^0$  mixing these coupling constants are defined in Eq. (37) of Sec. III B and for  $B_d - \bar{B}_d$  and  $B_s - \bar{B}_s$  mixings the coupling constants are given by substitution of flavor indices. In the MSSM box diagrams exchanging charged Higgs, neutralino, chargino and gluino can contribute to these coupling constants. We first define the following neutralino, chargino and gluino vertices for quarks and squarks,

$$\begin{aligned} \mathcal{L} \equiv & \sum_{i=1}^3 \sum_{A=1}^4 \sum_{X=1}^6 \left\{ \overline{d}_i \left( N_{iAX}^{dL} P_L + N_{iAX}^{dR} P_R \right) \tilde{\chi}_A^0 \tilde{d}_X \right. \\ & \left. + \overline{u}_i \left( N_{iAX}^{uL} P_L + N_{iAX}^{uR} P_R \right) \tilde{\chi}_A^0 \tilde{u}_X \right\} \\ & + \sum_{i=1}^3 \sum_{A=1}^2 \sum_{X=1}^6 \left\{ \overline{d}_i \left( C_{iAX}^{dL} P_L + C_{iAX}^{dR} P_R \right) \tilde{\chi}_A^- \tilde{u}_X \right. \\ & \left. + \overline{u}_i \left( C_{iAX}^{uL} P_L + C_{iAX}^{uR} P_R \right) \tilde{\chi}_A^- \tilde{d}_X \right\} \\ & + \sum_{i=1}^3 \sum_{X=1}^6 \sum_{a=1}^8 \left\{ \overline{d}_i \left( \Gamma_{iX}^{dL} P_L + \Gamma_{iX}^{dR} P_R \right) \tilde{G}^a T^a \tilde{d}_X \right. \end{aligned}$$

$$+\overline{u}_i \left( \Gamma_{iX}^{uL} P_L + \Gamma_{iX}^{uR} P_R \right) \tilde{G}^a T^a \tilde{u}_X \} + \text{H.c.}, \quad (\text{C1})$$

where  $P_L$  and  $P_R$  are projection operators defined by  $P_L = (1 - \gamma_5)/2$  and  $P_R = (1 + \gamma_5)/2$  and  $T^a$  is the generator of SU(3) gauge group. The neutralino-squark coupling constants appear in the above formula are given by

$$N_{iAX}^{dL} = -\sqrt{2}g_2 \left\{ \frac{1}{3} \tan \theta_W (O_N)_{A1} (U_d^*)_{Xi+3} + \frac{m_{di}}{2m_W \cos \beta} (O_N)_{A3} (U_d^*)_{Xi} \right\}, \quad (\text{C2a})$$

$$N_{iAX}^{dR} = -\sqrt{2}g_2 \left[ \left\{ -\frac{1}{2} (O_N^*)_{A2} + \frac{1}{6} \tan \theta_W (O_N^*)_{A1} \right\} (U_d^*)_{Xi} + \frac{m_{di}}{2m_W \cos \beta} (O_N^*)_{A3} (U_d^*)_{Xi+3} \right], \quad (\text{C2b})$$

$$N_{iAX}^{uL} = -\sqrt{2}g_2 \left\{ -\frac{2}{3} \tan \theta_W (O_N)_{A1} (U_u^*)_{Xi+3} + \sum_{j=1}^3 \frac{m_{ui} (V_{\text{CKM}})^i_j}{2m_W \sin \beta} (O_N)_{A3} (U_u^*)_{Xj} \right\}, \quad (\text{C2c})$$

$$N_{iAX}^{uR} = -\sqrt{2}g_2 \left[ \left\{ \frac{1}{2} (O_N^*)_{A2} + \frac{1}{6} \tan \theta_W (O_N^*)_{A1} \right\} (U_u^*)_{Xi} + \sum_{j=1}^3 \frac{(V_{\text{CKM}}^\dagger)^i_j m_{uj}}{2m_W \sin \beta} (O_N^*)_{A3} (U_u^*)_{Xj+3} \right], \quad (\text{C2d})$$

where  $g_2$  is the SU(2) gauge coupling constant.  $O_N$  is the diagonalization matrix for neutralino mass matrix defined in Appendix B.  $U_d$  and  $U_u$  are unitary matrices which appear in diagonalization of the  $6 \times 6$  squark mass matrices,  $m_d^2$  and  $m_u^2$  as follows:

$$U_d m_d^2 U_d^\dagger = \text{diag}(m_{d_1}^2, m_{d_2}^2, m_{d_3}^2, m_{d_4}^2, m_{d_5}^2, m_{d_6}^2),$$

$$m_d^2 = \begin{pmatrix} m_Q^2 + m_d^\dagger m_d & \frac{v}{\sqrt{2}} \cos \beta (\tilde{y}_d + y_d \mu^* \tan \beta)^\dagger \\ +m_Z^2 \cos 2\beta (-\frac{1}{2} + \frac{1}{3} \sin^2 \theta_W) \mathbf{1} & m_D^2 + m_d m_d^\dagger \\ \frac{v}{\sqrt{2}} \cos \beta (\tilde{y}_d + y_d \mu^* \tan \beta) & -\frac{1}{3} m_Z^2 \cos 2\beta \sin^2 \theta_W \mathbf{1} \end{pmatrix}, \quad (\text{C3a})$$

$$U_u m_u^2 U_u^\dagger = \text{diag}(m_{u_1}^2, m_{u_2}^2, m_{u_3}^2, m_{u_4}^2, m_{u_5}^2, m_{u_6}^2),$$

$$m_u^2 = \begin{pmatrix} m_Q^2 + m_u^\dagger m_u & -\frac{v}{\sqrt{2}} \sin \beta (\tilde{y}_u + y_u \mu^* \cot \beta)^\dagger \\ +m_z^2 \cos 2\beta (\frac{1}{2} - \frac{2}{3} \sin^2 \theta_W) \mathbf{1} & m_U^2 + m_u m_u^\dagger \\ -\frac{v}{\sqrt{2}} \sin \beta (\tilde{y}_u + y_u \mu^* \cot \beta) & +\frac{2}{3} m_z^2 \cos 2\beta \sin^2 \theta_W \mathbf{1} \end{pmatrix}, \quad (\text{C3b})$$

where generation indices are suppressed and the mass matrices for down-type and up-type quarks are given by  $(m_d)_{ij} = m_{di} \delta_j^i$  and  $(m_u)_{ij} = m_{ui} (V_{\text{CKM}})^i_j$ . The chargino-squark coupling constants in Eq. (C1) are given by

$$C_{iAX}^{dL} = g_2 \frac{m_{di}}{\sqrt{2} m_W \cos \beta} (O_{CL}^*)_{A2} (U_u^*)_{Xi}, \quad (\text{C4a})$$

$$C_{iAX}^{dR} = -g_2 \left\{ (O_{CR}^*)_{A1} (U_u^*)_{Xi} - \sum_{j=1}^3 \frac{(V_{\text{CKM}}^\dagger)^i_j m_{uj}}{\sqrt{2} m_W \sin \beta} (O_{CR}^*)_{A2} (U_u^*)_{Xj+3} \right\}, \quad (\text{C4b})$$

$$C_{iAX}^{uL} = g_2 \sum_{j=1}^3 \frac{m_{ui} (V_{\text{CKM}})^i_j}{\sqrt{2} m_W \cos \beta} (O_{CR})_{A2} (U_d^*)_{Xj}, \quad (\text{C4c})$$

$$C_{iAX}^{uR} = -g_2 \left\{ (O_{CL})_{A1} (U_d^*)_{Xi} - \frac{m_{di}}{\sqrt{2} m_W \cos \beta} (O_{CL})_{A2} (U_d^*)_{Xi+3} \right\}, \quad (\text{C4d})$$

where  $O_{CL}$  and  $O_{CR}$  are the diagonalization matrices for chargino mass matrix defined in Appendix B. The gluino-squark coupling constants in Eq. (C1) are given by

$$\Gamma_{iX}^{dL} = -\sqrt{2} g_3 (U_d^*)_{Xi+3}, \quad (\text{C5a})$$

$$\Gamma_{iX}^{dR} = \sqrt{2} g_3 (U_d^*)_{Xi}, \quad (\text{C5b})$$

$$\Gamma_{iX}^{uL} = -\sqrt{2} g_3 (U_u^*)_{Xi+3}, \quad (\text{C5c})$$

$$\Gamma_{iX}^{uR} = \sqrt{2} g_3 (U_u^*)_{Xi}. \quad (\text{C5d})$$

where  $g_3$  is the SU(3) gauge coupling constant.

The SUSY contribution to the effective FCNC coupling constants is divided into six parts as follows:

$$g = g(H^-) + g(H^-W) + g(\tilde{\chi}^0) + g(\tilde{\chi}^-) + g(\tilde{G}) + g(\tilde{G}\tilde{\chi}^0), \quad (\text{C6})$$

where  $g$  represents the effective coupling constants in Eq. (37) of Sec. IIIB and its generalization for  $B^0 - \bar{B}^0$  mixing. In the following, coupling constants  $g$  are associated with

indices  $i, j$ .  $K^0 - \bar{K}^0$  mixing corresponds to  $i = 1, j = 2$  and  $B_d - \bar{B}_d$  ( $B_s - \bar{B}_s$ ) mixing corresponds to  $i = 1, j = 3$  ( $i = 2, j = 3$ ). The contribution from box diagrams including charged Higgs and up-type quark is given by

$$g_R^V(H^-) = -\frac{\sqrt{2}G_F}{16\pi^2} \sum_{k,l=1}^3 (V_{\text{CKM}}^\dagger)^j_l (V_{\text{CKM}})^l_i (V_{\text{CKM}}^\dagger)^j_k (V_{\text{CKM}})^k_i \times m_{d_j}^2 m_{d_i}^2 \tan^4 \beta d_2(m_{H^-}^2, m_{H^-}^2, m_{u_k}^2, m_{u_l}^2), \quad (\text{C7a})$$

$$g_L^V(H^-) = -\frac{\sqrt{2}G_F}{16\pi^2} \sum_{k,l=1}^3 (V_{\text{CKM}}^\dagger)^j_l (V_{\text{CKM}})^l_i (V_{\text{CKM}}^\dagger)^j_k (V_{\text{CKM}})^k_i \times m_{u_l}^2 m_{u_k}^2 \cot^4 \beta d_2(m_{H^-}^2, m_{H^-}^2, m_{u_k}^2, m_{u_l}^2), \quad (\text{C7b})$$

$$g_{RR}^S(H^-) = -\frac{\sqrt{2}G_F}{16\pi^2} \sum_{k,l=1}^3 (V_{\text{CKM}}^\dagger)^j_l (V_{\text{CKM}})^l_i (V_{\text{CKM}}^\dagger)^j_k (V_{\text{CKM}})^k_i \times m_{d_j}^2 m_{u_l}^2 m_{u_k}^2 d_0(m_{H^-}^2, m_{H^-}^2, m_{u_k}^2, m_{u_l}^2), \quad (\text{C7c})$$

$$g_{LL}^S(H^-) = -\frac{\sqrt{2}G_F}{16\pi^2} \sum_{k,l=1}^3 (V_{\text{CKM}}^\dagger)^j_l (V_{\text{CKM}})^l_i (V_{\text{CKM}}^\dagger)^j_k (V_{\text{CKM}})^k_i \times m_{u_l}^2 m_{u_k}^2 m_{d_i}^2 d_0(m_{H^-}^2, m_{H^-}^2, m_{u_k}^2, m_{u_l}^2), \quad (\text{C7d})$$

$$g_{RR}^{S'}(H^-) = g_{LL}^{S'}(H^-) = 0, \quad (\text{C7e})$$

$$g_{RL}^S(H^-) = -\frac{\sqrt{2}G_F}{16\pi^2} \sum_{k,l=1}^3 (V_{\text{CKM}}^\dagger)^j_l (V_{\text{CKM}})^l_i (V_{\text{CKM}}^\dagger)^j_k (V_{\text{CKM}})^k_i \times m_{d_j} m_{u_l}^2 m_{u_k}^2 m_{d_i} d_0(m_{H^-}^2, m_{H^-}^2, m_{u_k}^2, m_{u_l}^2), \quad (\text{C7f})$$

$$g_{RL}^{S'}(H^-) = \frac{\sqrt{2}G_F}{8\pi^2} \sum_{k,l=1}^3 (V_{\text{CKM}}^\dagger)^j_l (V_{\text{CKM}})^l_i (V_{\text{CKM}}^\dagger)^j_k (V_{\text{CKM}})^k_i \times m_{d_j} m_{u_k}^2 m_{d_i} d_2(m_{H^-}^2, m_{H^-}^2, m_{u_k}^2, m_{u_l}^2). \quad (\text{C7g})$$

where  $m_{H^-}$  is the charged Higgs mass. The contribution from box diagrams including charged Higgs, W boson and up-type quark is given by

$$g_R^V(H^- W) = 0, \quad (\text{C8a})$$

$$\begin{aligned}
g_L^V(H^-W) = & -\frac{\sqrt{2}G_F}{8\pi^2} \sum_{k,l=1}^3 (V_{\text{CKM}}^\dagger)^j_l (V_{\text{CKM}})^l_i (V_{\text{CKM}}^\dagger)^j_k (V_{\text{CKM}})^k_i \\
& \times m_{u_l}^2 m_{u_k}^2 \cot^2 \beta \left\{ d_2(m_{H^-}^2, m_W^2, m_{u_k}^2, m_{u_l}^2) \right. \\
& \left. - m_W^2 d_0(m_{H^-}^2, m_W^2, m_{u_k}^2, m_{u_l}^2) \right\}, \quad (\text{C8b})
\end{aligned}$$

$$g_{RR}^S(H^-W) = g_{LL}^S(H^-W) = g_{RR}^{S'}(H^-W) = g_{LL}^{S'}(H^-W) = 0, \quad (\text{C8c})$$

$$\begin{aligned}
g_{RL}^S(H^-W) = & \frac{\sqrt{2}G_F}{2\pi^2} \sum_{k,l=1}^3 (V_{\text{CKM}}^\dagger)^j_l (V_{\text{CKM}})^l_i (V_{\text{CKM}}^\dagger)^j_k (V_{\text{CKM}})^k_i \\
& \times m_{d_j} m_{d_i} m_W^2 \tan^2 \beta \left\{ d_2(m_{H^-}^2, m_W^2, m_{u_k}^2, m_{u_l}^2) \right. \\
& \left. - \frac{m_{u_k}^2 m_{u_l}^2}{4m_W^2} d_0(m_{H^-}^2, m_W^2, m_{u_k}^2, m_{u_l}^2) \right\}, \quad (\text{C8d})
\end{aligned}$$

$$g_{RL}^{S'}(H^-W) = 0. \quad (\text{C8e})$$

The contribution from box diagrams including neutralino and down-type squark is given by

$$\begin{aligned}
g_R^V(\tilde{\chi}^0) = & -\frac{\sqrt{2}}{128\pi^2 G_F} \sum_{A,B=1}^4 \sum_{X,Y=1}^6 N_{jBY}^{dL} N_{iAY}^{dL*} \\
& \times \left\{ N_{jAX}^{dL} N_{iBX}^{dL*} d_2(m_{\chi_A^0}^2, m_{\chi_B^0}^2, m_{\tilde{d}_X}^2, m_{\tilde{d}_Y}^2) \right. \\
& \left. + N_{jBX}^{dL} N_{iAX}^{dL*} \frac{m_{\chi_A^0} m_{\chi_B^0}}{2} d_0(m_{\chi_A^0}^2, m_{\chi_B^0}^2, m_{\tilde{d}_X}^2, m_{\tilde{d}_Y}^2) \right\}, \quad (\text{C9a})
\end{aligned}$$

$$\begin{aligned}
g_{RR}^S(\tilde{\chi}^0) = & \frac{\sqrt{2}}{128\pi^2 G_F} \sum_{A,B=1}^4 \sum_{X,Y=1}^6 N_{jBY}^{dR} N_{iAY}^{dL*} N_{jBX}^{dR} N_{iAX}^{dL*} \\
& \times m_{\tilde{\chi}_A^0} m_{\tilde{\chi}_B^0} d_0(m_{\tilde{\chi}_A^0}^2, m_{\tilde{\chi}_B^0}^2, m_{\tilde{d}_X}^2, m_{\tilde{d}_Y}^2), \quad (\text{C9b})
\end{aligned}$$

$$\begin{aligned}
g_{RR}^{S'}(\tilde{\chi}^0) = & \frac{\sqrt{2}}{128\pi^2 G_F} \sum_{A,B=1}^4 \sum_{X,Y=1}^6 N_{jBY}^{dR} N_{iAY}^{dL*} (N_{jBX}^{dR} N_{iAX}^{dL*} - N_{jAX}^{dR} N_{iBX}^{dL*}) \\
& \times m_{\tilde{\chi}_A^0} m_{\tilde{\chi}_B^0} d_0(m_{\tilde{\chi}_A^0}^2, m_{\tilde{\chi}_B^0}^2, m_{\tilde{d}_X}^2, m_{\tilde{d}_Y}^2), \quad (\text{C9c})
\end{aligned}$$

$$\begin{aligned}
g_{RL}^S(\tilde{\chi}^0) = & \frac{\sqrt{2}}{64\pi^2 G_F} \sum_{A,B=1}^4 \sum_{X,Y=1}^6 N_{jBY}^{dR} N_{iAY}^{dL*} (N_{jBX}^{dL} N_{iAX}^{dR*} + N_{jAX}^{dL} N_{iBX}^{dR*}) \\
& \times d_2(m_{\tilde{\chi}_A^0}^2, m_{\tilde{\chi}_B^0}^2, m_{\tilde{d}_X}^2, m_{\tilde{d}_Y}^2), \quad (\text{C9d})
\end{aligned}$$

$$\begin{aligned}
g_{RL}^{S'}(\tilde{\chi}^0) = & -\frac{\sqrt{2}}{128\pi^2 G_F} \sum_{A,B=1}^4 \sum_{X,Y=1}^6 N_{jBY}^{dR} N_{iAY}^{dR*} \\
& \left\{ 2N_{jBX}^{dL} N_{iAX}^{dL*} d_2(m_{\tilde{\chi}_A^0}^2, m_{\tilde{\chi}_B^0}^2, m_{\tilde{d}_X}^2, m_{\tilde{d}_Y}^2) \right. \\
& \left. + N_{jAX}^{dL} N_{iBX}^{dL*} m_{\tilde{\chi}_A^0} m_{\tilde{\chi}_B^0} d_0(m_{\tilde{\chi}_A^0}^2, m_{\tilde{\chi}_B^0}^2, m_{\tilde{d}_X}^2, m_{\tilde{d}_Y}^2) \right\}, \quad (C9e)
\end{aligned}$$

The contribution from box diagrams including chargino and up-type squark is given by

$$g_R^V(\tilde{\chi}^-) = -\frac{\sqrt{2}}{128\pi^2 G_F} \sum_{A,B=1}^2 \sum_{X,Y=1}^6 C_{jBY}^{dL} C_{iAY}^{dL*} C_{jAX}^{dL} C_{iBX}^{dL*} d_2(m_{\tilde{\chi}_A^-}^2, m_{\tilde{\chi}_B^-}^2, m_{\tilde{u}_X}^2, m_{\tilde{u}_Y}^2), \quad (C10a)$$

$$g_{RR}^S(\tilde{\chi}^-) = 0, \quad (C10b)$$

$$\begin{aligned}
g_{RR}^{S'}(\tilde{\chi}^-) = & -\frac{\sqrt{2}}{128\pi^2 G_F} \sum_{A,B=1}^2 \sum_{X,Y=1}^6 C_{jBY}^{dR} C_{iAY}^{dL*} C_{jAX}^{dR} C_{iBX}^{dL*} \\
& \times m_{\tilde{\chi}_A^-} m_{\tilde{\chi}_B^-} d_0(m_{\tilde{\chi}_A^-}^2, m_{\tilde{\chi}_B^-}^2, m_{\tilde{u}_X}^2, m_{\tilde{u}_Y}^2), \quad (C10c)
\end{aligned}$$

$$g_{RL}^S(\tilde{\chi}^-) = \frac{\sqrt{2}}{64\pi^2 G_F} \sum_{A,B=1}^2 \sum_{X,Y=1}^6 C_{jBY}^{dR} C_{iAY}^{dL*} C_{jAX}^{dL} C_{iBX}^{dR*} d_2(m_{\tilde{\chi}_A^-}^2, m_{\tilde{\chi}_B^-}^2, m_{\tilde{u}_X}^2, m_{\tilde{u}_Y}^2), \quad (C10d)$$

$$\begin{aligned}
g_{RL}^{S'}(\tilde{\chi}^-) = & -\frac{\sqrt{2}}{128\pi^2 G_F} \sum_{A,B=1}^2 \sum_{X,Y=1}^6 C_{jBY}^{dL} C_{iAY}^{dL*} C_{jAX}^{dR} C_{iBX}^{dR*} \\
& \times m_{\tilde{\chi}_A^-} m_{\tilde{\chi}_B^-} d_0(m_{\tilde{\chi}_A^-}^2, m_{\tilde{\chi}_B^-}^2, m_{\tilde{u}_X}^2, m_{\tilde{u}_Y}^2), \quad (C10e)
\end{aligned}$$

The contribution from box diagrams including gluino and down-type squark is given by

$$\begin{aligned}
g_R^V(\tilde{G}) = & -\frac{\sqrt{2}}{128\pi^2 G_F} \sum_{X,Y=1}^6 \Gamma_{jY}^{dL} \Gamma_{iY}^{dL*} \Gamma_{jX}^{dL} \Gamma_{iX}^{dL*} \left\{ \frac{11}{18} d_2(M_3^2, M_3^2, m_{\tilde{d}_X}^2, m_{\tilde{d}_Y}^2) \right. \\
& \left. + \frac{1}{18} M_3^2 d_0(M_3^2, M_3^2, m_{\tilde{d}_X}^2, m_{\tilde{d}_Y}^2) \right\}, \quad (C11a)
\end{aligned}$$

$$g_{RR}^S(\tilde{G}) = -\frac{\sqrt{2}}{128\pi^2 G_F} \sum_{X,Y=1}^6 \frac{17}{36} \Gamma_{jY}^{dR} \Gamma_{iY}^{dL*} \Gamma_{jX}^{dR} \Gamma_{iX}^{dL*} M_3^2 d_0(M_3^2, M_3^2, m_{\tilde{d}_X}^2, m_{\tilde{d}_Y}^2), \quad (C11b)$$

$$g_{RR}^{S'}(\tilde{G}) = \frac{\sqrt{2}}{128\pi^2 G_F} \sum_{X,Y=1}^6 \frac{1}{12} \Gamma_{jY}^{dR} \Gamma_{iY}^{dL*} \Gamma_{jX}^{dR} \Gamma_{iX}^{dL*} M_3^2 d_2(M_3^2, M_3^2, m_{\tilde{d}_X}^2, m_{\tilde{d}_Y}^2), \quad (C11c)$$

$$\begin{aligned}
g_{RL}^S(\tilde{G}) = & -\frac{\sqrt{2}}{128\pi^2 G_F} \sum_{X,Y=1}^6 \left\{ \left( -\frac{1}{3} \Gamma_{jY}^{dR} \Gamma_{iY}^{dR*} \Gamma_{jX}^{dL} \Gamma_{iX}^{dL*} - \frac{11}{18} \Gamma_{jY}^{dL} \Gamma_{iY}^{dR*} \Gamma_{jX}^{dR} \Gamma_{iX}^{dL*} \right) \right. \\
& \left. \times d_2(M_3^2, M_3^2, m_{\tilde{d}_X}^2, m_{\tilde{d}_Y}^2) \right\}
\end{aligned}$$

$$+\frac{7}{12}\Gamma_{jY}^{dL}\Gamma_{iY}^{dL*}\Gamma_{jX}^{dR}\Gamma_{iX}^{dR*}M_3^2 d_0(M_3^2, M_3^2, m_{\tilde{d}_X}^2, m_{\tilde{d}_Y}^2)\Big\}, \quad (\text{C11d})$$

$$g_{RL}^{S'}(\tilde{G}) = -\frac{\sqrt{2}}{128\pi^2 G_F} \sum_{X,Y=1}^6 \left\{ \left( -\frac{5}{6}\Gamma_{jY}^{dL}\Gamma_{iY}^{dR*}\Gamma_{jX}^{dR}\Gamma_{iX}^{dL*} + \frac{5}{9}\Gamma_{jY}^{dR}\Gamma_{iY}^{dR*}\Gamma_{jX}^{dL}\Gamma_{iX}^{dL*} \right) \right. \\ \times d_2(M_3^2, M_3^2, m_{\tilde{d}_X}^2, m_{\tilde{d}_Y}^2) \\ \left. + \frac{1}{36}\Gamma_{jY}^{dL}\Gamma_{iY}^{dL*}\Gamma_{jX}^{dR}\Gamma_{iX}^{dR*}M_3^2 d_0(M_3^2, M_3^2, m_{\tilde{d}_X}^2, m_{\tilde{d}_Y}^2) \right\}, \quad (\text{C11e})$$

The contribution from box diagrams including neutralino, gluino and down-type squark is given by

$$g_R^V(\tilde{G}\tilde{\chi}^0) = -\frac{\sqrt{2}}{128\pi^2 G_F} \sum_{A=1}^4 \sum_{X,Y=1}^6 \left\{ \frac{2}{3}N_{jAY}^{dL}\Gamma_{iY}^{dL*}\Gamma_{jX}^{dL}N_{iAX}^{dL*} d_2(m_{\tilde{\chi}_A^0}^2, M_3^2, m_{\tilde{d}_X}^2, m_{\tilde{d}_Y}^2) \right. \\ \left. + \frac{1}{6} \left( N_{jAY}^{dL}\Gamma_{iY}^{dL*}N_{jAX}^{dL}\Gamma_{iX}^{dL*} + \Gamma_{jY}^{dL}N_{iAY}^{dL*}\Gamma_{jX}^{dL}N_{iAX}^{dL*} \right) \right. \\ \left. \times m_{\tilde{\chi}_A^0} M_3 d_0(m_{\tilde{\chi}_A^0}^2, M_3^2, m_{\tilde{d}_X}^2, m_{\tilde{d}_Y}^2) \right\}, \quad (\text{C12a})$$

$$g_{RR}^S(\tilde{G}\tilde{\chi}^0) = -\frac{\sqrt{2}}{128\pi^2 G_F} \sum_{A=1}^4 \sum_{X,Y=1}^6 \left\{ N_{jAY}^{dR}\Gamma_{iY}^{dL*}\Gamma_{jX}^{dR}N_{iAX}^{dL*} \right. \\ \left. - \frac{1}{3} \left( N_{jAY}^{dR}\Gamma_{iY}^{dL*}N_{jAX}^{dR}\Gamma_{iX}^{dL*} + \Gamma_{jY}^{dR}N_{iAY}^{dL*}\Gamma_{jX}^{dR}N_{iAX}^{dL*} \right) \right\} \\ \times m_{\tilde{\chi}_A^0} M_3 d_0(m_{\tilde{\chi}_A^0}^2, M_3^2, m_{\tilde{d}_X}^2, m_{\tilde{d}_Y}^2), \quad (\text{C12b})$$

$$g_{RR}^{S'}(\tilde{G}\tilde{\chi}^0) = \frac{\sqrt{2}}{128\pi^2 G_F} \sum_{A=1}^4 \sum_{X,Y=1}^6 \frac{1}{3} \left( N_{jAY}^{dR}\Gamma_{iY}^{dL*}\Gamma_{jX}^{dR}N_{iAX}^{dL*} \right. \\ \left. + N_{jAY}^{dR}\Gamma_{iY}^{dL*}N_{jAX}^{dR}\Gamma_{iX}^{dL*} + \Gamma_{jY}^{dR}N_{iAY}^{dL*}\Gamma_{jX}^{dR}N_{iAX}^{dL*} \right) \\ \times m_{\tilde{\chi}_A^0} M_3 d_0(m_{\tilde{\chi}_A^0}^2, M_3^2, m_{\tilde{d}_X}^2, m_{\tilde{d}_Y}^2), \quad (\text{C12c})$$

$$g_{RL}^S(\tilde{G}\tilde{\chi}^0) = -\frac{\sqrt{2}}{128\pi^2 G_F} \sum_{A=1}^4 \sum_{X,Y=1}^6 \left[ \left\{ \frac{1}{3}(N_{jAY}^{dL}\Gamma_{iY}^{dR*} + \Gamma_{jY}^{dL}N_{iAY}^{dR*})(\Gamma_{jX}^{dR}N_{iAX}^{dL*} + N_{jAX}^{dR}\Gamma_{iX}^{dL*}) \right. \right. \\ \left. \left. + (N_{jAY}^{dR}\Gamma_{iY}^{dR*}N_{jAX}^{dL}\Gamma_{iX}^{dL*} + \Gamma_{jY}^{dR}N_{iAY}^{dR*}\Gamma_{jX}^{dL}N_{iAX}^{dL*}) \right\} \right. \\ \left. \times d_2(m_{\tilde{\chi}_A^0}^2, M_3^2, m_{\tilde{d}_X}^2, m_{\tilde{d}_Y}^2) \right]$$

$$\begin{aligned}
& + \frac{1}{2} \left( N_{jAY}^{dL} \Gamma_{iY}^{dL*} \Gamma_{jX}^{dR} N_{iAX}^{dR*} + \Gamma_{jY}^{dL} N_{iAY}^{dL*} N_{jAX}^{dR} \Gamma_{iX}^{dR*} \right) \\
& \times m_{\tilde{\chi}_A^0} M_3 d_0(m_{\tilde{\chi}_A^0}^2, M_3^2, m_{\tilde{d}_X}^2, m_{\tilde{d}_Y}^2) \Big], \quad (C12d)
\end{aligned}$$

$$\begin{aligned}
g_{RL}^{S'}(\tilde{G}\tilde{\chi}^0) &= \frac{\sqrt{2}}{128\pi^2 G_F} \sum_{A=1}^4 \sum_{X,Y=1}^6 \left[ \left\{ (N_{jAY}^{dL} \Gamma_{iY}^{dR*} + \Gamma_{jY}^{dL} N_{iAY}^{dR*}) (N_{jAX}^{dR} \Gamma_{iX}^{dL*} + \Gamma_{jX}^{dR} N_{iAX}^{dL*}) \right. \right. \\
& + \frac{1}{3} \left( N_{jAY}^{dR} \Gamma_{iY}^{dR*} N_{jAX}^{dL} \Gamma_{iX}^{dL*} + \Gamma_{jY}^{dR} N_{iAY}^{dR*} \Gamma_{jX}^{dL} N_{iAX}^{dL*} \right) \Big\} \\
& \times d_2(m_{\tilde{\chi}_A^0}^2, M_3^2, m_{\tilde{d}_X}^2, m_{\tilde{d}_Y}^2) \\
& + \frac{1}{6} \left( N_{jAY}^{dL} \Gamma_{iY}^{dL*} \Gamma_{jX}^{dR} N_{iAX}^{dR*} + \Gamma_{jY}^{dL} N_{iAY}^{dL*} N_{jAX}^{dR} \Gamma_{iX}^{dR*} \right) \\
& \times M_3 m_{\tilde{\chi}_A^0} d_0(m_{\tilde{\chi}_A^0}^2, M_3^2, m_{\tilde{d}_X}^2, m_{\tilde{d}_Y}^2) \Big], \quad (C12e)
\end{aligned}$$

The neutralino, chargino, gluino and neutralino-gluino contributions to  $g_L^V$ ,  $g_{LL}^S$  and  $g_{LL}^{S'}$  are obtained by replacing the suffix  $R$  with  $L$  and  $L$  with  $R$  in the corresponding formulas for  $g_R^V$ ,  $g_{RR}^S$  and  $g_{RR}^{S'}$ , respectively. The mass functions which appear in the above formulas are defined as follows:

$$\begin{aligned}
d_0(x, y, z, w) &= \frac{x \ln(x)}{(y-x)(z-x)(w-x)} + \frac{y \ln(y)}{(x-y)(z-y)(w-y)} \\
& + \frac{z \ln(z)}{(x-z)(y-z)(w-z)} + \frac{w \ln(w)}{(x-w)(y-w)(z-w)}, \quad (C13a)
\end{aligned}$$

$$\begin{aligned}
d_2(x, y, z, w) &= \frac{1}{4} \left\{ \frac{x^2 \ln(x)}{(y-x)(z-x)(w-x)} + \frac{y^2 \ln(y)}{(x-y)(z-y)(w-y)} \right. \\
& + \left. \frac{z^2 \ln(z)}{(x-z)(y-z)(w-z)} + \frac{w^2 \ln(w)}{(x-w)(y-w)(z-w)} \right\}. \quad (C13b)
\end{aligned}$$

## REFERENCES

- [1] Muon  $g - 2$  Collaboration, H.N. Brown *et al.*, hep-ex/0102017.
- [2] J. Ellis and D.V. Nanopoulos, Phys. Lett. B **110**, 44 (1982); R. Barbieri and R. Gatto, Phys. Lett. B **110**, 211 (1982); T. Inami and C.S. Lim, Nucl. Phys. **B207**, 533 (1982).
- [3] M.J. Duncan, Nucl. Phys. **B221**, 285 (1983); J.F. Donoghue, H.P. Nilles and D. Wyler, Phys. Lett. B **128**, 55 (1983); A. Bouquet, J. Kaplan and C.A. Savoy, Phys. Lett. B **148**, 69 (1984).
- [4] L.J. Hall, V.A. Kostelecky and S. Raby, Nucl. Phys. **B267**, 415 (1986).
- [5] T. Kurimoto, Phys. Rev. D **39**, 3447 (1989); G.C. Branco, G.C. Cho, Y. Kizukuri and N. Oshimo, Phys. Lett. B **337**, 316 (1994).
- [6] S. Bertolini, F. Borzumati, A. Masiero and G. Ridolfi, Nucl. Phys. **B353**, 590 (1991).
- [7] T. Goto, T. Nihei and Y. Okada, Phys. Rev. D **53**, 5233 (1996); Erratum-*ibid.* **54**, 5904 (1996); T. Goto, Y. Okada and Y. Shimizu, Phys. Rev. D **58**, 094006 (1998).
- [8] T. Goto, Y. Okada and Y. Shimizu, KEK-Preprint-99-72, KEK-TH-611, hep-ph/9908499.
- [9] F. Gabbiani and A. Masiero, Nucl. Phys. **B322**, 235 (1989); J.S. Hagelin, S. Kelley and T. Tanaka, Nucl. Phys. **B415**, 293 (1994).
- [10] R. Barbieri and L.J. Hall, Phys. Lett. B **338**, 212 (1994); R. Barbieri, L. Hall and A. Strumia, Nucl. Phys. **B445**, 219 (1995).
- [11] R. Barbieri, L. Hall and A. Strumia, Nucl. Phys. **B449**, 437 (1995); N. G. Deshpande, B. Dutta and S. Oh, Phys. Rev. Lett. **77**, 4499 (1996).
- [12] P. Ciafaloni, A. Romanino and A. Strumia, Nucl. Phys. **B458**, 3 (1996); N. Arkani-Hamed, H. Cheng and L.J. Hall, Phys. Rev. D **53**, 413 (1996); T.V. Duong, B. Dutta and E. Keith Phys. Lett. B **378**, 128 (1996); M.E. Gómez and H. Goldberg, Phys.

- Rev. D **53**, 5244 (1996); N.G. Deshpande, B. Dutta and E. Keith Phys. Rev. D **54**, 730 (1996); J. Hisano, T. Moroi, K. Tobe and M. Yamaguchi, Phys. Lett. B **391**, 341 (1997), Erratum-*ibid.* **397**, 357 (1997); J. Hisano, D. Nomura, Y. Okada, Y. Shimizu and M. Tanaka, Phys. Rev. D **58**, 116010 (1998); G. Barenboim, K. Huitu and M. Raidal, Phys. Rev. D **63**, 055006 (2001).
- [13] Super-Kamiokande Collaboration, Y. Fukuda *et al.*, Phys. Rev. Lett. **81**, 1562 (1998); E. Kearns, talk at the 30th International Conference on High Energy Physics (ICHEP 2000), Osaka, 2000.
- [14] T. Yanagida, in *Proceedings of the Workshop on Unified Theory and Baryon Number of the Universe*, Tsukuba, Japan, 1979, edited by O. Sawada and A. Sugamoto; M. Gell-Mann, P. Ramond and R. Slansky, in *Supergravity*, 1979, edited by P. van Nieuwenhuizen and D. Freedman (North-Holland, Amsterdam).
- [15] F. Borzumati and A. Masiero, Phys. Rev. Lett. **57**, 961 (1986); J. Hisano, T. Moroi, K. Tobe, M. Yamaguchi and T. Yanagida, Phys. Lett. B **357**, 579 (1995); J. Hisano, T. Moroi, K. Tobe and M. Yamaguchi, Phys. Rev. D **53**, 2442 (1996); J.A. Casas and A. Ibarra, hep-ph/0103065.
- [16] J. Hisano and D. Nomura, T. Yanagida Phys. Lett. B **437**, 351 (1998).
- [17] J. Hisano and D. Nomura, Phys. Rev. D **59**, 116005 (1999).
- [18] M.E. Gómez, G.K. Leontaris, S. Lola and J.D. Vargados, Phys. Lett. B **459**, 116009 (1999); W. Buchmuller, D. Delepine and F. Vissani, Phys. Lett. B **459**, 171 (1999); J. Ellis, M.E. Gómez, G.K. Leontaris, S. Lola and D.V. Nanopoulos, Eur. Phys J. C **14**, 319 (2000); W. Buchmuller, D. Delepine, L.T. Handoko Nucl. Phys. **B576**, 445 (2000); J.L. Feng, Y. Nir and Y. Shadmi, Phys. Rev. D **61**, 113005 (2000); J. Sato, K. Tobe, T. Yanagida, Phys. Lett. B **498**, 189 (2001); J. Sato and K. Tobe, hep-ph/0012333.
- [19] S. Baek, T. Goto, Y. Okada and K. Okumura, Phys. Rev. D **63**, 051701(R) (2001); talk

- at the 30th International Conference on High-Energy Physics (ICHEP 2000), Osaka, 2000, hep-ph/0009196.
- [20] T. Moroi, J. High Energy Phys. **03**, 019 (2000); Phys. Lett. B **493**, 366 (2000).
  - [21] A. Czarnecki and W.J. Marciano, hep-ph/0102122; L. Everett, G.L. Kane, S. Rigolin and L.-T. Wang, hep-ph/0102145; J.L. Feng and K. Matchev, hep-ph/0102146; E.A. Baltz, P. Gondolo, hep-ph/0102147; U. Chattopadhyay and P. Nath, hep-ph/0102157; S. Komine, T. Moroi and M. Yamaguchi, hep-ph/0102204; J. Hisano and K. Tobe, hep-ph/0102315; T. Ibrahim, U. Chattopadhyay and P. Nath, hep-ph/0102324; J. Ellis, D.V. Nanopoulos and K.A. Olive, hep-ph/0102331; K. Choi, K. Hwang, S.K. Kang, K.Y. Lee and W.Y. Song, hep-ph/0103048; S. Baek, P. Ko and H.S. Lee, hep-ph/0103218; D.F. Carvalho, J. Ellis, M.E. Gómez and S. Lola, hep-ph/0103256; H. Baer, C. Balázs, J. Ferrandis and X. Tata, hep-ph/0103280.
  - [22] Z. Maki, M. Nakagawa, S. Sakata, Prog. Theor. Phys. **28**, 870 (1962).
  - [23] CHOOZ Collaboration, M. Apollonio *et al.*, Phys. Lett. B **466**, 466 (1999).
  - [24] P. Fayet, in Unification of the Fundamental Particles Interactions, edited by S. Ferrara, J. Ellis and P. van Nieuwenhuizen (Plenum, New York, 1980) p. 587; J.A. Grifols and A. Mendez, Phys. Rev. D **26**, 1809 (1982); J. Ellis, H.S. Hagelin and D.V. Nanopoulos, Phys. Lett. B **116**, 283 (1982); R. Barbieri and L. Maiani, Phys. Lett. B **117**, 203 (1982); D.A. Kosower, L.M. Krauss, and N. Sakai, Phys. Lett. B **133**, 305 (1983); T.C. Yuan, R. Arnowitt, A.H. Chamseddine, and P. Nath, Z. Phys. C **26**, 407 (1984); T. Moroi, Phys. Rev. D **53**, 6565 (1996).
  - [25] J. Lopez, D.V. Nanopoulos and X. Wang, Phys. Rev. D **49**, 366 (1994); U. Chattopadhyay and P. Nath, Phys. Rev. D **53**, 1648 (1996).
  - [26] Y. Okada, K. Okumura and Y. Shimizu, Phys. Rev. D **61**, 094001 (2000).
  - [27] R. Kitano and Y. Okada, KEK-preprint-2000-131, KEK-TH-732, hep-ph/0012040, to

be published in Phys. Rev. D .

- [28] D. Atwood, M. Gronau and A. Soni, Phys. Rev. Lett. **79**, 185 (1997); C. Chua, X. He and W. Hou, Phys. Rev. D **60**, 014003 (1999).
- [29] A.J. Buras, M. Jamin and P.H. Weisz, Nucl. Phys. **B347**, 491 (1990); I.I. Bigi and F. Gabbiani, Nucl. Phys. **B352**, 309 (1991); S. Herrlich and U. Nierste, Nucl. Phys. **B419**, 292 (1994); S. Herrlich and U. Nierste, Nucl. Phys. **B476**, 27 (1996); J. Urban, F. Krauss, U. Jentschura and G. Soff, Nucl. Phys. **B523**, 40 (1998).
- [30] CDF Collaboration, Phys. Rev. D **56**, 1357 (1997); D0 Collaboration, Phys. Rev. Lett. **75**, 618 (1995); ALEPH Collaboration, Phys. Lett. B **499**, 67 (2001).
- [31] ALEPH Collaboration, Phys. Lett. B **499**, 53 (2001); L3 Collaboration, Phys. Lett. B **503**, 21 (2001); DELPHI Collaboration, Phys. Lett. B **499**, 23 (2001); OPAL Collaboration, Phys. Lett. B **499**, 38 (2001).
- [32] CLEO Collaboration, T. Coan, talk at the 30th International Conference on High-Energy Physics (ICHEP 2000), Osaka, 2000; Belle Collaboration, KEK-preprint-2001-3, BELLE-preprint-2001-2 , hep-ex/0103042.
- [33] L. Chau and W. Keung, Phys. Rev. Lett. **53**, 1802 (1984).
- [34] MEGA Collaboration, M.L. Brooks *et al.*, Phys. Rev. Lett. **83**, 1521 (1999).
- [35] Belle Collaboration, Phys. Rev. Lett. **86**, 2509 (2001); BaBar Collaboration, Phys. Rev. Lett. **86**, 2515 (2001).
- [36] N. Yamada, S. Hashimoto, K. Ishikawa, H. Matsufuru and T. Onogi, Nucl. Phys. Proc. Suppl. **83**, 340 (2000); JLQCD Collaboration, S. Aoki *et al.*, Phys. Rev. D **60**, 034511 (1999); R. Gupta, T. Bhattacharya and S. Sharpe, Phys. Rev. D **55**, 4036 (1997); M. Ciuchini *et al.*, J. High Energy Phys. **10**, 008 (1998); CP-PACS Collaboration, A. Ali Khan *et al.*, Nucl. Phys. Proc. Suppl. **83**, 265 (2000).

- [37] CDF Collaboration, Phys. Rev. D **61**, 072005 (2000).
- [38] T. Goto and T. Nihei, Phys. Rev. D **59**, 115009 (1999); K.S. Babu and M.J. Strassler, hep-ph/9808447; T. Goto and T. Nihei, in *Proceedings of the KIAS-CTP International Symposium on Supersymmetry, Supergravity and Superstring*, Seoul, Korea, 1999, edited by J.E. Kim and C. Lee.
- [39] J. Hisano, H. Murayama and T. Yanagida, Phys. Lett. B **291**, 263 (1992); K.S. Babu and S.M. Barr, Phys. Rev. D **48**, 5354 (1993); J. Hisano, T. Moroi, K. Tobe and T. Yanagida, Phys. Lett. B **342**, 138 (1995); K.S. Babu and S.M. Barr, Phys. Rev. D **51**, 2463 (1995).
- [40] Y. Kuno and Y. Okada, Rev. Mod. Phys. **73**, 151 (2001).
- [41] A. Czarnecki, W.J. Marciano and K. Melnikov, in *Proceedings of Workshop on Physics at the First Muon Collider and at the Front End of the Muon Collider*, Fermilab, 1997, edited by S.H. Geer and R. Raja, AIP Conf. Proc. No. 435 (AIP, New York), p.409.
- [42] P.G. Harris *et al.*, Phys. Rev. Lett. **82**, 904 (1999).
- [43] E.D. Commins *et al.*, Phys. Rev. A **50**, 2960 (1994).
- [44] L.M. Barkov *et al.*, “Search for the decay  $\mu^+ \rightarrow e^+ \gamma$  down to  $10^{-14}$  branching ratio”, Research Proposal to Paul Scherrer Institut (1999).
- [45] MECO Collaboration, M. Bachman *et al.*, “A Search for  $\mu^- N \rightarrow e^- N$  with sensitivity below  $10^{-16}$ ”, experimental proposal E940 to Brookhaven National Laboratory, AGS (1997).

TABLES

$m_t^{\text{pole}}$	$m_b^{\text{pole}}$	$m_s^{\overline{\text{MS}}}(2 \text{ GeV})$	$V_{cb}$	$ V_{ub}/V_{cb} $	$\delta_{13}$
175 GeV	4.8 GeV	120 MeV	0.04	0.08	$60^\circ$

TABLE I. Input parameters used in the numerical calculation.  $|V_{ub}/V_{cb}|$  and  $\delta_{13}$  are varied in Fig. 14.

	LMA	SMA
$\sin^2 2\theta_{\text{sun}}$	1	$5.5 \times 10^{-3}$
$\sin^2 2\theta_{\text{atm}}$	1	1
$\theta_{13}$	0	0
$\Delta m_{12}^2 \text{ (eV}^2\text{)}$	$1.8 \times 10^{-5}$	$5.0 \times 10^{-6}$
$\Delta m_{23}^2 \text{ (eV}^2\text{)}$	$3.5 \times 10^{-3}$	$3.5 \times 10^{-3}$
$m_{\nu_1} \text{ (eV)}$	$4.0 \times 10^{-3}$	$2.2 \times 10^{-3}$

TABLE II. Parameters for the neutrino sector. LMA (SMA) corresponds to the large (small) mixing angle MSW solution for the solar neutrino anomaly.

	(a)	(b)	(c)	(d)	(e)	(f)	(g)
neutrino	LMA	LMA	LMA	LMA	LMA	SMA	SMA
$M_R \text{ (GeV)}$	$4 \times 10^{13}$	$4 \times 10^{13}$	$4 \times 10^{13}$	$4 \times 10^{13}$	$4 \times 10^{14}$	$4 \times 10^{13}$	$4 \times 10^{14}$
$\theta_D$	0	0	$45^\circ$	0	0	0	0
$\tan \beta$	20	20	20	5	20	20	5
$A_0$	0	2	0	0	0	0	2.5

TABLE III. Parameters for Fig. 11.

$f_{B_d}$	$f_{B_s}/f_{B_d}$	$B_B$	$(B_B)_{RL}^S$	$(B_B)_{RL}^{S'}$	$B_K$	$(B_K)_{RL}^S$	$(B_K)_{RL}^{S'}$
210 MeV	1.17	0.8	0.8	0.8	0.69	1.03	0.73

TABLE IV. Decay constants and bag parameters for  $B^0 - \bar{B}^0$  and  $K^0 - \bar{K}^0$  mixing matrix elements used in the numerical calculation [36].

	(a)	(b)	(c)	(d)	(e)	(f)	(g)
$a_\mu^{\text{SUSY}} [10^{-10}]$	$\lesssim 50$	$\lesssim 50$	$\lesssim 10$	–	–	$\lesssim 50$	–
$B(\mu \rightarrow e \gamma)$	$\checkmark$	$\checkmark$	$\checkmark$	$\lesssim 10^{-13}$	$\checkmark$	$\lesssim 10^{-13}$	$\checkmark$
$B(\tau \rightarrow \mu \gamma)$	$\lesssim 10^{-9}$	$\lesssim 10^{-9}$	$\lesssim 10^{-9}$	$\lesssim 10^{-10}$	$\lesssim 10^{-9}$	$\lesssim 10^{-8}$	$\lesssim 10^{-7}$
$\varepsilon_K/(\varepsilon_K)_{\text{SM}} - 1$	$\lesssim 0.1$	$\lesssim 0.5$	$\lesssim 1$	$\lesssim 0.05$	$\lesssim 0.5$	–	$\lesssim 0.5$
$\Delta m_{B_d}/(\Delta m_{B_d})_{\text{SM}} - 1$	–	–	–	–	–	–	–
$\Delta m_{B_s}/(\Delta m_{B_s})_{\text{SM}} - 1$	–	–	–	–	$\lesssim 0.05$	–	$\lesssim 1$

TABLE V. Summary of the SUSY contributions to the observables in Fig. 11. “ $\checkmark$ ” shows that some parameter region is excluded by the  $\mu \rightarrow e \gamma$  constraint and hence the branching ratio can be just below the present upper bound. “–” means that the SUSY contribution is negligible.

# FIGURES

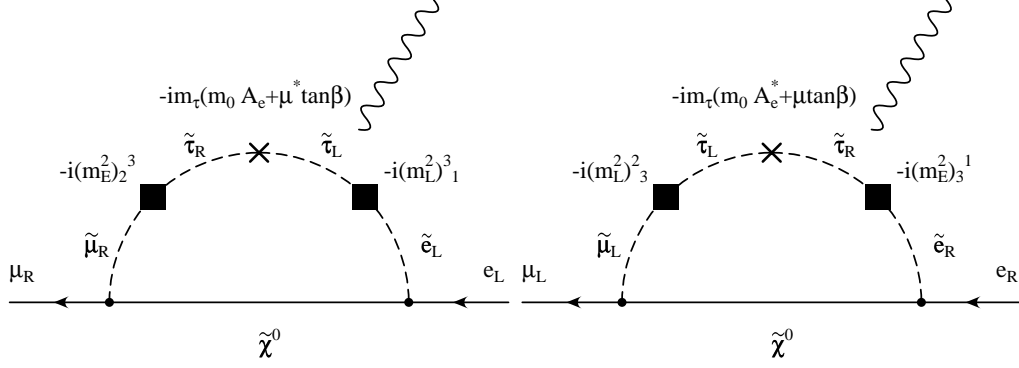


FIG. 1. Possible large contributions to  $\mu \rightarrow e \gamma$  amplitudes,  $A_R^{21}$  and  $A_L^{21}$  in the present model. They are enhanced with a factor  $m_\tau/m_\mu$  compared to the other contributions.

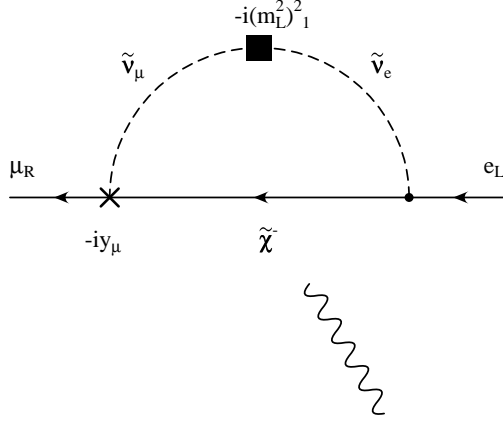


FIG. 2. A possible large contribution to  $\mu \rightarrow e \gamma$  amplitude  $A_R^{21}$  in the present model.

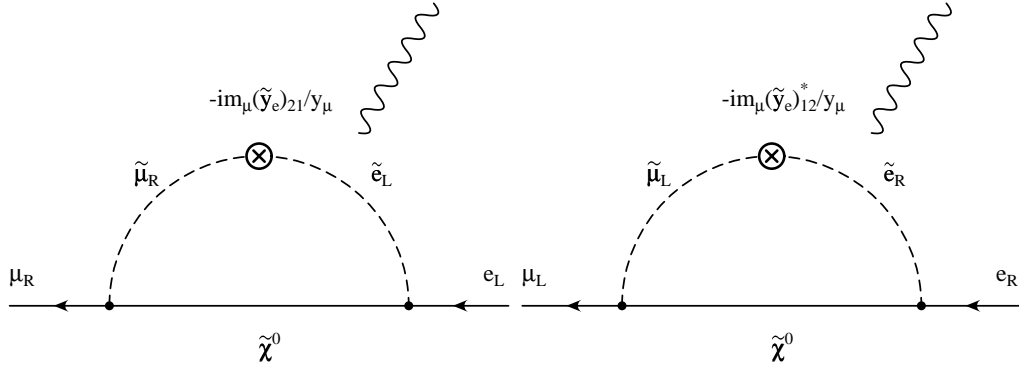


FIG. 3. Possible large contributions to  $\mu \rightarrow e \gamma$  amplitudes  $A_R^{21}$  and  $A_L^{21}$  in the present model. The flavor mixing in the left-right mixing is induced by the gauge interaction between the Planck scale and the GUT scale through the wavefunction renormalization of **24** Higgs supermultiplet.

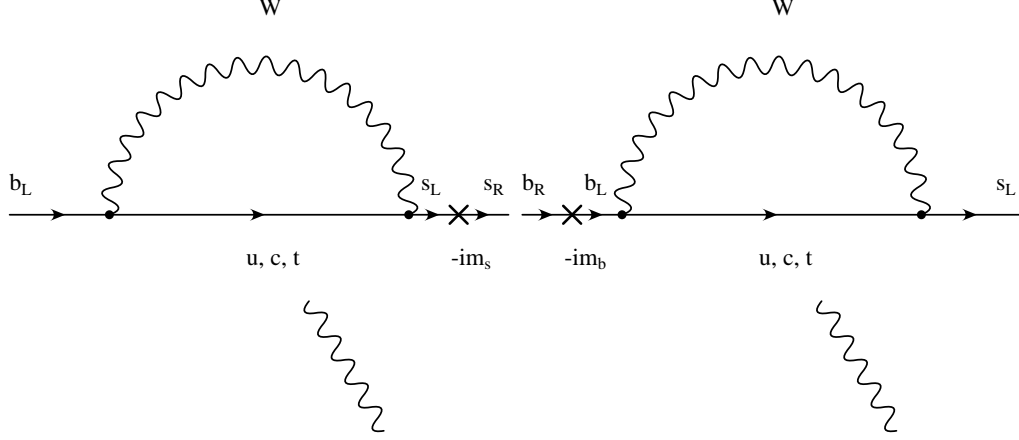


FIG. 4. One-loop diagrams which contribute to  $b \rightarrow s \gamma$  in the SM. The contribution to  $C'_7$  (left) is suppressed by  $m_s/m_b$  compared to the contribution to  $C_7$  (right).

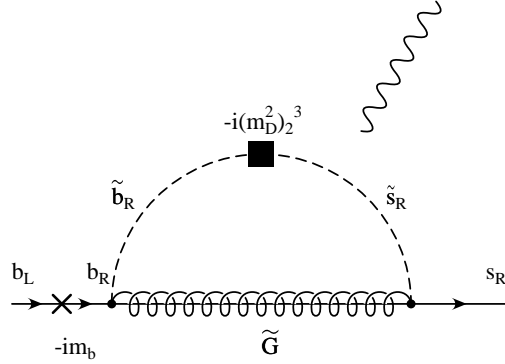


FIG. 5. A possible large contribution to  $b \rightarrow s \gamma$  amplitude  $C'_7$  in the SU(5)RN SUSY GUT which is not suppressed by  $m_s/m_b$ .

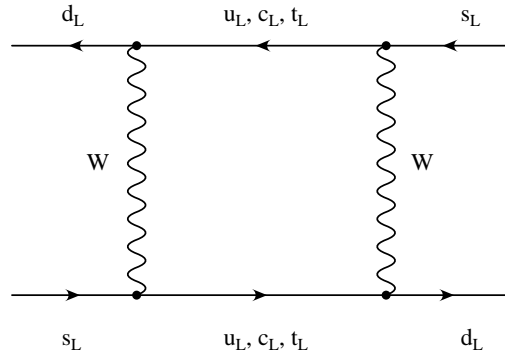


FIG. 6. A one-loop diagram which contributes to  $\epsilon_K$  in the SM. A similar diagram which contribute to  $B_d - \bar{B}_d$  ( $B_s - \bar{B}_s$ ) mixing in the SM can be obtained by replacing quarks in the external lines so that  $s \rightarrow b$  ( $s \rightarrow b$  and  $d \rightarrow s$ ).

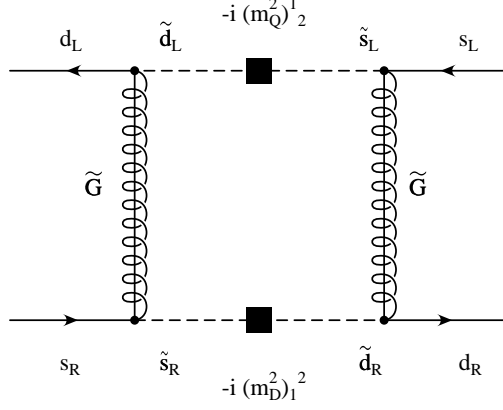


FIG. 7. A possible large contribution to  $\varepsilon_K$  in the SU(5)RN SUSY GUT. There is also a crossed diagram because of Majorana nature of gluino.

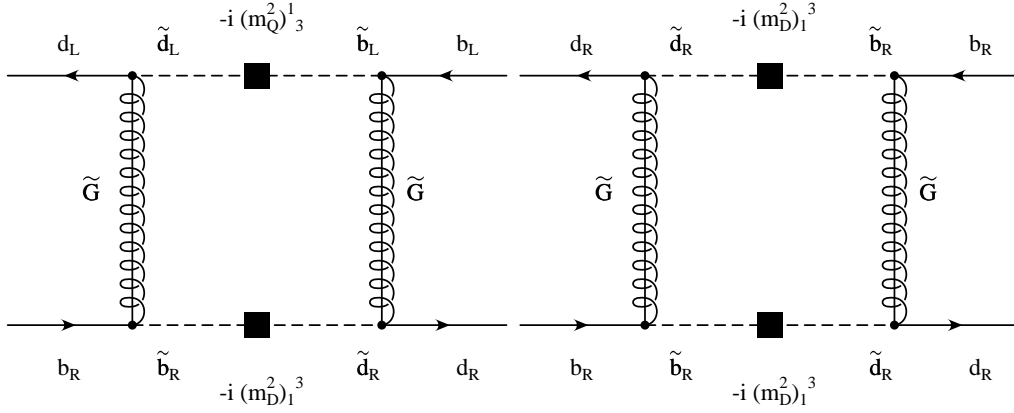


FIG. 8. Possible large contributions to  $B_d - \bar{B}_d$  mixing in the present model. Similar diagrams which contribute to  $B_s - \bar{B}_s$  mixing can be obtained by replacing the down quark/squark in the diagrams to the strange quark/squark. There are also crossed diagrams.

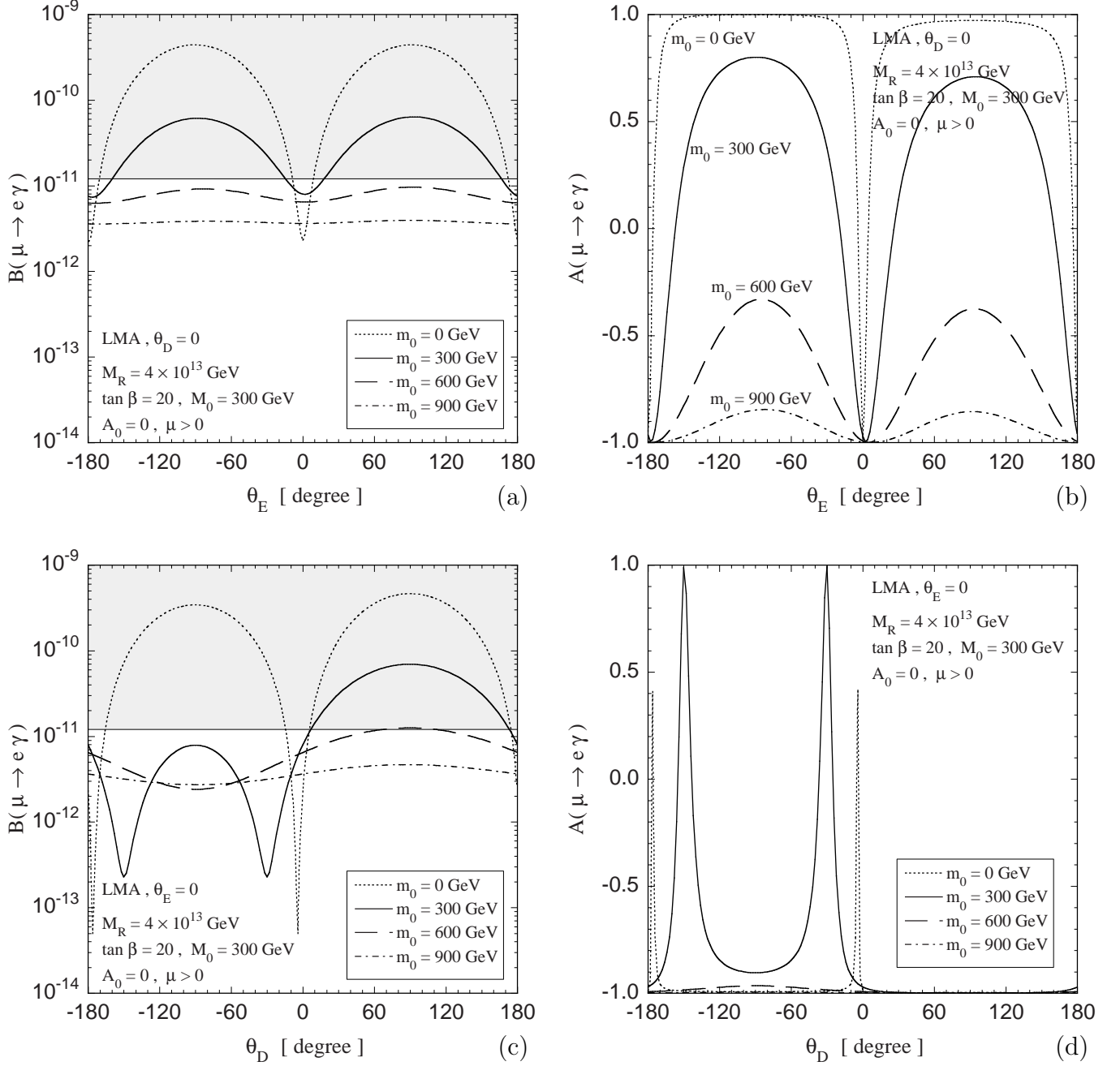


FIG. 9. Branching ratio and P-odd asymmetry of  $\mu \rightarrow e\gamma$  as functions of  $\theta_E$  and  $\theta_D$ .

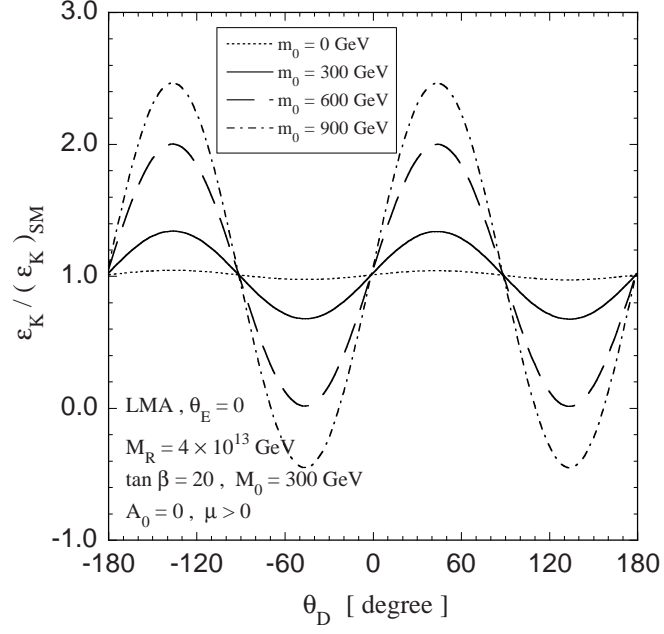
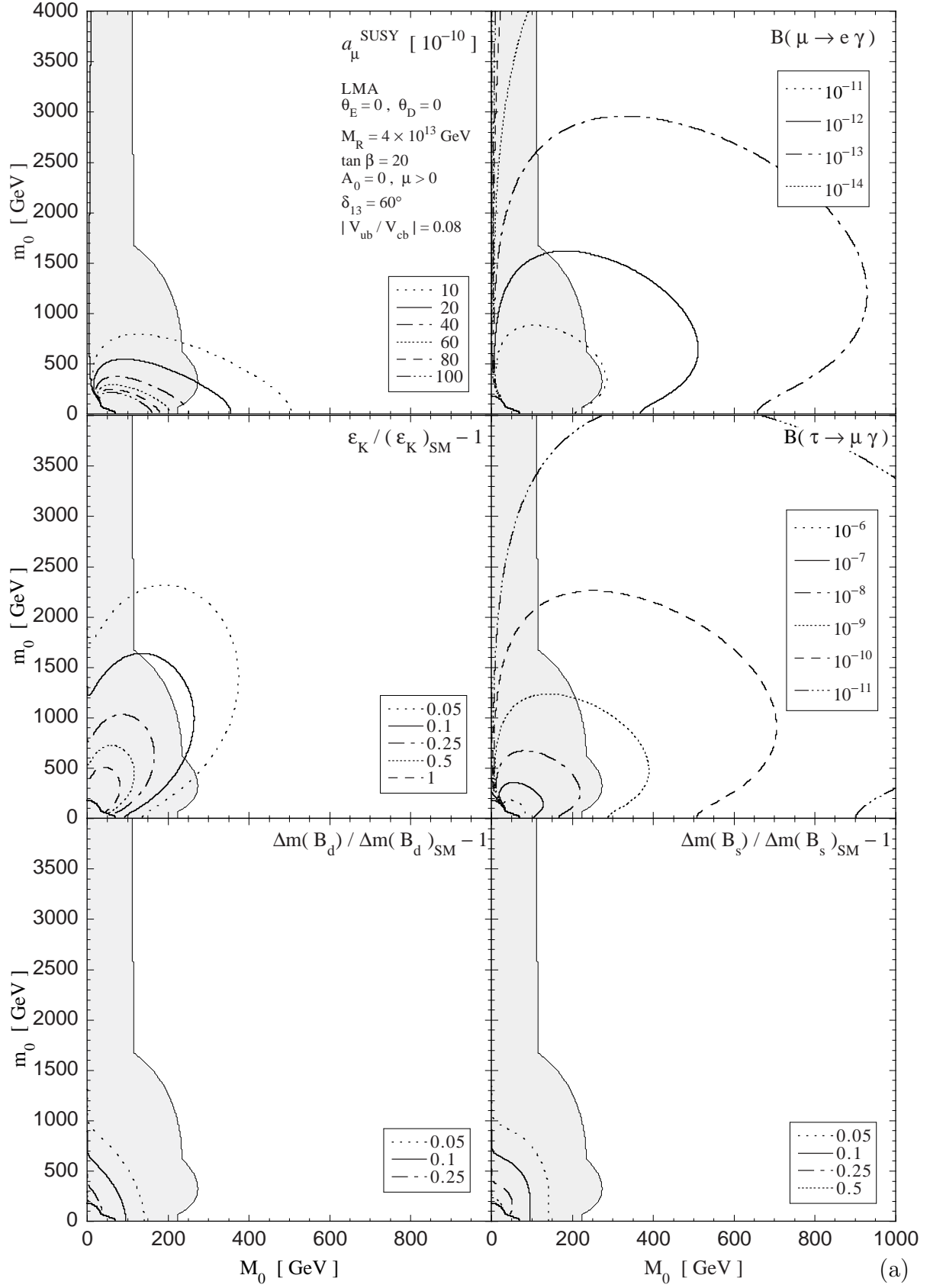
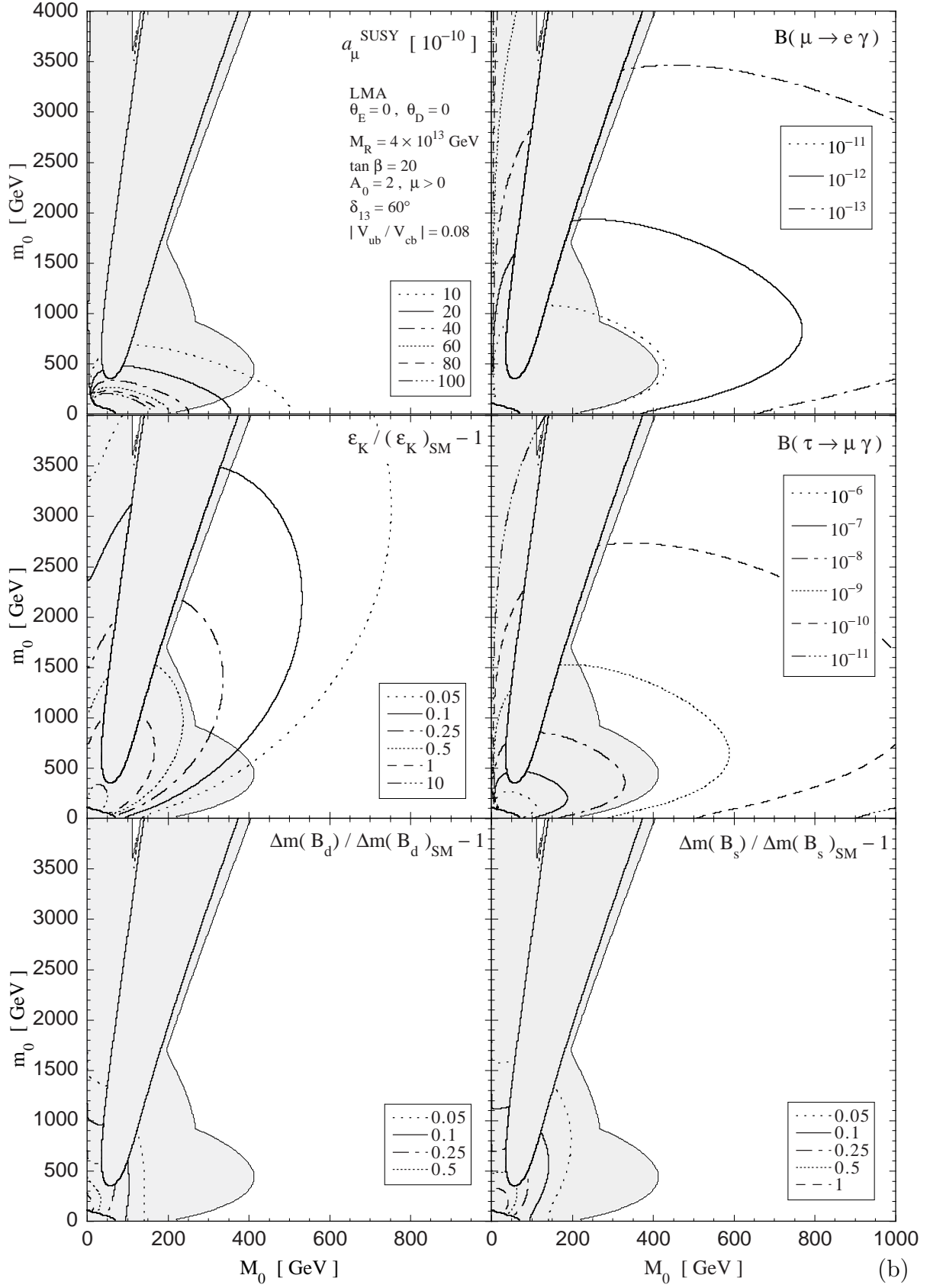
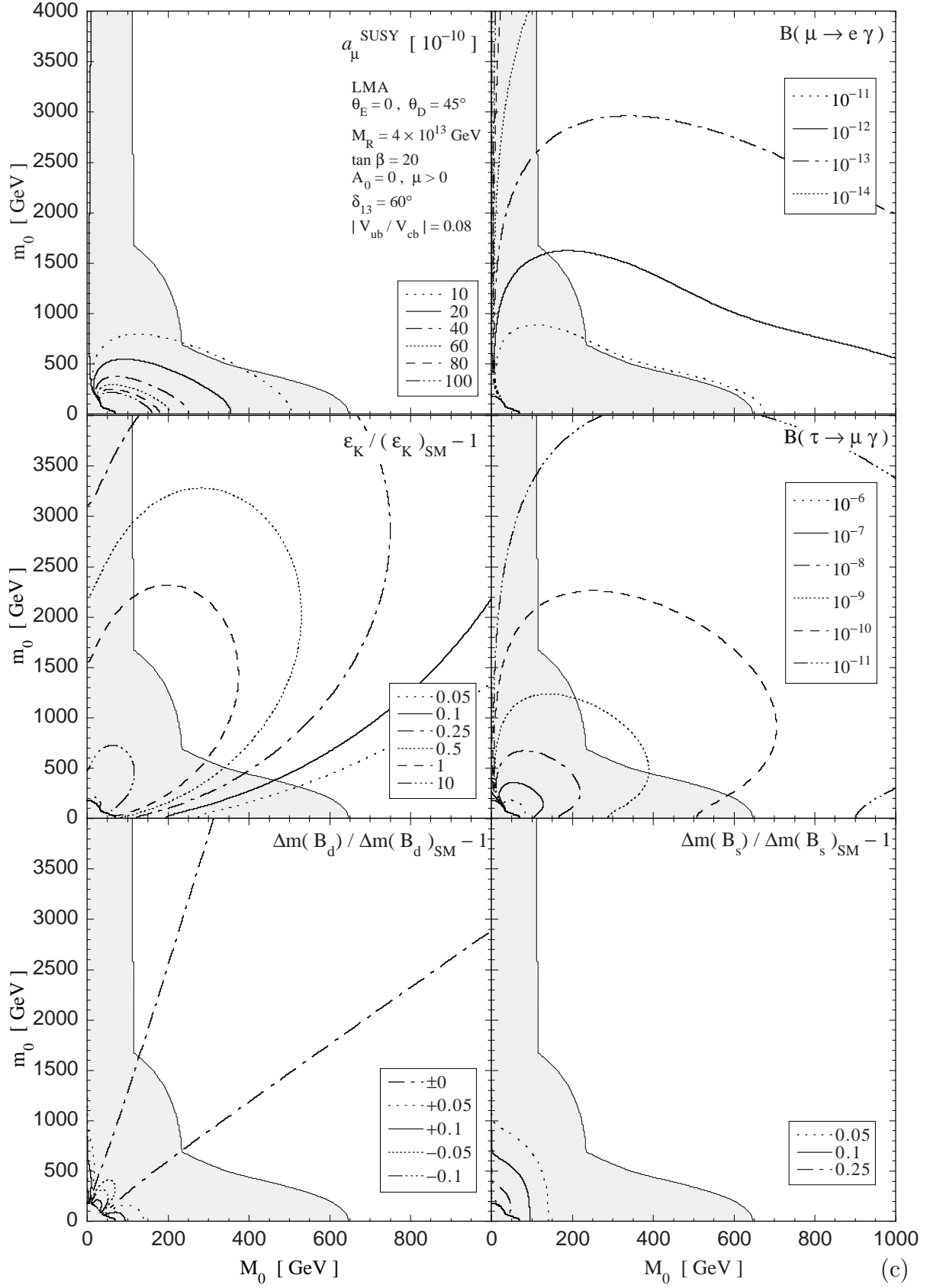
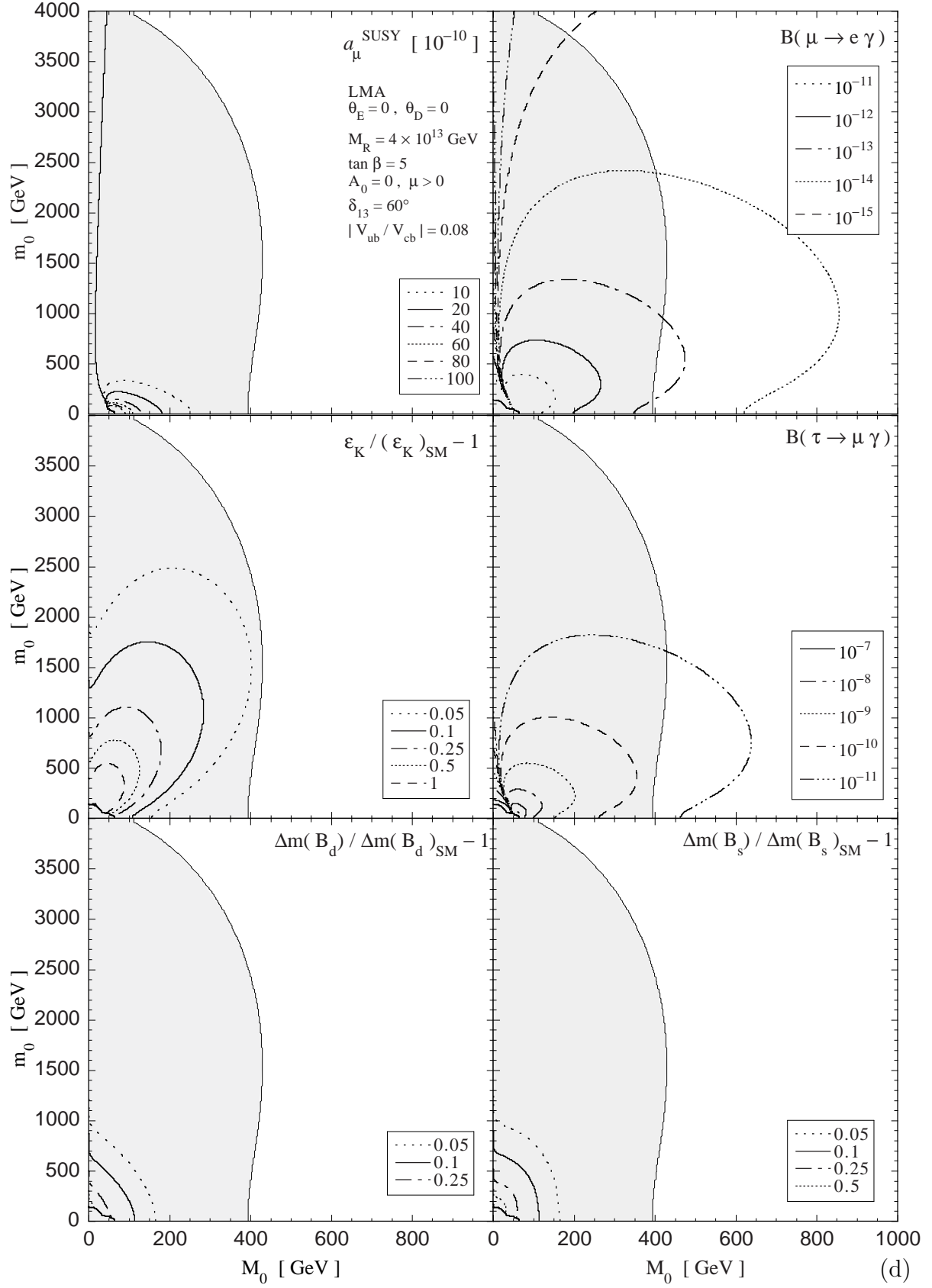


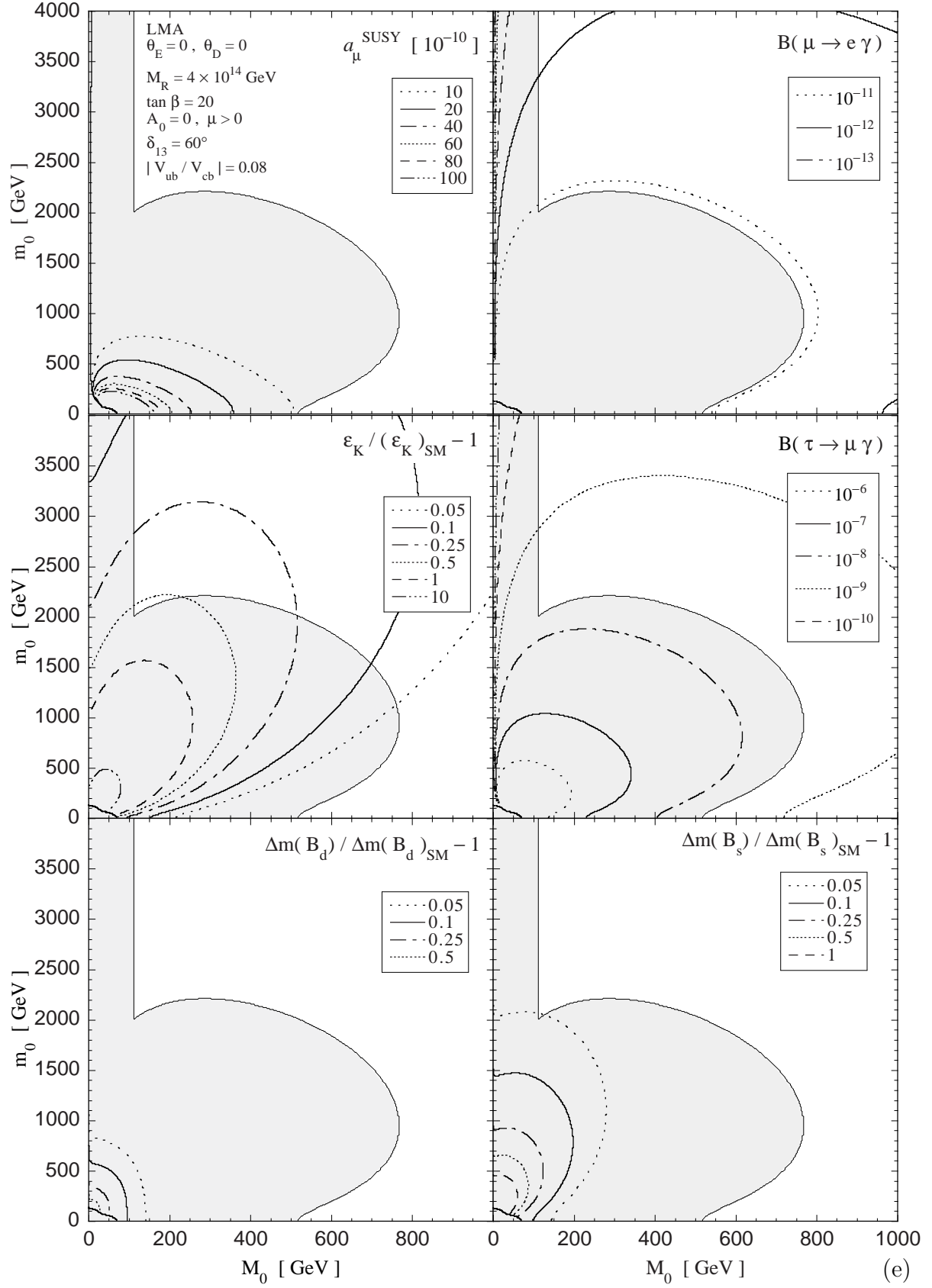
FIG. 10.  $\varepsilon_K$  normalized to the SM value as a function of  $\theta_D$ . Parameters are the same as those in Fig. 9(c) and (d).

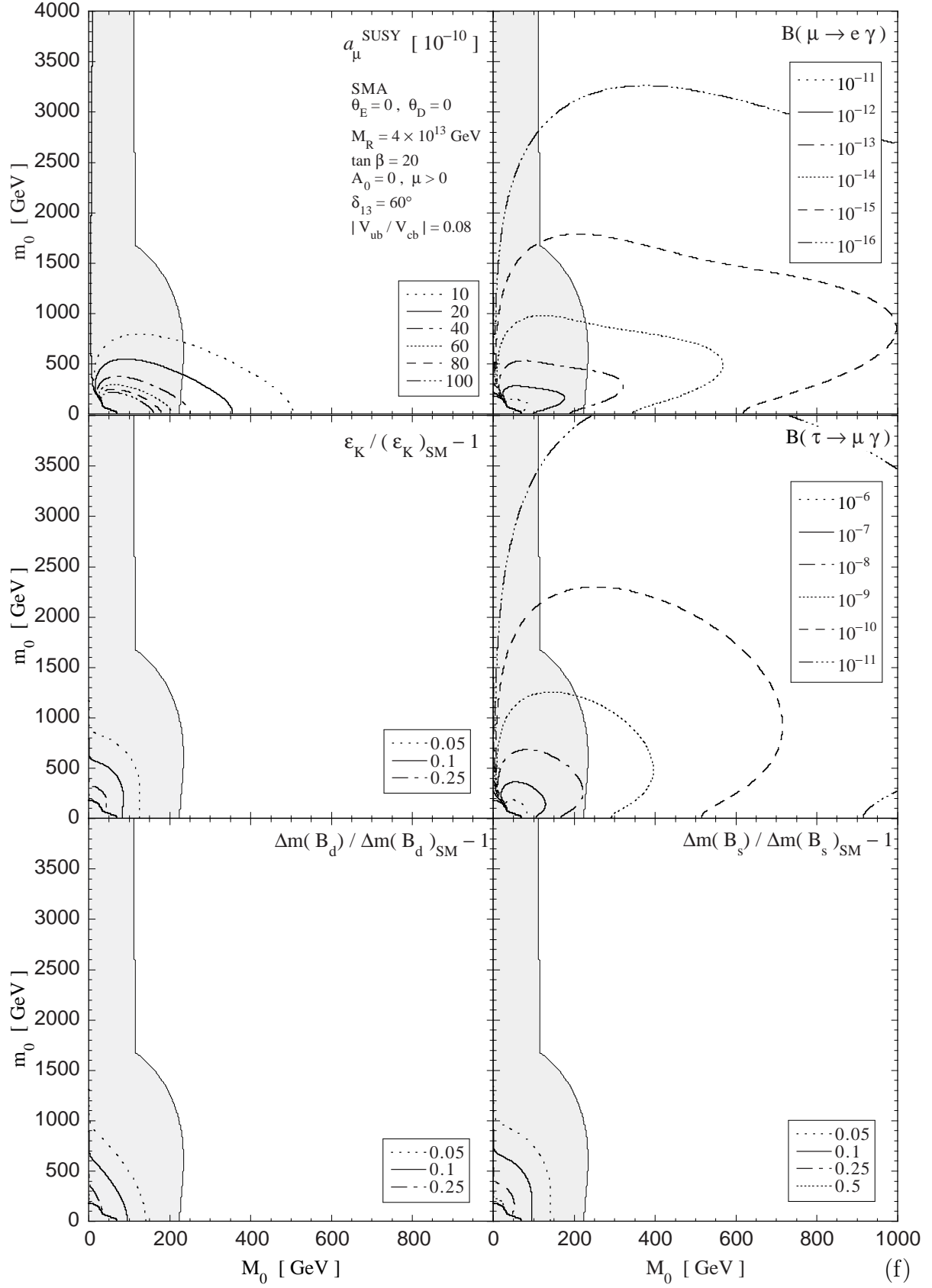












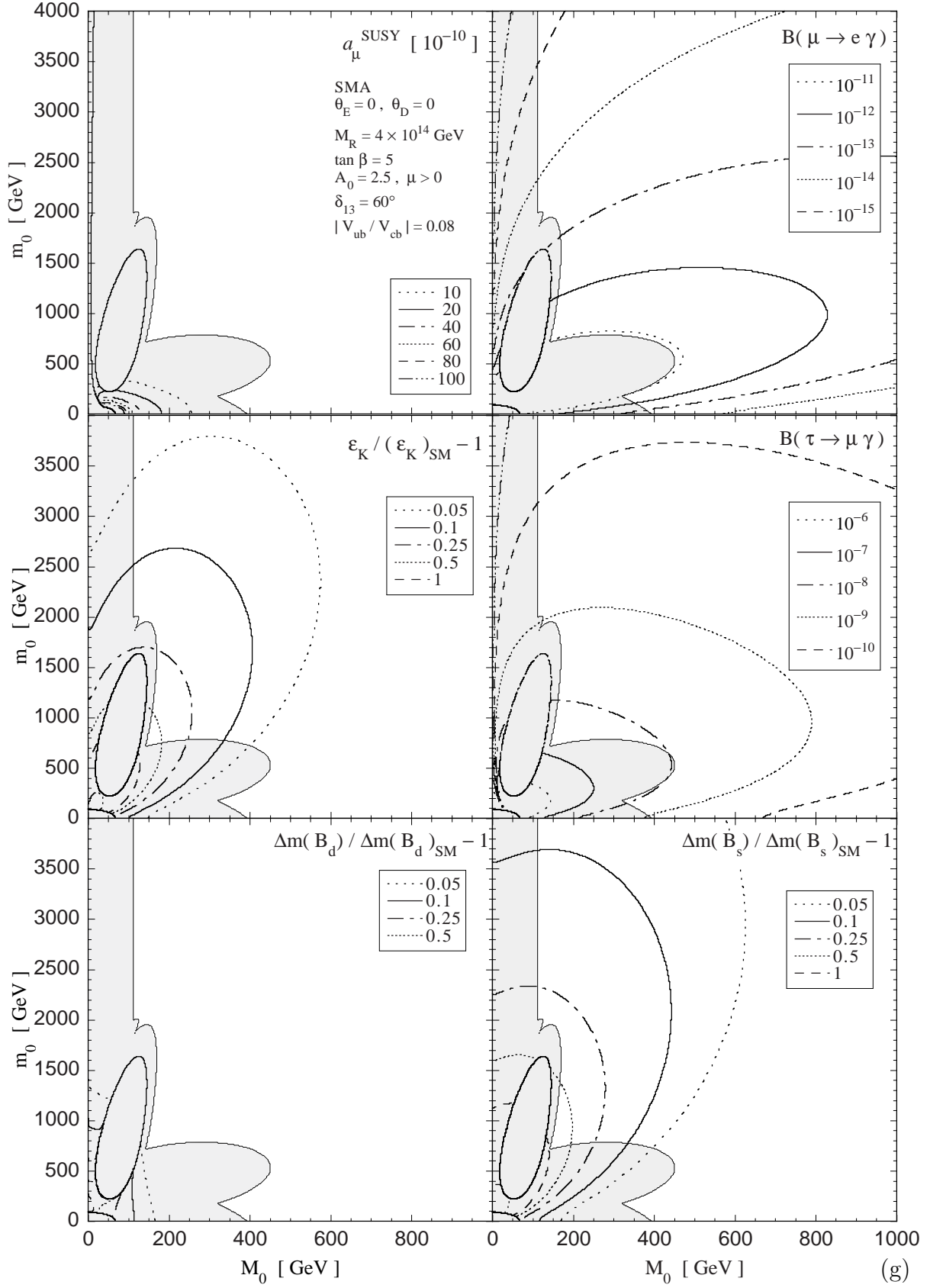


FIG. 11. Contour plots of  $a_\mu^{\text{SUSY}}$ ,  $B(\mu \rightarrow e \gamma)$ ,  $B(\tau \rightarrow \mu \gamma)$ ,  $\varepsilon_K/\varepsilon_K^{\text{SM}} - 1$ ,  $\Delta m_{B_d}/\Delta m_{B_d}^{\text{SM}} - 1$  and  $\Delta m_{B_s}/\Delta m_{B_s}^{\text{SM}} - 1$  on the  $m_0$ - $M_0$  plane for various choices of the parameters given in Table III. CKM parameters are fixed as  $\delta_{13} = 60^\circ$  and  $|V_{ub}/V_{cb}| = 0.08$  and  $\mu$  is taken as positive. Shaded regions are excluded experimentally (see text). In (b) and (g), the excluded regions correspond to negative stop mass squared are also shown.

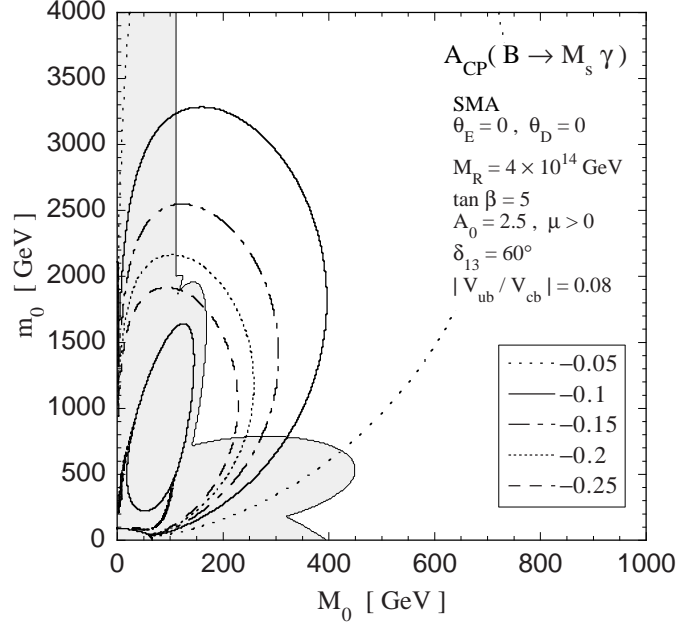


FIG. 12. Contour plot of the time-dependent CP asymmetry of  $B \rightarrow M_s \gamma$  decay with the same parameter set as Fig. 11(g).

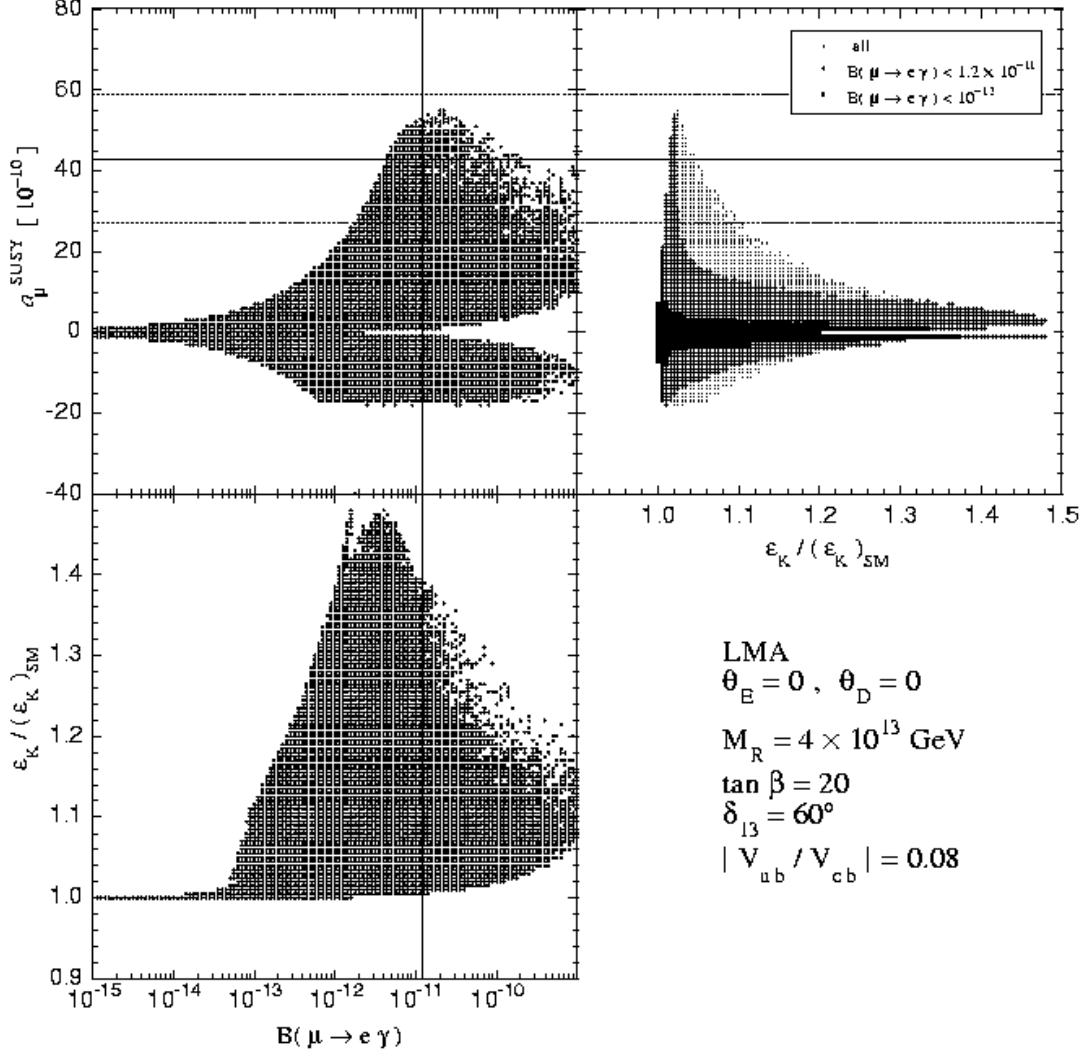


FIG. 13. Correlation among  $a_\mu^{\text{SUSY}}$ ,  $B(\mu \rightarrow e \gamma)$  and  $\epsilon_K$ . The vertical line shows the experimental upper bound  $B(\mu \rightarrow e \gamma) < 1.2 \times 10^{-11}$  [34] and the horizontal solid and dotted lines show the E821-favored region  $a_\mu^{\text{SUSY}} = (43 \pm 16) \times 10^{-10}$  [1].

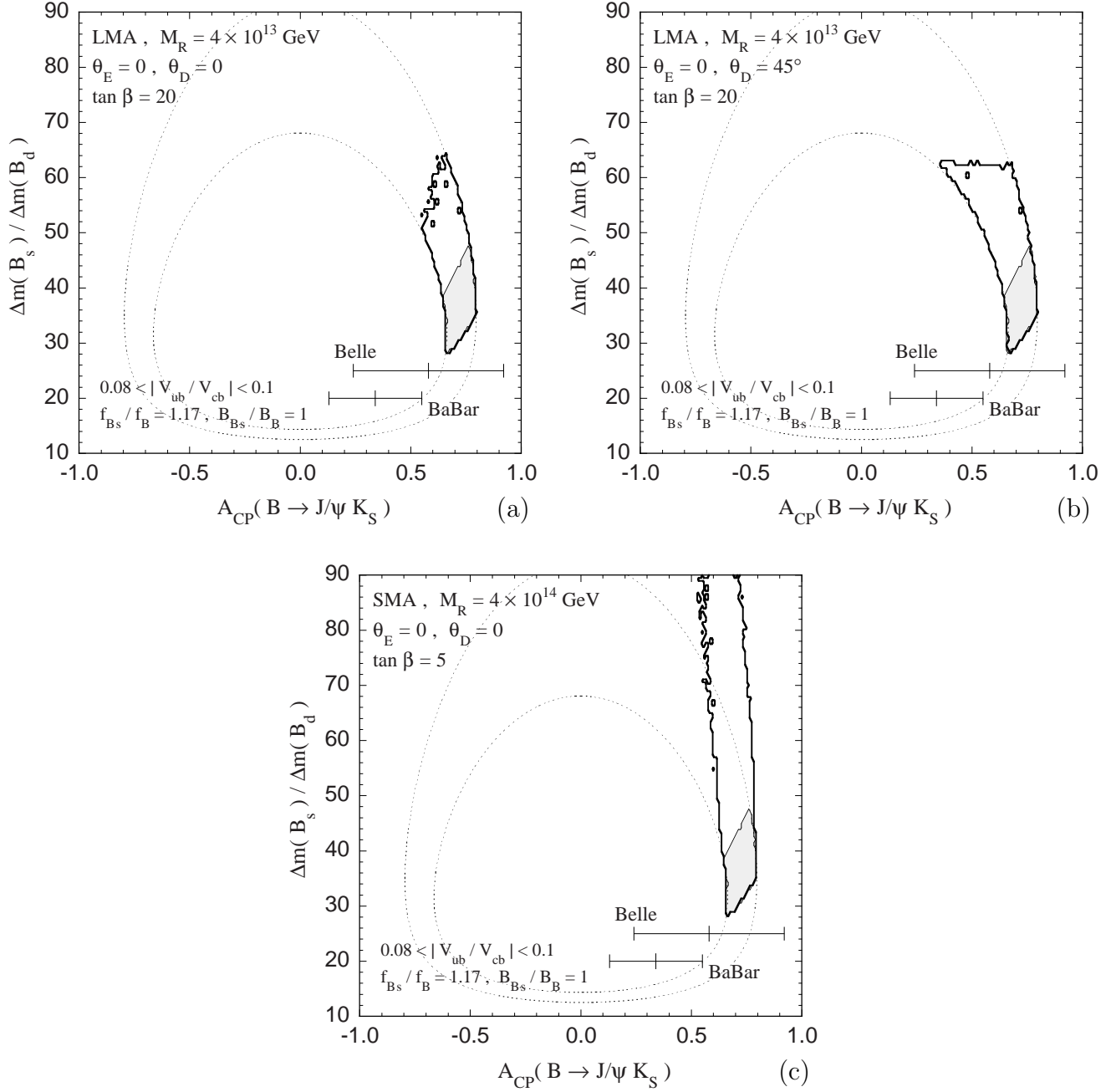


FIG. 14. Allowed region in  $\Delta m_{B_s}/\Delta m_{B_d}$ - $A_{CP}(B \rightarrow J/\psi K_S)$  plane.  $\delta_{13}$  and  $|V_{ub}/V_{cb}|$  are varied and constraints from  $\varepsilon_K$ ,  $\Delta m_{B_d}$  and  $\Delta m_{B_s}/\Delta m_{B_d}$  are imposed.  $1 \sigma$  ranges of the CP asymmetry from Belle and BaBar experiments are also shown [35].